The glycolytic inhibitor 2-deoxyglucose as a novel therapeutic agent to prevent cortical network dysfunction after traumatic brain injury

A thesis submitted by

Jenny Bryne Koenig

in partial fulfillment of the requirements for the degree of

PhD

in

Neuroscience

Tufts University

Sackler School of Graduate Biomedical Sciences

August 2019

Advisor: Chris G. Dulla, PhD

Abstract

Traumatic brain injury (TBI) is a significant cause of disability worldwide, as it can cause a wide range of chronic complications associated with disrupted brain function. Multiple molecular, cellular, and network pathologies occur following injury, but the pathophysiology of post-TBI cortical dysfunction is not well-understood. Many studies have demonstrated that GABAergic inhibitory network function is compromised following TBI, which may contribute to cortical hyperexcitability and motor, behavioral, and cognitive deficits. The loss or dysfunction of inhibitory interneurons may also contribute to the development of new-onset seizure activity observed commonly after TBI, in a condition known as post-traumatic epilepsy (PTE). Preserving the function of GABAergic interneurons, therefore, is a rational therapeutic strategy to preserve cortical function after TBI and prevent long-term clinical complications.

Following TBI, there is a complex landscape of metabolic changes that evolve over days and weeks. Based on rich clinical and preclinical data of these post-TBI changes in glucose utilization, combined with the success of metabolic therapies like the ketogenic diet in treating epilepsy, interest has grown in determining whether manipulating metabolic activity following traumatic brain injury may have therapeutic value to prevent post-traumatic epileptogenesis.

In this thesis, I explore whether the use of a glycolytic inhibitor, 2-deoxyglucose (2-DG), affects post-TBI cortical pathology. First, I outline the therapeutic rationale behind this approach by examining changes in glucose utilization and glycolytic activity in the brain following traumatic brain injury and during seizures. In this section, I also

outline potential paths forward to utilize glycolytic inhibitors as a disease-modifying therapy for post-traumatic epilepsy.

Then, I tested whether the use of 2-DG attenuates cortical dysfunction after TBI in a mouse model of focal brain contusion. Employing the controlled cortical impact (CCI) model of TBI, we found that *in vitro* 2-DG treatment rapidly attenuated epileptiform activity seen in acute cortical slices 3-5 weeks after TBI. One week of *in vivo* 2-DG treatment immediately after TBI prevented the development of epileptiform activity, restored excitatory and inhibitory synaptic activity, and attenuated the loss of parvalbumin-expressing inhibitory interneurons. Further, I found that acute *in vitro* application of 2-DG decreased the excitability of excitatory neurons, but not inhibitory interneurons, suggesting a possible cell type-specific mechanism for 2-DG's effects. In summary, the glycolytic inhibitor 2-DG may have therapeutic potential to restore network function following TBI.

Dedication

The years spent developing this work are dedicated to my future students and patients.

I hope that I can help, teach, support, share with, and inspire you in the same way that my mentors have done for me.

Acknowledgments

First and foremost, I would like to thank my amazing mentor, Dr. Chris Dulla. None of this work would have been possible without your endless support, guidance, and affirmation. Thank you for training me how to think, for encouraging me through every day and every experiment (regardless of its success or failure), for finding opportunities for me to grow and network, and for continually challenging me to become a better version of myself. I now embrace my full potential as a scientist, and I have you to thank for that.

Next, I would like to thank my thesis advisory committee (TAC) chair, Dr. Jamie Maguire, and my TAC members, Dr. Maribel Rios and Dr. Dong Kong, for their invaluable guidance and suggestions throughout my thesis project. I would also like to thank Dr. Michael Whalen for serving as my outside thesis examiner and for lending his expertise in TBI.

I'd like to acknowledge the members of the Dulla lab, past and present, who have been present during every single step of my project. Special thanks to Dr. David Cantu, who originally began our investigations of the effects of 2-DG treatment after CCI, and to Mary Sommer, Danielle Croker, Ashley Ortiz, and Cho Low (from the Kong lab) for contributing your time and efforts toward data collection for my thesis project. Thank you to Drs. Lauren Lau, Liz Hanson, and Jen Shih for showing me how to be a productive graduate student and for serving as excellent peer mentors (and lab friends!). Finally, thank you to Dr. Moritz Armbruster, who has magical hands at the electrophysiology rig and has given me excellent technical guidance throughout my experiments.

This work would not have been possible without generous funding support from the National Institute for Neurological Disorders and Stroke and the United States Department of Defense. Thank you to my NINDS program officer, Dr. Vicky Whittemore, for your support of my fellowship application and for your mentorship!

Thank you to the Neuroscience Program and the Medical Scientist Training Program at Tufts for your support. I'd particularly like to thank my advisors in the MD/PhD program, Dr. Jim Schwob, Dr. Naomi Rosenberg, and Dr. Gordon Huggins for believing in my potential as a physician-scientist and giving me the opportunity to pursue this career path! I'd also like to thank the awesome administrators who have allowed the PhD process to run smoothly – Shelley Antonio, Alison Hochler, Brian Lynch, Ledja Lera, Jeff Miller, Sara Abbott-Darcy, and all the others in the dean's office and medical school Office for Student Affairs. Finally, I'd like to acknowledge the Tufts Center for Neuroscience Research core facilities, including Andrew Tarr in the behavior core and Alenka Lovy in the imaging core, for their technical support.

I've had the opportunity to interact with, and become integrated into, the epilepsy research community through the Gordon Research Conferences on Epilepsy and the American Epilepsy Society annual meetings. Thank you for welcoming me into the field – I look forward to our future collaborations!

Thank you to my prior mentors for helping me reach this milestone in my career! I'd specifically like to thank Dr. Robert Sapolsky and Dr. Iris Jaffe (my former research mentors), as well as Dr. Melissa Works for showing me the ropes of lab work while I was an undergrad. I'd also like to thank Mrs. Cathy Alexander, who has believed in my potential and has cheered for my progress ever since I took her algebra class at 10 years

old – I look forward to sharing this achievement with you, and am grateful that I will finally live up to the “Dr. Jenny B. Koenig” plaque you gifted me with at my high school graduation!

I’ve been at Tufts for several years now, and I’ve been extremely lucky to share my time with an amazing cohort of MD/PhD students – Liz, Dave, Seth, Craig, Bobby – thanks for taking on this marathon effort with me! Also, a special thanks to my grad school friends for helping me think through problems, taking coffee breaks with me, and generally making the PhD process much more enjoyable (there are too many awesome people to name here, but I’m especially looking at you, Dom, Minagi, and Michaela!).

During this PhD, I have also been lucky to be a part of the dance community in Boston. To all the amazing humans in Boston Community Dance Project – thank you for allowing me to express myself, embrace my imperfections, and grow as a human and artist. You all have become my New England family!

Finally, and most importantly, I must thank my parents, Harris and Angela Koenig. There are truly no words to express my gratitude for you and for all you have done to help me achieve my dreams. Thank you for believing in me, thank you for keeping me grounded, thank you for encouraging me, thank you for loving me unconditionally. I could not have done this without you.

Table of Contents

List of Tables

List of Figures

List of Copyrighted Materials Produced by the Author

J. B. Koenig, C. G. Dulla, Dysregulated Glucose Metabolism as a Therapeutic Target to Reduce Post-traumatic Epilepsy. *Front Cell Neurosci* **12**, 350 (2018).

J. B. Koenig, D. Cantu, C. Low, M. Sommer, F. Noubary, D. Croker, M. Whalen, D. Kong, C. G. Dulla, Glycolytic inhibitor 2-deoxyglucose prevents cortical hyperexcitability after traumatic brain injury. In revision at *JCI Insight.*

List of Abbreviations

2-DG = 2-deoxyglucose
4-AP = 4-aminopyridine
aCSF = artificial cerebrospinal fluid
AD = Alzheimer's disease
ANLS = astrocyte-neuron lactate shuttle
ANOVA = analysis of variance
AP = action potential
ATP = adenosine triphosphate
BBB = blood-brain-barrier
CCI = controlled cortical impact
CHI = closed head injury
CR = calretinin
CT = computed tomography
CTE = chronic traumatic encephalopathy
EEG = electroencephalogram
EPM = elevated plus maze
fEPSP = field excitatory postsynaptic potential
FPI = fluid percussion injury
FST = forced swim test
GAD67 = glutamic acid decarboxylase 67
GFAP = glial acidic fibrillary protein
ICP = intracranial pressure
IP = intraperitoneal
KD = ketogenic diet
LG = low glucose
LMM = linear mixed model
MCT = monocarboxylate transporter
mEPSC = miniature excitatory postsynaptic current
mIPSC = miniature inhibitory postsynaptic current
MRI = magnetic resonance imaging
MWM = Morris water maze
NNT = number needed to treat
OF = open field
PB = phosphate buffer
PBS = phosphate-buffered saline
PCS = post-concussive syndrome
PET = positron emission tomography
PFA = paraformaldehyde
PID = post-injury day
PPP = pentose phosphate pathway
PTE = post-traumatic epilepsy
PV = parvalbumin
RR = Rotarod
SE = status epilepticus

sEPSC = spontaneous excitatory postsynaptic current
sIPSC = spontaneous inhibitory postsynaptic current
SSC = somatosensory cortex
SST = somatostatin
TBI = traumatic brain injury
TCA = tricarboxylic acid
tdT = tdTomato

Chapter 1 : Introduction

1.1 What is traumatic brain injury?

Traumatic brain injury (TBI) is one of the leading causes of long-term disability in the United States and around the world. According to the Centers for Disease Control and Prevention (CDC), TBI results in 1.36 million emergency room visits, 275,000 hospitalizations, and 52,000 deaths per year in the United States [1]. The numbers reported above are likely an underrepresentation of the true prevalence of TBI, as many individuals suffering from mild TBI or concussion do not seek clinical treatment. Further, the extensive acute and chronic complications of TBI, including cognitive deficits, behavioral changes, and seizure activity, each decrease the quality-of-life of patients suffering from brain injuries. Unfortunately, the pathophysiologic mechanisms linking the initial TBI to long-term pathologies are not well-understood, thus limiting the ability of physicians to intervene to prevent them.

The term "TBI" encompasses a broad range of disease mechanisms and severities and therefore corresponds to a very heterogeneous patient population. Traumatic brain injury can be most simply defined as an external insult to the brain that disrupts its normal function [2]. This insult is most traditionally due to mechanical blunt impact (such as hitting your head during a fall or motor vehicle accident) but can also result from blast waves (from being too close to a detonating explosive). The injury can occur with the skull intact (closed head injury) or can be penetrating, where both the skull and dura mater are compromised by a bullet, piece of shrapnel, bone fragment, or other object [3]. Additionally, the TBI may be focal, presenting with effects in a particular area of the brain where the force was applied (and sometimes in an opposing area of the brain, known as the contrecoup), or may be diffuse where there is evidence of axonal injury

across the brain parenchyma. In all injury types, acceleration-deceleration forces of the brain within the skull, as well as angular, rotational, and shear forces within the brain parenchyma, can cause additional mechanical insult that contributes to vascular and cellular injury. In fact, the forces associated with subconcussive hits (which are considered lower-severity than TBI) are sufficient to cause persistent changes in cognition and cortical white matter in collegiate contact sport athletes [4-6].

Epidemiologically, patients who are very young (<5 years old), adolescent (15-19 years old), or elderly (>75 years old) are more likely to sustain a TBI than patients in other age groups [7]. In these patients, accidents (such as falls) are an important contributor to the TBI rates. Among all age groups, patients >75 years old are most likely to require hospitalization or to die following a TBI [7]. Overall, TBI is more common in males than females (547.6 versus 385.9 per 100,000 persons [8]). Additionally, specific patient populations including contact sport athletes and war veterans are at especially increased risk of sustaining TBI and suffering from its long-term consequences. The patient epidemiology of TBI is important to consider, as some patient factors (such as age and pre-TBI cognitive function) are key indicators of the likelihood of developing long-term dysfunction [9].

In studying TBI, it is helpful to divide the heterogeneous patient population into sub-groups to better understand patient prognosis and to determine which patients would most likely benefit from specific interventions [3]. One important classification is by injury mechanism or etiology – for example, a blunt closed-head injury may result in very different pathophysiology and patient outcome than a penetrating stab wound or a blast wound. Another important classification is by injury severity, which can range

from mild (known as mTBI or concussion) to severe. This classification is less straightforward, and multiple different systems have been proposed to categorize TBI in this way. One classification system relies on the Glasgow Coma Scale, which utilizes functional readouts from the patient such as verbal response and eye opening, to determine injury severity. The Glasgow Coma Scale is scored from 3-15, and a TBI resulting in a score ≤8 is generally considered severe [3]. TBI can also be classified using data collected from brain imaging. Computed tomography (CT) is often performed to rule out intracranial bleeding and other TBI comorbidities, and thus, is commonly used to help classify TBI severity through the Marshall CT score or Rotterdam CT score systems [10]. Magnetic resonance imaging (MRI) can also be utilized for classification, but it is more expensive than CT and therefore is generally reserved for specific diagnostic purposes (such as examining diffuse axonal injury). One of the key efforts of the CDC under the Congressional TBI Act of 2008 is to standardize these different TBI classification systems to allow better comparison across preclinical and clinical studies.

The heterogeneity of TBI patients and their outcomes contributes to the complexity of this field of research and the difficulty in developing treatments for TBI. When a patient presents with a TBI, the current standard-of-care is purely supportive [2]. In severe TBI, physicians will usually intubate the patient to protect the airway, monitor and treat hypotension and electrolyte abnormalities, and maintain the patient's fluid status with normal saline. In terms of protecting the brain, they monitor intracranial pressure (as increased ICP is associated with worsened outcomes and brain herniation) and will treat increases in ICP with osmotic therapies or a surgical intervention to remove part of the skull (decompressive craniectomy). Standard management of acute severe TBI usually

also includes at least one week of seizure prophylaxis with levetiracetam or phenytoin to reduce acute seizure activity and lower the risk of status epilepticus (SE) in the acute period. SE, defined as seizure activity lasting > 5 minutes without recovery of consciousness, is acutely life-threatening and is associated with extremely high mortality (>50% in some studies). Finally, physicians seek to maintain normothermia and normoglycemia (range 140-180 mg/dL), as fever, hyperglycemia, and hypoglycemia have each been shown to be associated with worsened outcomes [11, 12]. While still somewhat controversial in the field, the use of therapeutic induced hypothermia (which is thought to reduce ICP and cerebral metabolic activity) has not been shown to be neuroprotective and is usually not performed [13]. Currently, there are no treatments for TBI that have been shown to effectively reduce the risk of long-term TBI complications, despite their clearly devastating patient-oriented and economic effects.

1.2 TBI pathophysiology: primary and secondary injury mechanisms

In an effort to develop novel therapies to treat TBI and prevent its chronic complications, significant preclinical work has been done to understand the pathophysiologic events that occur following a TBI. At a basic level, these can be divided into primary and secondary injury mechanisms (Table 1.1). The primary injury occurs at the time of the TBI and is a direct result of the external force applied to the brain. This includes widespread shearing of axonal and other cellular membranes and mechanical disruption of vascular architecture, including the blood-brain-barrier (BBB). This, in turn, can cause intracranial bleeding and the formation of a bruise/contusion on the brain surface. While primary prevention strategies (use of helmets or avoidance of situations

that leave a patient accident-prone) can reduce the incidence of a TBI altogether, the timing of the primary injury pathologies (instantaneous to minutes following TBI) does not allow an intervention to reduce or prevent them once a TBI occurs.

Following the primary injury, multiple secondary injury mechanisms evolve in the hours to days following TBI. Secondary injury includes the recruitment of inflammatory cells, increased intracranial pressure, changes in cellular metabolic activity, altered synaptic and network activity, widespread cell death, and many other cellular-level changes (Table 1.1). In many preclinical and clinical studies, these cellular mechanisms have been associated with worsened outcomes, including epileptogenesis [14]. Of particular importance to the studies presented here, changes in glucose utilization after injury are associated with both acute changes in neuronal activity and long-term functional deficits [15].

Primary Injury	Secondary Injury
• External force applied to the brain • Acceleration/deceleration forces acting focally and at contrecoup • Cortical contusion • Possible penetrating injury • Possible epidural or subdural hematoma • Membrane disruption, including disruption of BBB • Massive release of neurotransmitters and other intracellular contents	• Neuroinflammation • Altered synaptic and network activity • Apoptosis • Mitochondrial dysfunction • Free radical injury • Electrolyte imbalances • Vasospasm or vascular occlusion • BBB dysfunction • Cerebral edema • Excitotoxicity • Changes in glucose utilization

Table 1.1 Mechanisms of primary and secondary injury.

While classified broadly as “secondary injury,” it isn’t entirely clear whether all of the changes in Table 1.1 are purely pathologic, or whether some represent the system’s physiologic compensatory response to the initial insult. Nonetheless, the timing of

secondary injury (hours to days following TBI) allows the opportunity for clinical intervention to prevent its detrimental effects and its contribution to long-term pathology. A better understanding of how different aspects of secondary injury contribute to long-term brain dysfunction and clinical complications will aid in the development of interventional therapies. This provides the basis of the investigation presented in this thesis: to better understand how manipulation of glucose metabolism acutely after TBI (via delivery of glycolytic inhibitor, 2-deoxyglucose) can affect long-term cortical function.

1.3 Sub-acute and chronic complications of TBI

Since TBI, by definition, causes a change in "normal brain function," it can result in a broad range of cognitive and behavioral changes. At the time of the TBI, physicians can conclude that brain function was altered if they observe any of the following clinical signs:

> "a. Any period of loss of or decreased consciousness;
>
> b. Any loss of memory for events immediately before (retrograde amnesia) or after the injury (post-traumatic amnesia);
>
> c. Neurologic deficits such as muscle weakness, loss of balance and coordination, disruption of vision, change in speech and language, or sensory loss;
>
> d. Any alteration in mental state at the time of the injury such as confusion, disorientation, slowed thinking, or difficulty with concentration." [16]

These initial findings can resolve within minutes or hours following TBI, but some patients will never fully recover from these cognitive and neurologic deficits.

In the sub-acute period, patients can suffer from post-concussive syndrome (PCS). PCS refers to a constellation of vague neurologic symptoms, often including headache, dizziness, decreased attention, insomnia, and other cognitive/psychologic deficits [17]. PCS is most commonly associated with mild TBI, although it can occur after moderate or severe TBI. Patients who are female, elderly, or who have comorbid post-traumatic stress disorder (PTSD) are more likely to have prolonged or worsened PCS. The pathophysiology of PCS is not well understood, and likely includes both structural and psychogenic mechanisms. Importantly, most patients' PCS symptoms resolve within a few weeks following the TBI and only a minority of patients (10-15%) are diagnosed with persistent PCS (lasting >1 year) [17].

Post-traumatic complications can continue to emerge months to years following a TBI. These complications include cognitive and behavioral deficits, as well as the development of secondary psychiatric, sleep, neurodegenerative, and seizure disorders. Each of these complications can significantly impair patients' quality-of-life and ability to contribute to society. As further evidence of the devastation of post-TBI sequelae, 1.1% of the United States population (an estimated 3.17 million people in 2005) are living with long-term disability as a result of TBI [18]. It is not well-understood how TBI leads to long-term neurologic dysfunction, although early secondary injury mechanisms are likely to play a role. If the secondary injury after a TBI alters underlying cellular function and network connectivity permanently, then this would support TBI's capacity to increase risk for later CNS dysfunction. Interestingly, not all patients develop post-TBI complications, suggesting that having a TBI may be an important risk modifier that has

its greatest impact in patients that are already genetically or environmentally vulnerable to neurological problems.

One of the most devastating complications after TBI is neurodegeneration, as TBI patients are at increased risk to develop a broad range of neurodegenerative disorders including Alzheimer's disease, Parkinson's disease, frontotemporal dementia, amyotrophic lateral sclerosis, and mild/moderate cognitive impairment [19]. One possible contributor to post-TBI neurodegeneration is the release of tau into the brain parenchyma as a result of axonal injury [20]. TBI can also cause Aβ plaque deposition, as is observed in non-traumatic AD [21]. Further, chronic inflammation after TBI may disrupt physiologic clearance dynamics and promote pathologic plaque formation [20]. Interestingly, post-TBI neurodegeneration shares some important characteristics with non-traumatic AD, including increased risk in patients with the APOE ε4 allele and regionally selective cerebral atrophy starting in the hippocampus and amygdala [22].

This section would be incomplete without discussion of chronic traumatic encephalopathy (CTE, previously known as dementia pugilistica). Unlike many of the other post-TBI complications, where risk correlates with TBI severity, CTE is most commonly associated with repeated *mild* TBIs or concussive injuries. Thus, CTE is very prevalent in athletes engaging in contact sports. The prior classification of "dementia pugilistica" has been observed in ~20% of professional boxers [23]. Further, in a shocking study published in 2017, Mez and colleagues (led by Dr. Ann McKee) found evidence of CTE in 87% of a convenience sample of brains donated from American football players, including CTE findings in 110/111 former professional players from the National Football League [24]. While CTE is primarily neurodegenerative, it can be

distinguished from other dementias because of its clinical presentation and neuroanatomical pattern of tau pathology. Patients usually present first with behavioral deficits, including agitation, impulsivity, and personality changes, and then can further develop cognitive impairment, memory loss, and mood disorders (often presenting as depression with suicidal ideation). Pathologically, the patterns of tau accumulation in CTE are distinct from Alzheimer's and other dementias, as the abnormal hyper-phosphorylated tau is concentrated in the superficial cortical layers and surrounding the blood vessels in the depths of cortical sulci. While CTE is not the central focus of this thesis, coverage of CTE in the popular media has provided important urgency for and interest in my research within scientific and lay communities alike – because this work has been conducted during a time of greatly increased attention on TBI, a lot of people are invested in finding new ways to prevent its devastating long-term complications.

1.4 Post-traumatic epilepsy

Following a TBI, patients are predisposed to developing seizure activity. These seizures can be divided into two main classes based on when they emerge: early seizures and post-traumatic epilepsy (PTE). Early seizures occur within the first week after TBI in ~10-20% of severe TBI patients [25] and are usually associated with the massive release of glutamate and increase in intracerebral pressure that occur acutely after injury. Patients with more severe TBIs are at greater risk for early seizure activity, and in turn, early seizures predispose patients for worsened outcomes and increased mortality [26]. As mentioned above, severe TBI patients are often put on seizure prophylaxis with levetiracetam or phenytoin during the first week after injury in an effort to reduce the risk

of entering status epilepticus (which can be fatal) and to limit additional damage to the brain.

Weeks, months, or even years after a TBI, patients can present with new-onset seizures related to their original brain insult; this seizure disorder is referred to as post-traumatic epilepsy (PTE). The incidence of PTE in TBI patients varies broadly across studies, ranging from <5% in mild TBI populations to 53% in a population of veterans with penetrating TBI [27]. The delayed onset of PTE can make it difficult to attribute new-onset seizures to a prior TBI, such that a portion of patients with "idiopathic" epilepsies may actually have PTE as a result of prior undiagnosed (or unreported) TBI. Patients are at increased risk of developing PTE if they sustain a severe TBI (especially one that is penetrating), if they require surgical intervention to evacuate an intracranial hematoma, or if they are elderly. The presence of early seizures also correlates with increased risk of developing PTE, although it is unclear whether this is due to common pathophysiology between early and delayed-onset seizures, or whether the early seizures independently contribute to epileptogenesis.

Following one post-traumatic seizure, patients are very likely to have additional seizure activity (86% will have seizure recurrence within two years [28]). Thus, once diagnosed with PTE, most patients are maintained on long-term anticonvulsant therapy to reduce seizure frequency and its associated risks (accidents secondary to loss-of-consciousness, kindling, status epilepticus, etc). However, anticonvulsants cause a broad range of adverse effects, ranging from drowsiness to electrolyte imbalances to the fatal condition toxic epidermal necrolysis [29]. Additionally, as in other etiologies of epilepsy, a large portion of PTE patients are refractory to the currently available

anticonvulsant therapies and have uncontrolled seizure activity, further reducing quality-of-life and resulting in increased morbidity and mortality.

There are currently no therapeutic options available to prevent the development of epilepsy following TBI. As with other post-TBI complications, the pathophysiology underlying the development of PTE is not well-understood. However, the latent period between the TBI and the onset of seizure activity provides a valuable therapeutic opportunity to intervene and prevent epileptogenesis.

1.4.1 Does prophylaxis with anticonvulsant therapy prevent the development of PTE?

There have been several clinical studies to examine whether anticonvulsant therapy before seizure onset can prevent the development of PTE. Specifically, physicians treated TBI patients at increased risk of PTE (such as those with severe, penetrating injuries, or those who experienced early seizures) with various anticonvulsants to determine whether this intervention effectively reduced the risk of later epilepsy. A recent Cochrane systematic review performed a meta-analysis on all of the clinical trials which have examined anticonvulsant or neuroprotective interventions to prevent post-traumatic epilepsy [30]. There have been ten clinical trials to date, including 2326 patients. Thompson and colleagues found that treatment with anticonvulsants following TBI did not reduce the risk for “late seizures” (with onset > 1 week following TBI) and did not reduce mortality across a 3-24 month follow-up. The Cochrane review also examined one trial with a possible neuroprotective agent (magnesium), which found no evidence of improved outcomes [31].

The negative results of these clinical trials predicate the need for novel therapeutic approaches that are based on an understanding of the pathophysiology of post-traumatic neurologic dysfunction.

1.4.2 Using preclinical models to identify and assess potential therapeutic targets

In order to delineate the pathophysiology of the long-term complications of TBI, several animal models have been developed [32]. Each of these models can be modified to produce injuries of different severities, depending on the type of research questions being explored. Overall, animal models allow experimenters to produce a TBI in a way that is controlled and reproducible across experimental subjects. While some aspects of brain injury, such as hypoxia or ischemia, can be modeled in cell culture conditions, studying network pathology after TBI requires an intact brain. (However, there have been efforts to model other aspects of brain trauma in cultured cells, such as in the *in vitro* traumatic axonal injury model [33].)

The most commonly used models of TBI in small animals are controlled cortical impact (CCI) and fluid percussion injury (FPI). Both CCI and FPI generate a primarily focal injury, although the CCI is a blunt force with a piston directly to the brain surface, while the FPI is produced by a fluid wave impacting the brain. By changing the location and type of force applied to the brain, these models can produce quite different pathologic responses. Another way to model TBI is with "weight drop," which as the name suggests, involves dropping a weight from a designated height to produce an injury. There are several different versions of this approach, including dropping the weight directly onto the brain through a craniectomy, or in contrast, dropping the weight onto an intact skull to more closely resemble human concussion (this is often referred to

separately as the closed head injury (CHI) model). Recently, models of penetrating and blast injuries have been developed, although they are less well-characterized and seem to be less consistent across subjects. Finally, there are modified approaches (of both CCI [34] and CHI [35]) that been developed in swine in an effort to better mimic the complex linear, rotational, and shear forces that occur in human TBI. A key advantage to modeling TBI in pigs is that their brain is gyrated and thus, may physically respond to external forces more similarly to the human brain than the lissencephalic rodent brain. The neuron-to-glia ratio and relative myelin content in the pig brain also resembles that of humans. Thus, TBI models in swine may more closely resemble human pathophysiology, although the high expense and limited accessibility to pigs as research subjects make this model unlikely to be broadly adopted by preclinical TBI researchers.

The pathophysiologic similarities across multiple TBI models can provide valuable insight into disease mechanisms that may be consistent across the heterogeneous TBI patient population. For example, loss and/or dysfunction of inhibitory interneurons has been shown across the CCI [36], FPI [37], and weight drop [38] models and is also found in human postmortem tissue following TBI [39]. Thus, these common pathologies shed light on which avenues of therapeutic exploration could be effectively translated to humans.

1.5 Developing this thesis work: targeting metabolism as a therapeutic approach

A prior study from our lab investigated the effects of controlled cortical impact (CCI) on cortical function, including changes in stimulus-evoked field potentials, excitatory neurotransmitter levels, inhibitory interneuron density, and synaptic activity

[36]. Our lab utilizes the CCI model because it allows us to precisely control the severity and location of the TBI across experimental subjects. Further, CCI is well-characterized and results in spontaneous seizure activity [40, 41] at similar rates (~10-30%) as severe human TBI. Cantu and colleagues from our lab found robust epileptiform activity that was elicited in stimulus-evoked field excitatory postsynaptic potentials (fEPSPs) in the cortex as early as 2 weeks post-CCI. Using a FRET-based glutamate biosensor [42] in acute cortical slices, the authors observed an increased concentration of glutamate present in the deep cortical layers near the CCI lesion. Additionally, the authors examined synaptic activity onto Layer V pyramidal neurons 2-4 weeks after CCI and found an increased frequency of spontaneous excitatory postsynaptic currents (sEPSCs) and a decreased frequency of spontaneous inhibitory postsynaptic currents (sIPSCs). Finally, Cantu utilized immunohistochemistry to examine the density of different types of interneurons in the perilesional cortex and found a decreased density of parvalbumin-expressing and somatostatin-expressing cells near the edge of the CCI cavitation. Overall, this work identified several key changes in both excitatory and inhibitory cortical activity that occur following a moderate-to-severe intensity CCI and that may contribute to cortical hyperexcitability and epileptogenesis.

Our next step was to develop a model of how cellular and network dysfunction emerges following CCI. We decided to focus on metabolic changes for two key reasons – (1) the ketogenic diet (KD) was already well-established as an effective metabolic approach to control seizure activity, and small-molecule mimics of KD were beginning to be explored for their use as anticonvulsants, and (2) dynamic changes in glucose utilization after TBI had been identified as a possible secondary injury mechanism in

both humans and animal models. We hypothesized that acute activity-dependent increases in glycolysis after TBI contributed to aberrant excitation of interneurons, resulting in interneuron loss or dysfunction, and ultimately leaving the cortical network prone to hyperexcitability (Figure 1.1). Further, we hypothesized that intervening with glycolytic inhibitor 2-deoxyglucose (2-DG) would reduce hyper-glycolysis after TBI and could attenuate downstream cortical pathology. Using similar approaches to those in our lab's prior publication by Cantu and colleagues, we sought to assess whether *in vivo* 2-DG treatment attenuated the electrophysiological and immunohistochemical changes that had been reported. This thesis will present the results of these studies.

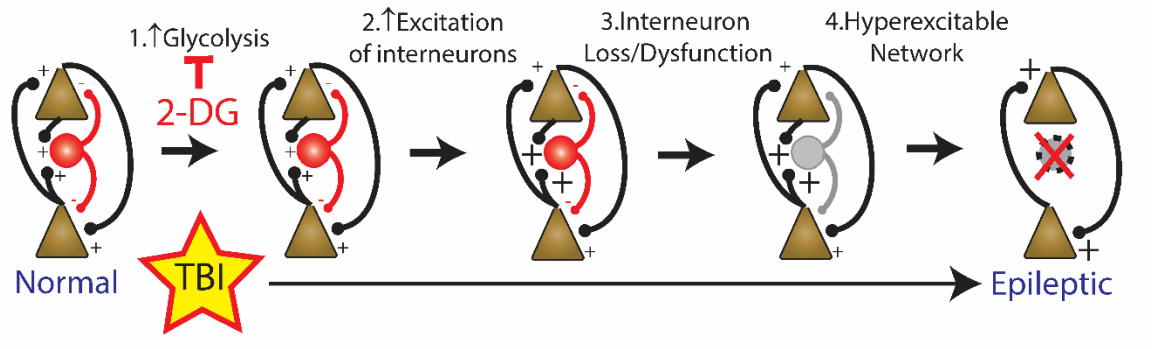

Figure 1.1 Schematic of our model for epileptogenesis after TBI. Brown triangles = excitatory pyramidal neurons; red circles = inhibitory interneurons.

1.5.1 An aside: the structure of this thesis

In this first chapter, I have presented a basic background of TBI, have introduced the complexity of the clinical manifestations and complications of the disease, and have given the readers a brief summary of the central hypotheses that drove my thesis work. In the next two chapters, I will present two manuscripts that I have produced with the guidance of my mentor, Dr. Chris Dulla, and with the technical assistance and intellectual

support of several co-authors (see footnote 2 at the beginning of Chapter 3 for full list). The first manuscript (Chapter 2) is a comprehensive review of the preclinical and clinical literature of glucose utilization in TBI and seizures, which poses acute hyper-glycolysis as a rational therapeutic target to reduce post-TBI hyperexcitability and PTE [15]. The second manuscript (Chapter 3) presents the data accumulated throughout my experimentation of 2-DG as a potential disease-modifying agent following CCI in mice. In Chapter 3, the reader will find my key results, as well as a brief discussion of the results and a description of the materials and methods I used throughout the work. Chapter 4 contains a more general discussion of the broader implications of my thesis work, including a section on the translational potential of our therapeutic approach and an exploration of future studies that will further advance our understanding of how metabolism can be harnessed to manipulate network activity in neurological disorders. Finally, the Appendix (Chapter 5) contains additional data collected during my time in the Dulla lab, further examining the effects of 2-DG after CCI. Overall, I hope this thesis work orients the reader to the potential therapeutic opportunity of targeting aberrant glucose utilization to prevent post-TBI complications.

Chapter 2 : Dysregulated Glucose Metabolism as a Therapeutic Target to Reduce Post-traumatic Epilepsy[1]

[1] Koenig, JB; Dulla, CG. 2018. *Frontiers in Cellular Neuroscience.* 12: 350.
Reprinted here with permission of publisher.

While accounting for only 2% of the body's weight, the human brain accounts for 20% of its energy utilization [43]. In pathological states, such as following a brain injury or during a seizure, the brain's energy usage is significantly disrupted. In this review, we explore brain metabolism and glucose utilization as therapeutic targets to prevent the pathophysiological changes that may cause epileptogenesis following brain injury.

The brain requires energy in the form of ATP to power its cellular processes. The ability of the brain to conduct electrical signals between cells requires a steep electrochemical gradient to be maintained across cellular membranes. Reestablishing the electrochemical gradient following synaptic activity accounts for ≈80% of the total brain energy costs [44], with action potential (AP) firing contributing to a smaller, but important, component of energy utilization. Active transport of neurotransmitter into presynaptic vesicles, as well as vesicle recycling [45], also requires ATP. Thus, the brain has many energetically-intensive tasks in addition to basic cellular functions.

The obligatory fuel of the brain is glucose, which is transported across the blood-brain-barrier by GLUT1 transporters (see Figure 2.1). The systemic delivery of multiple kinds of fuel (glucose, fructose, glycolytic end-products lactate and pyruvate, and ketone body β-hydroxybutyrate) results in an increase in extracellular glucose in the brain [46], suggesting that it is the preferred fuel. Only in extreme cases, such as during starvation or in the condition of the anticonvulsant ketogenic diet (discussed below), does the brain switch to utilizing a different energy source (ketone bodies) to generate ATP. In addition to glucose, the brain also requires oxygen. Both glucose and oxygen are delivered to the brain parenchyma through the vasculature, a process which is dynamically regulated by regionally- and temporally-specific changes in vasoconstriction and vasodilation. Thus,

there is coupling between brain function and local vascular supply (first proposed by Roy and Sherrington in 1890), such that ultimately, energy delivery and utilization are activity-dependent processes.

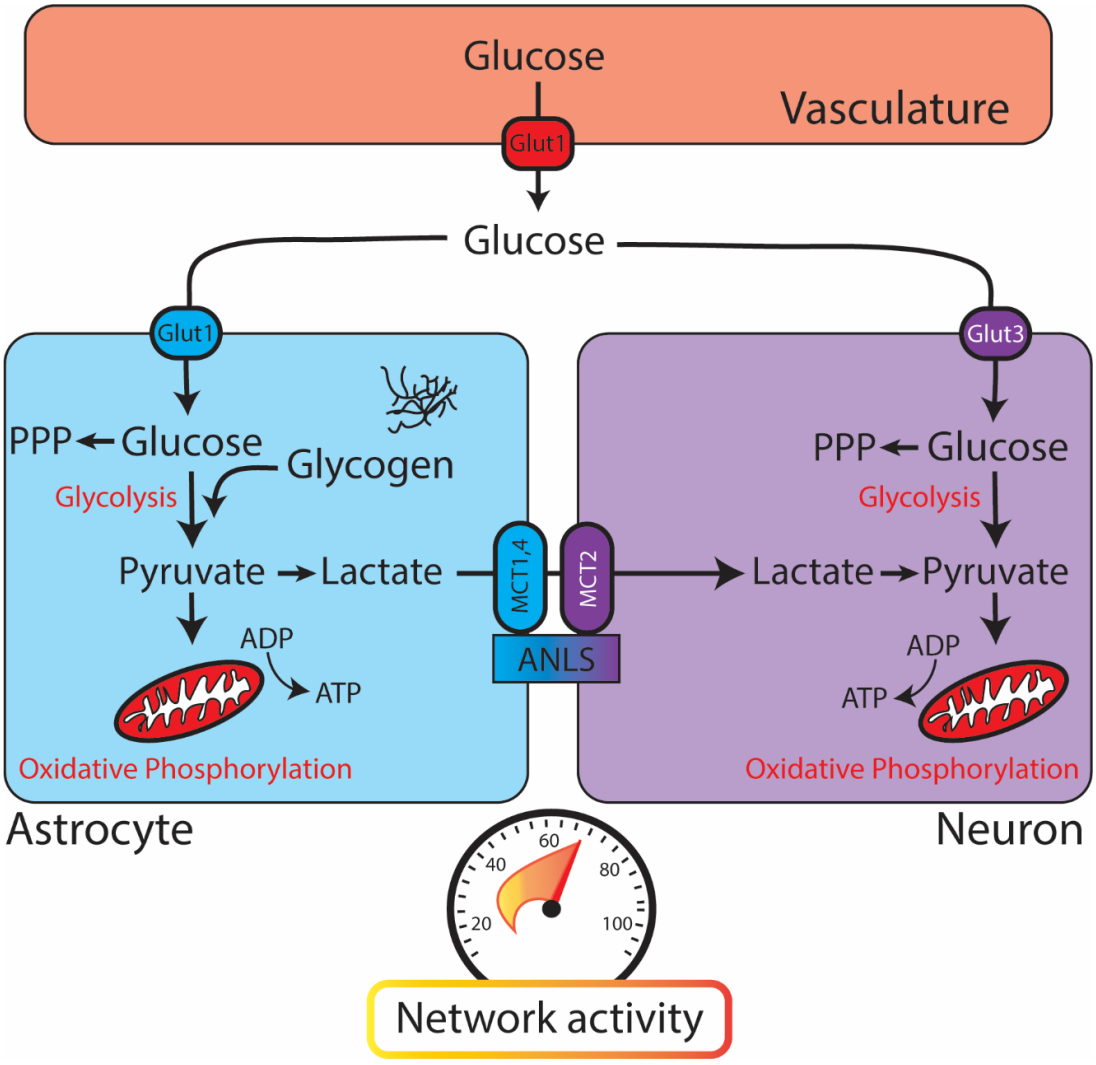

Figure 2.1: Glucose utilization in the brain relies on neuronal and astrocytic pathways. When glucose leaves the vasculature (red, top) it enters the brain parenchyma and is transported into astrocytes (blue) or neurons (purple). Both astrocytes and neurons contain glycolytic enzymes. The astrocyte-neuron lactate shuttle (ANLS) hypothesis posits that glycolysis is performed mainly in astrocytes, with lactate being delivered to neurons through monocarboxylate transporters (MCTs) for conversion to pyruvate and further metabolism through oxidative phosphorylation. PPP = pentose phosphate pathway. Bottom. Speedometer represents the activity-dependent nature of brain metabolism. As network activity increases, glucose metabolism and energy consumption also increase.

Once a glucose molecule leaves the vasculature and enters the brain parenchyma, it is transported into cells for metabolism (through GLUT3 in neurons or GLUT1 in astrocytes). Canonically, glycolysis converts glucose to pyruvate, which is then converted to acetyl-CoA to enter the citric acid (TCA) cycle and provide substrates for oxidative phosphorylation (Figure 2.2). While oxidative phosphorylation ultimately generates the majority of the ATP in aerobic respiration, it also requires oxygen and is much slower than the glycolytic production of ATP. Thus, these two processes might fuel different aspects of brain function. As an alternative to glycolysis, glucose can be shuttled into the pentose phosphate pathway, which generates reduced NADPH and supports the production of glutathione. Glutathione provides an important defense mechanism against oxidative stress, as it serves as an electron donor in the detoxification of reactive oxygen species.

Different cell types in the brain utilize fuel differently. Neurons utilize 80-90% of the ATP of the brain, even though they account for ≈50% of the cells [47]. A traditional view of brain glucose utilization poses astrocytes as a key metabolic support cell. In the "astrocyte-neuron lactate shuttle" (ANLS) model, glycolysis is performed in astrocytes and its product pyruvate is converted to lactate by lactate dehydrogenase (Figure 2.1). Lactate is then shuttled to neurons through monocarboxylate transporters (MCTs), converted back to pyruvate, and further metabolized through oxidative phosphorylation [48]. This model is similar to energy utilization in other body tissues, where glycolysis and the TCA cycle are uncoupled at the level of lactate [49]. While strong evidence supports the ANLS, there is robust evidence that glycolysis also occurs in neurons.

Examination of transcriptional expression and proteomics data reveals the presence of components of the glycolytic pathway in both astrocytes and neurons [50].

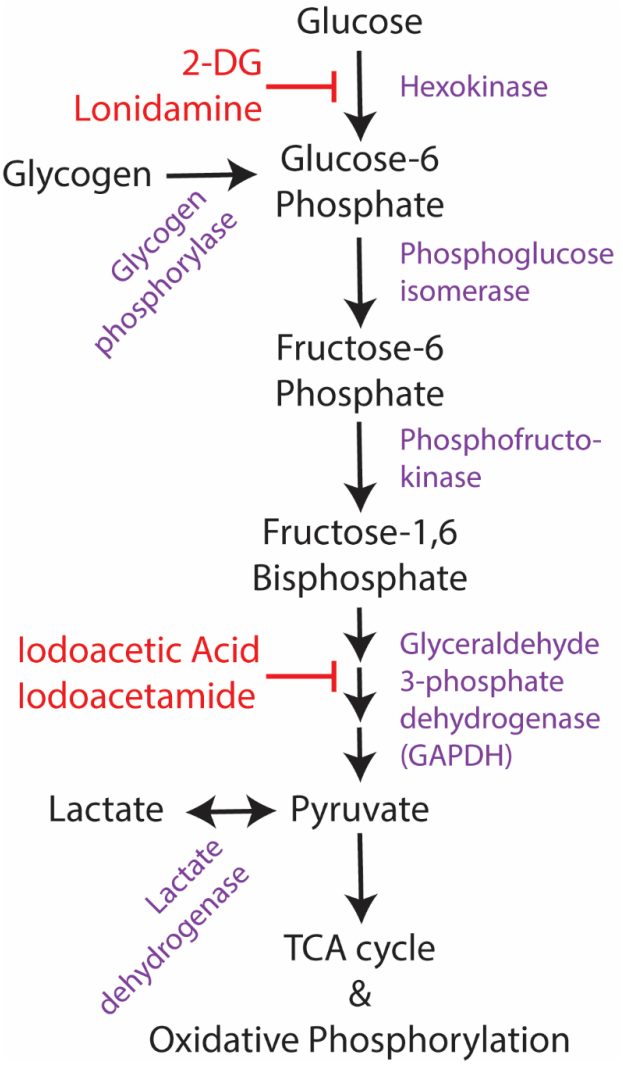

Figure 2.2: Overview of glucose utilization. Simplified schematic of glucose utilization, focusing on the steps of the glycolytic pathway. Enzymes shown in purple and pharmacological inhibitors in red. 2-DG = 2-deoxyglucose.

One of the challenges to understanding brain metabolism is effectively visualizing and integrating the movement of metabolites at the regional, cellular, and subcellular level. To understand large-scale changes, we can utilize whole brain imaging with

functional MRI (fMRI) or positron emission tomography (PET) scanning. fMRI relies on the signal of oxy- versus deoxy-hemoglobin, where changes in the "BOLD" signal can occur with blood flow or metabolic flux. PET scanning, on the other hand, utilizes tracers to label blood, glucose, or oxygen. For example, using 18F-labeled 2-deoxyglucose (F-DG), one can visualize the accumulation of "glucose" in areas of the brain which require more fuel, and are thus transporting more glucose and F-DG into the brain parenchyma. We can also look at metabolic flux in brain slices from animal models or in culture, using metabolomic or molecular imaging of pH, NADH [51, 52], ATP, or fluorescently labeled glucose [53]. Using these micro and macro views of brain metabolism, we can begin to understand system-level metabolic activity in the healthy, injured, and epileptic brain.

A better understanding of brain fuel utilization at baseline and in pathological states may allow us to harness the therapeutic potential of metabolic targets. Our motivation for this approach is based on the robust anticonvulsant and neuroprotective effects of the ketogenic diet in humans [54], where very low-carbohydrate, high-fat intake causes a shift of brain fuel utilization away from glucose and toward ketone bodies. A number of exciting studies have attempted to harness the power of the ketogenic diet either by providing ketones as an exogenous energy supply or by inhibiting glycolysis using pharmacological approaches. These manipulations can have far-reaching effects on brain activity and neurological outcomes, well beyond acute changes in metabolic activity. Here, we will explore glycolytic inhibition as a potential therapeutic entry point in treating traumatic brain injury (TBI) and post-traumatic epilepsy (PTE; Table 2.1).

Brain metabolism is dynamically regulated to accommodate changes in activity levels and injury states.	
SEIZURE * Metabolic activity and glucose utilization are increased acutely during a seizure. * There is evidence of a prolonged hypometabolic state following a seizure. * In patients with epilepsy, there are regions of both hyper- and hypo-metabolism, suggesting complex, regionally-specific pathophysiology.	**TRAUMATIC BRAIN INJURY** * There is an increase in fuel utilization and metabolic activity in the first week after TBI. * In the long-term after injury, there is widespread hypometabolism across multiple brain regions. * Patients are at risk of developing post-traumatic epilepsy after TBI.
Dysregulated glucose metabolism may be a valuable therapeutic target to prevent the development of epilepsy after traumatic brain injury.	

Table 2.1: Key points.

2.1 Metabolism is activity-dependent

As the energy requirements of the brain change, fuel utilization can be upregulated to accommodate these requirements. For example, fMRI studies have shown that visual tasks result in increased cerebral blood flow and increased oxidative metabolism in the visual cortex to meet the metabolic needs of the region [55]. However, there are many challenges in interpreting changes in cerebral blood flow and oxygen utilization at the level of the entire brain [56], so *in vitro* experiments can aid in elucidating the mechanisms by which activity results in metabolic changes.

2.1.1 *Activity-dependent changes in astrocytic glucose utilization*

As shown in Figure 2.1, changes in network activity can affect a broad range of metabolic processes in both astrocytes and neurons. Astrocytes are poised to detect local

changes in neuronal activity, and thus energetic need, in the brain. These cells have close interactions with synapses, and dynamically change their morphology in response to activity [57]. Astrocytes participate in glutamate uptake through transporters GLT-1 and GLAST, which themselves are upregulated by activity [58, 59]. Through this mechanism, astrocytes sense local changes in excitatory activity based on changes in glutamate concentration.

It has been previously shown that glutamate uptake requires re-establishment of the sodium gradient across the membrane (as glutamate is co-transported with sodium), which results in a decrease of ATP in astrocytes [60]. Alongside this energetic need, glutamate transport stimulates increased glucose uptake and increased lactate release from astrocytes in culture [61]. This study in particular provided key evidence for the astrocyte-neuron lactate shuttle (ANLS) hypothesis, which postulates that increases in activity result in astrocytic glycolysis and delivery of lactate to neurons as fuel. When glutamate uptake is reduced in GLT-1 or GLAST knockout mice, there is a decrease in glucose tracer uptake induced by unilateral whisker stimulation [62]. This lends further support, *in vivo*, that glutamate uptake in astrocytes plays a crucial role in glucose utilization. Additionally, astrocytes exhibit "metabolic waves" of fluorescently labeled glucose (2-NBD-glucose), where 2-NBD-glucose uptake parallels the spatial movement and kinetics of sodium transport into astrocytes [53]. The neuroenergetic coupling of stimulation to glucose movement is inhibited with glutamate transport blocker TBOA, suggesting a necessary role for glutamate transporters in the activity-dependent effects on astrocytic glucose uptake. While elevated extracellular glutamate results in increases in glucose utilization in astrocytes, the sodium co-transport through glutamate transporters

also acidifies mitochondrial pH such that oxidative phosphorylation is less effective [63]. This potential reduction in the efficiency of oxidative phosphorylation suggests a glutamate-uptake induced shift in astrocytic metabolism away from oxidative phosphorylation and toward glycolysis during periods of activity.

Other extracellular changes associated with neuronal activity also induce changes in astrocytic glycolysis. Increases in extracellular potassium concentration (such as following APs) result in increased deoxyglucose accumulation [64] and glycolytic activity in astrocytes [65]. This effect was found to be dependent on the Na^+/HCO_3^- cotransporter NBCe1 [66]. Additionally, noradrenaline (via β2- and β3-adrenoreceptors) or arachidonic acid can stimulate glucose uptake in astrocytes [67, 68].

Astrocytes are also able to mobilize energy for utilization through glycogenolysis, where astrocytic glycogen stores are catabolized into single glucose units. Extracellular potassium has been shown to induce glycogenolysis in mouse cortical slices in a calcium-dependent manner [69]. The breakdown of astrocytic glycogen stores can also be induced by adenosine, ATP, arachidonic acid, vasoactive intestinal peptide, and noradrenaline [70, 71].

2.1.2 Activity-dependent changes in neuronal glucose utilization

While astrocytes provide metabolic support to neurons through the astrocyte-neuron lactate shuttle, neurons are also able to upregulate their own metabolic processes in response to activity. The ANLS model suggests that glycolysis occurs mainly in astrocytes, but there is significant evidence supporting that glycolysis takes place in neurons as well (reviewed in [72]). First, neurons have enriched expression of three isoforms of the rate-limiting enzyme of glycolysis (hexokinase) relative to astrocytes

[73]. In addition, hexokinase-1 protein levels positively correlate with glucose uptake in neurons, suggesting that the cells with more hexokinase are more readily able to metabolize glucose through the glycolytic pathway. Finally, this study showed that functional activation with whisker stimulation increased *in vivo* glucose uptake in neurons, but not astrocytes, suggesting that neuronal glucose utilization is dynamic with activity state. Additionally, data mining of previously published transcriptomic and proteomic results show increased protein levels for many of the enzymes required for glycolysis in neurons relative to astrocytes [50]. Thus, neurons have the machinery required to utilize glucose through the glycolytic pathway.

As in astrocytic metabolism, activity also drives changes in neuronal metabolism. Synaptic activity requires ATP, however in normal conditions, ATP levels stay constant in neurons following activity [45]. Blocking either the glycolytic pathway or oxidative phosphorylation results in a precipitous drop in ATP levels following synaptic activity in neuronal culture [45]. Taken together, these findings suggest that activity drives neuronal ATP production in order to maintain consistent ATP levels within the cell sufficient to meet the significant energy demands of the synaptic vesicle cycle.

The first step in upregulating fuel utilization in response to activity is to increase glucose delivery to the neurons. Synaptic transmission in cortical neuronal cultures has been shown to increase surface expression of GLUT3, a key glucose transporter in neurons, in an NMDA receptor-dependent manner [74]. An additional glucose transporter, GLUT4, is also mobilized to the presynaptic surface as a result of synaptic firing [75]. Neurons with mutated GLUT4, which is defective in glucose transport, are

unable to maintain synaptic vesicle recycling with activity [75], suggesting a key role for fuel delivery to perform the energetically-demanding processes at the synapse.

In the ANLS model, lactate would be delivered to neurons from astrocytes, instead of neurons taking up glucose directly. However, it has been shown that glucose uptake (not lactate utilization) is positively correlated with NMDA receptor-mediated activity in neurons [76]. This finding was reproduced in hippocampal slices and *in vivo*, where activity caused an increase in glycolytic activity in neurons (measured by an increase in the cytosolic NADH:NAD^+ ratio, which was not affected by blocking lactate delivery to neurons through MCTs; [77]).

While some studies have suggested that neurons rely on oxidative metabolism [64, 78, 79], glycolysis may provide faster replenishment of ATP in cases of high activity or energy stress. For example, recent work described the formation of a "glycolytic metabolon" at presynaptic sites, where glycolytic enzymes are locally concentrated to accommodate for energy demands at active synapses [80]. This clustering allows for rapid, spatially-controlled delivery of ATP to the synapses with increased energy need to fuel activity. Additionally, AP bursting in primary hippocampal culture results in a shift of the neuronal transcriptional profile away from oxidative phosphorylation and toward the glycolytic pathway [81]. Thus, it seems that neurons may rely more heavily on oxidative phosphorylation at baseline, whereas a shift toward glycolysis during periods of high activity would allow rapid replenishment of energy to support synaptic function (resembling the distinction between "fast-twitch" muscle fibers which rely on glycolysis versus "slow-twitch" muscle fibers which utilize oxidative phosphorylation).

2.1.3 Changes in metabolism feed back to affect neuronal activity

Altering neuronal metabolism can have direct effects on neuronal excitability and activity. Glycolytic inhibition with the pharmacologic inhibitor iodoacetic acid alters the shape of the neuronal action potential, resulting in a smaller and broader presynaptic AP waveform [82]. Altering the availability of glucose can also have effects on broader network activity, such as reducing the power of gamma oscillations in hippocampal slices [83]. These effects may be mediated through molecules which can sense local energy state and affect neuronal excitability. For example, K_{ATP} channels conduct potassium in response to decreased ATP concentration, and can thus directly modulate neuronal activity by altering membrane resistance [84-86]. Another example of metabolism feeding back to neuronal excitability is through adenosine receptors. Adenosine release, which can occur via equilibrative transporters when ATP consumption is high and ATP production is low, decreases excitatory synaptic transmission during hypoxia via A_1 receptors, [87]. Conversely, adenosine can increase the intrinsic excitability of pyramidal neurons via A_{2A} receptors, [88]. Understanding how metabolic manipulations can impact neuronal activity will provide novel tools for us to control network output in cases of pathological activation, such as following a brain injury or during a seizure.

2.2 Glucose utilization during seizures

At the most basic level, metabolic activity increases acutely during a seizure or convulsion [89], with increased rates of both glucose and oxygen consumption [90]. Human imaging studies also show that glucose utilization is elevated in the hippocampus of patients with temporal lobe epilepsy during seizure activity [91]. This is thought to

represent a response to the increased energy demands associated with restoring ionic gradients, replenishing neurotransmitter vesicles, and compensating for cellular stress after ictal activity. However, the dynamic response of glucose utilization associated with seizure activity is much more complicated than this simplistic coupling.

2.2.1 Clinical perspective

Altered glucose utilization occurs in patients with epilepsy, with both hypo- and hyper-metabolism commonly seen. A recent retrospective study of over 500 PET scans of patients with intractable epilepsy found that approximately 6% showed significant hypermetabolism [92]. Similar increases in glucose utilization have been seen in various forms of epilepsy, including focal cortical dysplasia [93], Sturge-Weber Syndrome [94], and continuous spikes and waves during sleep [95]. The low incidence of hypermetabolism may reflect that the vast majority of human studies examine the interictal period, when seizure activity is not occurring. Hypometabolism is much more frequently reported in patients with epilepsy. Decreased FDG labeling in the temporal lobe is, in fact, a strong predictor of seizure control following resection of the temporal pole for intractable seizures [96]. While the mechanistic underpinning of hypometabolism is not known, many suspect that the loss of neurons associated with hippocampal sclerosis results in decreased energy demand. While this may be true, other studies suggest that hypometabolism may be prevalent in areas where sclerosis is minimal, such as hippocampal area CA3 [97]. Because of the variety of metabolic changes observed in patients with epilepsy, there have been some controversies regarding the value of metabolic imaging data.

The literature reporting seemingly incongruent results may reflect biological diversity, as studies using imaging technologies with higher spatial resolution suggest regionally heterogeneous metabolic activity in individual patients suffering from epilepsy. Recent work using FDG-PET combined with electrocorticography in patients before surgery for intractable epilepsy reports extremely complex changes. Areas of both hypo- and hyper-metabolism were seen, and these areas had variable spatial overlap with sites of seizure initiation [98]. This supports a complex spatiotemporal relationship between metabolism and seizure activity that can vary between patients, between brain regions in the same patient, and perhaps even between individual seizures in the same patient. Importantly, FDG-PET does not report on glycolytic activity directly, but rather indicates glucose uptake. Therefore, combining FDG-PET with other measures can help increase our understanding of glucose utilization.

Another set of commonly used, clinically available tools assay brain metabolic activity by measuring blood flow and blood oxygenation. In generalized spike-wave epilepsy, cerebral blood flow has been shown to increase prior to ictal activity and then decrease following the seizure [99]. Intraoperative monitoring of hemoglobin oxygenation in temporal lobe epilepsy suggests decreased cerebral perfusion prior to ictal activity, followed by a significant increase after the seizure ends [100]. BOLD signal derived from fMRI, which also monitors hemoglobin oxygenation status, suggests that metabolic changes precede seizure activity, with the pattern of activity with respect to the seizure focus varying widely from patient to patient [101]. When these measures of cerebral blood flow and oxygenation are combined with the FDG-PET findings discussed earlier, a picture begins to emerge regarding glucose utilization and the epileptic brain.

During ictal activity, glucose utilization is acutely increased. Interictally, metabolic activity can be regionally increased or decreased, and likely reflects complex pathophysiology including cell loss, altered neuronal activity, and inflammation [102], all of which lead to regionally-specific changes in metabolic activity. Because of the limitations of interrogating the human brain, preclinical studies have also been utilized to better understand the metabolic changes associated with seizure activity.

2.2.2 Preclinical perspective

Many of the clinical findings discussed above have been replicated in animal models. Glucose utilization is increased during experimental status epilepticus (SE) [103, 104] induced by bicuculline [105], pilocarpine, and kainic acid [106]. Multiple studies also show subsequent hypometabolism, as measured with PDG-PET, beginning approximately 1-2 days after chemoconvulsant-induced status epilepticus and lasting as long as 42 days [107, 108]. In fact, Jupp and colleagues showed that following kainic acid-induced status epilepticus, metabolic activity was decreased at one day post-SE, recovered slightly, and then decreased again during the chronic phase of epilepsy when spontaneous recurrent seizures appear [108]. This suggests that glucose consumption may fluctuate throughout the different phases of the epileptogenic process. Acute seizures lead to aberrant consumption of glucose to support cellular homeostasis. Quickly afterwards, glucose utilization is decreased during the post-ictal phase. Later, cellular- and network-level changes which contribute to the epileptogenic process result in varied metabolic needs. The dynamic nature of glucose utilization described here suggests that therapies targeting metabolism may have discrete windows of efficacy, paralleling the complex changes of metabolism observed in patients with epilepsy.

As with clinical studies, however, many of these assays monitor glucose uptake as a measure of metabolic activity. In the brain, glucose utilization is intimately linked with astrocytic metabolism, where astrocytes can mobilize glucose from glycogen stores or perform glycolysis to provide lactate to neurons for further metabolism. In a rat model of sustained seizures, glycogen concentrations were diminished after 20 minutes and 2 hours of status epilepticus. Interestingly, lactate levels were elevated after 20 minutes of SE, but were decreased after 2 hours of SE [109]. This suggests that seizure activity first results in glycogen store utilization to provide fuel in the form of lactate, but that the glycogen reserves are not sufficient to provide continuous fuel during a long period of SE. In a neonatal flurothyl seizure model, seizures induced an acute decrease in brain glucose levels (as measured by labeled carbon tracing) and a significant increase in lactate levels, although glycogen levels were stable [110]. This suggests that while glucose utilization during a seizure may be a global phenomenon, the source of glucose and how it is utilized may vary with age and experimental model [111]. Further complicating the picture, glucose may be directed to different metabolic processes depending on the oxygenation level. Glucose can provide energy via glycolysis under hypoxic or normoxic conditions, but once converted to pyruvate, further metabolism through oxidative phosphorylation requires oxygen, and thus requires normoxic conditions. In a canine model of epilepsy, MR spectroscopy was used to analyze brain metabolism postictally. Glycolytic end products appeared to increase gradually during seizures due to evolving anaerobic conditions during the ictal activity [112]. The relationship between oxygenation state and glycolytic activity, therefore, may contribute to the varying reports of glucose utilization in the epileptic brain. For example, if oxygen levels are low,

glycolysis may be relied upon more heavily than oxidative phosphorylation. However, because glycolysis produces fewer ATP molecules than oxidative phosphorylation per glucose molecule, this may explain the increased need for glucose uptake.

Preclinical models have also demonstrated that different types of seizures can lead to different metabolic changes. Using combined NADH and FAD^+ imaging alongside recording of oxygen levels, Ivanov and colleagues demonstrated unique metabolic changes in two *in vitro* models of seizure-like activity. In a zero-magnesium model, oxidative phosphorylation increased strongly during ictal activity and then decreased abruptly before the ictal activity ceased. Using a bicuculline model, oxidative phosphorylation increased in brief transients and then decreased during ictal activity [113]. This study also suggests that glycolysis precedes epileptiform activity, as NADH production occurs without oxygen utilization. In various *in vivo* models, we also observe different seizure subtypes utilizing different energy supplies. In a mouse model of flurothyl-induced seizures, labeled glucose was used to track cerebral metabolic flux. Surprisingly, labeled glucose was not converted into labeled lactate, even though total lactate levels rose. This suggests that during a seizure, lactate does not arise directly from glucose, but rather from utilization of glycogen stores. In this study, McDonald and Borges also reported a significant inhibition of pyruvate dehydrogenase (PDH), the enzyme which converts pyruvate into acetyl-CoA for entry into the TCA cycle [110]. This suggests that selective suppression of glucose-derived substrates from entering into oxidative phosphorylation occurs in this model of acute seizures, perhaps as a mechanism to reduce oxidative stress. Conversely, in a study examining how kainic acid-induced seizures affect cerebral glucose utilization [114], the authors reported that both a sub-

convulsive and convulsive dose of kainic acid led to an immediate increase in lactate levels. Interestingly, when a sub-convulsive dose was examined, astrocytic TCA cycle activity was increased but neuronal activity remained stable. When a convulsive dose was given, both neuronal and astrocytic metabolism were affected. This supports the idea that neuronal metabolic activity is preferentially enriched in states of energy crisis, whereas astrocytic metabolism is able to compensate in baseline or less-demanding activity states.

Throughout the examples described above, it is apparent that the metabolic changes associated with seizure activity are diverse, complicated, and variable depending on seizure type, regional focus, and individual patient. Therefore, in developing a metabolic therapy, it will be important to stratify patients based on the pathophysiologic processes contributing to their epilepsy. We will now turn our attention to the metabolic changes associated with traumatic brain injury (TBI), as patients who suffer from TBI are at increased risk of epileptogenesis. Because of the latent period between the injury and onset of seizures, this patient population represents a unique opportunity to develop a metabolic therapy targeted to the epileptogenic process.

2.3 Glucose metabolism is dysregulated following traumatic brain injury

Traumatic brain injury (TBI) occurs when a mechanical force acts on the brain and disrupts normal function. TBI encompasses a diverse range of injury types, severities, and patient demographics, and results in ≈ 2.8 million emergency room visits per year in the United States. Importantly, TBI can result in long-term neurological complications which affect patient quality-of-life, including neurodegeneration, behavioral dysfunction, and epilepsy. However, the heterogeneity of TBI in humans has

made it difficult to fully understand the pathophysiology of these long-term neurological disorders. As we have already discussed how metabolism is disrupted with changes in activity state and in hyperexcitable/seizure-prone neuronal networks, changes in glucose utilization may provide a clue as to how complications emerge following injury (Figure 2.3).

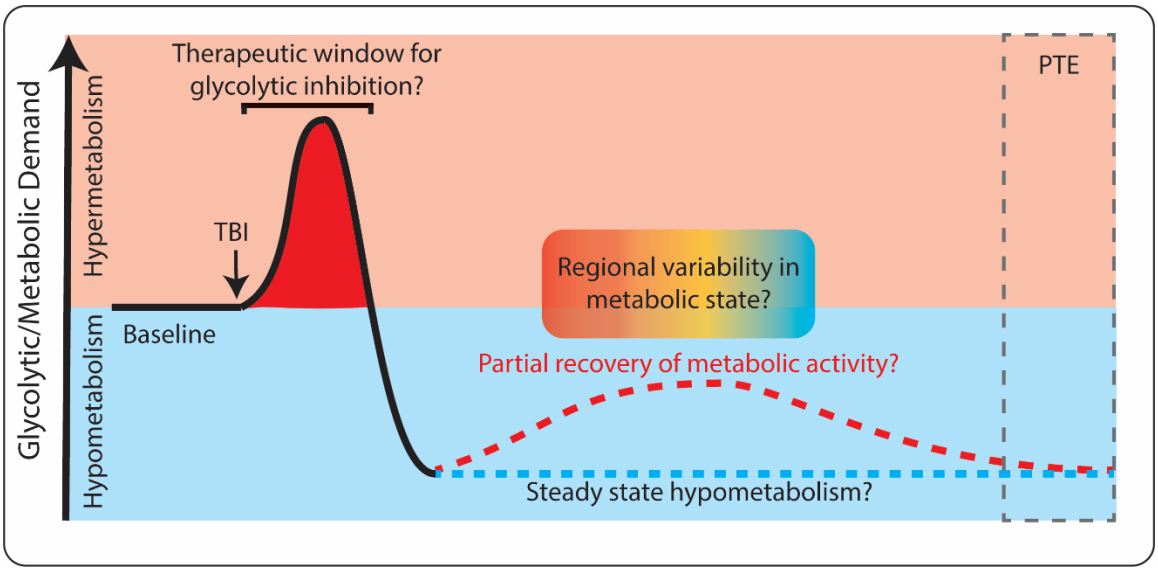

Figure 2.3 Dynamic glucose utilization following TBI. Both hyper-metabolism (red) and hypo-metabolism (blue) occur following TBI. Initially, glucose utilization increases, which may be a target for therapeutic intervention. Later, hypometabolism occurs and long-term complications such as post-traumatic epilepsy (PTE) can develop. Both consistent hypometabolism (blue dashed line) and partial recovery of hypometabolism (red dashed line) have been reported following TBI. There may also be spatially-specific changes in metabolism within individual patients (red/blue gradient).

The acceleration/deceleration and shearing forces associated with TBI disrupt cellular membranes and result in massive neurotransmitter release, blood-brain-barrier compromise [115], and loss of the electrochemical gradients required for neuronal signaling (reviewed in [116, 117]). Thus, during the acute period after injury, there is a significant change in energetic needs for the regions affected. Unfortunately, our

knowledge of how these molecular and cellular insults translate into changes in energy utilization is limited. Here, we review the multiple clinical and preclinical studies performed to gain a better understanding of how glucose utilization changes to compensate for this pathology.

2.3.1 Clinical perspective

Brain imaging in humans following TBI, including PET scanning and magnetic resonance spectroscopy [118], can reveal changes in glucose uptake/utilization. A study in 1997 examined 28 patients who suffered from a severe TBI, and found evidence of increased cerebral glucose utilization in the majority of patients within the first week following injury [119]. This study also revealed that some patients had increased glucose uptake in focal regions (particularly when associated with a focal mass lesion TBI), while others had increased uptake globally throughout the cortex. Later work revealed that global increases in glucose utilization are more common in severely injured TBI patients, relative to mild TBI patients [120]. When specifically examining the white matter after moderate to severe TBI, patients exhibited a decrease in oxygen utilization without a decrease in glucose utilization [121], suggesting a possible uncoupling of aerobic and anaerobic fuel utilization, as well as providing evidence for metabolic disruption in the setting of diffuse subcortical white matter injury. Patients with lower extracellular glucose and higher extracellular glutamate levels within the first week following injury, findings possibly associated with early hyperglycolysis and indicative of dysregulated glucose utilization, had worsened outcomes at 6 months post-injury [122]. This finding suggests a crucial role for metabolic and activity state changes in long-term patient outcomes. Importantly, acute metabolic changes may not be uniform across patients as

some studies have observed decreased glucose utilization in gray matter acutely following injury [123]. This underscores the importance of developing approaches to rapidly and quantitatively assay brain metabolic function so that patients with different injury types, severities, and timelines may be compared appropriately.

Following the initial stage of focal or global hypermetabolism, there is significant evidence of long-term hypometabolism across multiple brain regions in the months to years following TBI. As early as several days following injury, there is a decrease in cerebral blood flow and oxygen utilization in the peri-lesional area [124] . However, even when studied >1 year following diffuse axonal injury, there is decreased cerebral oxygen utilization in 60% of patients [125]. In fact, cerebral hypometabolism may be a prognostic indicator of long-term outcomes following TBI, as it is for outcomes following surgical resection in temporal lobe epilepsy [126]. There is a reported relationship between the degree of hypometabolism and the level of patient consciousness after TBI, where patients in a vegetative state had more widespread, reduced metabolic flux relative to patients with higher levels of function [127]. In fact, even within the acute period (first 5 days post-TBI), decreased glucose utilization in specific brain regions (thalamus, brainstem, and cerebellum) also correlated with patients' levels of consciousness [128]. Additionally, cerebral metabolism following TBI positively correlates with full-scale IQ scores [129], suggesting that decreased cerebral fuel utilization is associated with worsened cognitive and behavioral outcomes.

It is important to clarify that the findings of altered glucose uptake or oxygen utilization on imaging are not easily interpretable as changes in glycolysis/glucose utilization. Studies using microdialysis of metabolites, or tracking 13C-labeled carbon

from glucose through to its products [130], can help us better understand how glucose metabolism is altered following injury. When 13C was followed, Dusick and co-authors found a preferential increase in glucose flux into the pentose phosphate pathway, particularly in the first 48 hours after injury [131]. This finding argues against the traditional assumption that increased glucose uptake on PET scans indicates cerebral hyperglycolysis, although Jalloh and colleagues found increases in both glycolytic lactate production and flux through the pentose phosphate pathway after TBI [132]. Examination of lactate (product of anaerobic glycolysis) and pyruvate (product of aerobic glycolysis to be utilized in the TCA cycle) from intrasurgical microdialysis showed increases in both of these products with increased glucose uptake on PET scan [133]. No change in the lactate:pyruvate ratio in this study suggested that glucose utilization by both aerobic and anaerobic glycolysis was increased following injury. Another microdialysis study in conjunction with intracortical depth EEG found an increased lactate:pyruvate ratio specifically during seizures or periodic discharges after injury, suggesting transient metabolic crises during periods of altered brain activity [134] and preferential increases in anaerobic glycolysis during seizures, as described above [112].

While these human studies clearly reveal long-term dysregulation of glucose metabolism following traumatic brain injury, there are significant limitations in interpretation due to the inability to clearly track individual metabolic processes in brain tissue as well as the heterogeneity of patient injuries and timeline of study participation. The use of preclinical animal models has provided additional understanding of post-TBI pathophysiology by standardizing injury mechanism, location, and timeline [135, 136].

2.3.2 Preclinical perspective

There are multiple animal models of TBI used for preclinical experimentation, including controlled cortical impact (CCI), fluid percussion injury (FPI), and weight drop. Each of these models recapitulates aspects of human TBI, including cellular losses [36, 39], behavioral dysfunction [137-139], and post-traumatic epilepsy [140, 141], while allowing experimental control of injury type, location, and severity across subjects. Newer models of closed-head and repetitive brain injury may more closely resemble the injury mechanisms experienced by most human patients, although these have not been as extensively studied as CCI, FPI, and weight drop. Each of these preclinical models can produce different pathological outcomes, based on variables such as injury severity and location. Drawing conclusions based on data from multiple models may provide better understanding of TBI pathophysiology and more fully represent the diversity of real-world human brain injury.

Some animal models have recapitulated the early hypermetabolism and prolonged hypometabolism observed in humans. For example, after fluid percussion injury, there are local increases in glucose utilization at early time points [142], which then transition to a hypometabolic period that resolves to baseline by several days following injury [143]. Studies in juvenile rats follow this pattern [144, 145], but suggest that the metabolically depressed period may resolve faster in young animals or that the injury-induced energy crisis may be delayed in young relative to adult animals [146]. This phenomenon could begin to explain the resilience and relative neuroprotection of juveniles to TBI. As late as 3 months following mild TBI (weight drop) in rats, there are observable regionally-specific changes in glucose uptake [147]. As observed in humans,

long-term hypometabolism is associated with worsened outcomes in animal models. A composite score of serial PET scans from 1 week, 1 month, and 3 months after rat FPI revealed that hypometabolism in the hippocampus ipsilateral to injury was more significant in epileptic versus non-epileptic animals [148]. Interestingly, changes in glucose uptake in the acute, sub-acute, and chronic period are all associated with underlying regional pathophysiology such as reactive astrocytosis and microgliosis [149]. This association may provide a cellular-level explanation for the correlation between glucose metabolism and functional outcome, and may provide insight into possible human biomarkers or therapeutic targets.

Interestingly, the use of excitatory neurotransmitter antagonists, particularly APV to block NMDA receptors, prevented the increase in glucose utilization after FPI [150], suggesting that the metabolic changes after injury are in fact activity-dependent. There is also evidence that excessive activation during a vulnerable period after TBI results in worsened outcomes, as motor cortex stimulation 1 day after injury causes increased cortical degeneration [151]. Additionally, a repeated brain injury during a vulnerable metabolic period (such as 24 hours after a mild TBI) can lead to functional impairment, increased lesion volume, and increased reactive astrocytosis relative to repeated injury during a less vulnerable time (15 days after TBI) [152]. When the brain is already in a state of energy crisis, additional aberrant activation creates further energetic demands and can cause cell death, excitotoxicity, and ultimately worsened outcomes.

A key advantage of utilizing animal models is the ability to harvest brain tissue after injury to assess changes in expression patterns. These changes provide insight into which processes are up- or down-regulated following injury. Examination of the

transcriptome after CCI in mice shows increased expression of glycolytic enzymes at 6 hours after injury, with later decreases in glycolytic enzyme expression at later time points [153]. Similarly, severe FPI in rats resulted in increased expression and enzymatic activity of proteins involved in glycolysis at early time points after injury [154]. This study also found a slight delay in the hyperglycolytic response in animals with mild injury relative to severe injury. Together, these findings strongly support dynamic regulation of glycolytic activity following TBI in animal models.

Additionally, animal studies can begin to elucidate the cell type-specific changes of metabolism after injury. For example, GLUT3 expression (which is responsible for glucose transport into neurons) is increased by 300% from 4 hours-48 hours after injury, while glial transporter GLUT1 is not changed [155]. This finding suggests that neuronal glucose uptake and utilization is preferentially increased in the post-injury period, relative to astrocytic glucose uptake. By 14 days after injury, the oxidative metabolism of glucose is decreased preferentially in neurons but not astrocytes [156].

In addition to helping to identify the basic pathophysiology after TBI, preclinical models also allow for the study of possible therapeutic approaches. One example is the delivery of glycolytic end-product pyruvate to animals following injury, which has been shown to attenuate posttraumatic hypometabolism, be neuroprotective [157], and ameliorate deficits in working memory [158]. The ketogenic diet has also been investigated as a therapeutic approach following TBI (reviewed in [159]), and has been shown to decrease edema, cytochrome c release, Bax upregulation, and apoptotic cell death after weight drop in rats [160, 161].

As we begin to better understand the etiology of post-TBI complications, we can identify relevant biomarkers to assess the efficacy of various therapeutic approaches. As of now, there are no clear biomarkers that indicate risk for post-traumatic epileptogenesis after TBI. In the preclinical models discussed above, only some are associated with post-traumatic epilepsy. Further, within each model, only a small portion of rodents develop spontaneous electrographic and behavioral seizure activity while the others remain non-epileptic. This resembles human TBI, where depending on injury severity, only a subset of patients will go on to develop PTE. It is not well-understood why some animals (and humans) are more vulnerable than others to PTE, and without good biomarkers for epileptogenesis to stratify study subjects, it is difficult to power a preclinical drug study with our available models. However, since glucose metabolism is clearly dysregulated in both epileptic brains and following TBI, this may be an exciting area to look for possible biomarkers. Additionally, attempts to maintain physiologic glucose utilization (avoiding acute hyperglycolytic and chronic hypometabolic states) may constitute a valuable therapeutic approach that should be investigated.

2.4 A role for glycolytic inhibition in modulating aberrant network function

As described above, brain metabolism (particularly glucose utilization and glycolysis) plays a key role in maintaining network activity in both physiologic and pathologic states. There has been increasing interest in manipulating brain metabolism in order to control aberrant activity states. The rationale behind this approach is well-founded, based on the clinical success of the ketogenic diet (KD) in humans suffering from intractable epilepsy. This diet is very low in carbohydrates and high in fats, which is

thought to cause a shift in brain fuel utilization from glucose/glycolysis to ketone bodies/ketosis. Many molecular mechanisms have been proposed to modulate the antiepileptic effects of the KD, in an effort to find a small molecule mimic (reviewed in [162-166] and others). Additionally, the KD is now being utilized for other neurological conditions, including neurodegenerative diseases like amyotrophic lateral sclerosis, Alzheimer's disease, and Parkinson's disease (reviewed in [167]), and psychiatric conditions [168], although with limited evidence in humans in the latter case. Interestingly, the KD is also under investigation for treating cancer, where controlling metabolic substrate supply to the most metabolically active cancer cells may be a useful therapy.

The ketogenic diet is often difficult for patients to maintain, as the meal options are limited and sometimes difficult to access. Thus, how can we mimic the benefits of the KD with a pharmacological tool? Some studies have utilized β-hydroxybutyrate, which is one of the main ketone bodies upregulated in KD. Exposure to β-hydroxybutyrate in brain slices reduces glucose utilization and stimulates pyruvate consumption [169] suggesting a shift away from glycolysis. Ketone bodies have also been shown to effectively reduce hyperexcitability and seizures in multiple different *in vitro* and *in vivo* models (reviewed in [166]). On the other hand, a study in seizure-prone EL mice [170] showed that decreased glucose utilization (with decreased glucose in the diet, with or without the glycolytic inhibitor 2-DG) is required to replicate the protective effects of the KD, while β-hydroxybutyrate supplementation was not sufficient to protect against seizures [171].

Direct inhibition of glycolysis has been extensively studied as an anticonvulsant target, due to the known relationship between glucose utilization and neuronal excitability and activity. While there are multiple methods to inhibit glycolysis (Figure 2.2), including pharmacologic hexokinase inhibition with lonidamine [172], hexokinase feedback inhibition with its end-product glucose 6-phosphate [173], glyceraldehyde-3-phosphate dehydrogenase (GAPDH) inhibition with iodoacetic acid or iodoacetamide [174], and genetic manipulations to knock down enzymatic activity at different stages of glycolysis [175], the most commonly used method is 2-deoxyglucose. 2-deoxyglucose (2-DG) is a glucose analog that competitively inhibits glycolysis at the rate-limiting enzyme hexokinase. The end-product of 2-DG's interaction with hexokinase (2-deoxy-glucose-6-phosphate), lacks the hydroxyl group required for the action of the next glycolytic enzyme, phosphoglucose isomerase, so glycolysis is halted. 2-DG is already in use clinically as a chemotherapeutic agent for cancer [176], as neoplastic cells have increased glycolytic activity via the Warburg effect. 2-DG is well-tolerated in humans [176, 177] and is continuing to be investigated as a therapeutic adjuvant with other cancer treatments.

2-DG has been shown to have anticonvulsant properties in many different slice and *in vivo* models of epilepsy (reviewed in [178]). In key work by Stafstrom and Sutula [179], the authors showed a decrease in interictal epileptiform bursts in hippocampal slices treated with 7.5 mM [K^+], 4-aminopyridine (4-AP), or bicuculline (all *in vitro* models of hyperexcitability). They showed an increase in the after-discharge threshold in the perforant path kindling model with 2-DG (also shown by [180]), suggesting antiepileptic action. As more evidence *in vivo*, 2-DG has been shown to decrease seizure

severity and duration following pilocarpine [181] and to increase the seizure threshold in the 6-Hz corneal stimulation model [182]. More recently, bath-applied 2-DG has been shown to suppress spontaneous neuronal firing and zero-magnesium-induced epileptiform bursts in hippocampal slices, while intracellular application of 2-DG to a single neuron is not sufficient to reduce its spontaneous firing [183]. This study suggests a network effect of glycolytic inhibition beyond what is capable by controlling a single neuron's activity. Taken together, these results strongly support the role of 2-DG as an anticonvulsant target.

While there have been reports of 2-DG decreasing seizure threshold or initiating epileptogenesis [182, 184], these findings may be attributable to the fact that chronic hypometabolism or severe glucose deprivation can independently cause seizures. Also, several clinically effective anticonvulsants have mixed effects in animal models [185], depending on the exact mechanism of action of the drug. Further, a new study by Nedergaard shows that the proconvulsant effect of 2-DG can be reproduced by blocking oxidative phosphorylation [186], providing a possible mechanism to describe ictal facilitation by 2-DG that is distinct from the anticonvulsant effects of glycolytic inhibition. Thus, the varied results of 2-DG do not rule out glycolysis as a key anticonvulsant target.

There have been several mechanisms of action proposed for the anticonvulsant effects of 2-DG. First, 2-DG can directly suppress synaptic transmission, hyperpolarize neurons, and decrease membrane resistance [187]. This study implicated an adenosine-dependent increase in potassium conductance as a possible mechanism for the change in neuronal membrane properties. A study from 2016 identified an additional bicuculline-

sensitive tonic current with 2-DG application, suggesting a role for the potentiation of GABAergic conductances as an additional mechanism for 2-DG's anticonvulsant effects in the 4-AP slice model of hyperexcitability [188]. In addition to its direct effects on neuronal excitability, 2-DG has also been reported to alter transcriptional activity. For example, 2-DG has been shown to attenuate electrical kindling-induced upregulation of brain-derived neurotrophic factor (BDNF) through an NRSF-dependent mechanism [180]. 2-DG has also been shown to increase expression of K_{ATP} channel subunits Kir6.1 and Kir6.2 following pilocarpine [189], which could explain the increased potassium conductance and anticonvulsant effect of the treatment. Thus, 2-DG is likely acting through rapid, reversible effects on neuronal excitability as well as through longer-term mechanisms affecting neuronal expression profiles.

Other metabolic molecular targets that shift neuronal metabolism away from glycolysis have been investigated for their anticonvulsant properties, including lactate dehydrogenase (LDH), BAD/K_{ATP} channels, and fructose-1,6-diphosphate. LDH is a component of the ANLS, which allows for the conversion of lactate to pyruvate after delivery to neurons. Using an anticonvulsant screen, it was found that clinical anticonvulsant stiripentol exerted its effects through LDH inhibition, which hyperpolarized neurons and could be counteracted with delivery of glycolytic end product pyruvate [190]. The Yellen group has explored a K_{ATP}-channel-dependent mechanism through which the BAD knockout mouse is resistant to picrotoxin-induced epileptiform activity. Specifically, they found that the protective effect of BAD knockout (a protein which is involved in apoptosis and glucose metabolism) in reducing epileptiform activity is abolished through genetic or pharmacologic blockade of K_{ATP}

channels [50, 191]. Finally, fructose-1,6-diphosphate, which is thought to shift glucose utilization away from glycolysis and toward the pentose phosphate pathway [192], has been shown to be anticonvulsant in multiple rat models of epilepsy [181] and protective against epileptogenesis in an amygdaloid-kindling seizure model in rats [193].

2.5 Can inhibiting glycolysis reduce post-traumatic epilepsy following traumatic brain injury?

2.5.1 Broad spectrum intervention in a complex environment

To date, no clinical treatments exist which can reduce the incidence of post-traumatic epilepsy following traumatic brain injury. Anticonvulsants (such as phenytoin and levetiracetam) and glucocorticoids have been examined in clinical trials to prevent PTE, but have not shown significant long-term beneficial effects [194-196]. Could metabolic therapies provide a novel way forward? As described above, preclinical studies support the use of glycolytic inhibition to reduce seizures in multiple models. These studies, however, draw on 2-deoxyglucose's *anticonvulsant* effects and have not explored the possible disease-modifying, anti-epileptogenic effects of the treatment. In addition to 2-DG's anticonvulsant effects, glycolytic inhibition following traumatic brain injury may result in other benefits that prevent the development of post-traumatic epilepsy. Metabolic manipulation as a therapeutic target is a rational approach based on the body of evidence presented above. First, diverse and robust metabolic changes occur following TBI. At a basic level, this implicates metabolism as a part of disease pathology, and therefore a potential avenue for therapeutic intervention. Second, inhibiting metabolic systems offers the opportunity to affect a wide range of energy-dependent

processes that may contribute to disease pathology. Neurotransmission, maintenance of ionic gradients, and inflammatory processes (among others) all have significant energy demands and may contribute to disease progression. While disrupting metabolism may lack specificity, its breadth of effects may contribute to a truly disease-modifying approach. Additionally, this approach may be more specific than first appreciated, as it aims to decrease the activity of only the most active cells. Third, increased metabolic activity acutely following brain injury may drive secondary injury processes that contribute to epileptogenesis. To date, no data exists to support or refute a direct link between them, but a deeper understanding of how different pathophysiological processes interact to result in post-traumatic epileptogenesis will help drive novel therapeutic approaches. If intervening in metabolic pathways after injury is protective, it is likely not via acute anticonvulsant effects, as other traditional anticonvulsant drugs have failed to prevent PTE. Instead, it may be acting by preventing other epileptogenic processes. Finally, manipulating metabolism, in some ways, is reminiscent of TBI treatment with hypothermia. While hypothermia has many effects, it slows metabolic activity via its effects on enzyme kinetics. A recent meta-analysis of therapeutic hypothermia for TBI suggests it may improve neurological outcomes for adults following focal TBI ([197]; but see also [198, 199]). Because the mechanistic rationale is strong and the need for disease-modifying therapies to prevent PTE is great, it makes sense to consider how we might harness 2-DG (or other strategies to inhibit glycolysis) to improve patient outcomes following TBI.

2.5.2 Metabolic intervention considerations: timing may be essential

Based on the existing evidence, attenuating glycolysis may only be advantageous during the first hours to days following TBI (as depicted in Figure 2.3). Clinical literature supports that TBI-induced hypermetabolism occurs only in the short term after TBI. The injury itself causes cells to rupture and release their intracellular contents (including pro-excitatory species like glutamate), breaches the blood-brain barrier, activates immune and inflammatory cascades, and reduces local blood flow and oxygenation. All of these events could favor the use of glycolysis to power neuronal activity and inflammatory activity, especially in a local low-oxygen environment. If any of these early events, and their immediate downstream effects, contribute to the development of PTE and rely on increased glycolysis, then attenuating excessive glycolytic activity may be beneficial. The time window in which hypermetabolism occurs may be extremely short, perhaps lasting only minutes to hours following injury [117, 150, 200]. Once the initial hypermetabolic state is resolved, the brief window of opportunity to provide metabolic intervention is likely lost. As outlined above, a period of hypometabolism occurs in humans and animal models in the days to months following TBI. During this phase, there would no longer be rationale to inhibit glycolysis, as we would not want to further reduce metabolic activity.

2.5.3 What pathological events following TBI could be targeted to avoid PTE?

There are surprisingly few risk factors identified that clearly correlate with an increased risk of developing PTE following TBI. The only clear prognostic indicators are the severity of the injury and age at time of injury [201-203]. How do we know which aspects of TBI pathophysiology should be targeted to reduce PTE? Recent preclinical studies have identified hippocampal shape changes visualized using MRI that reliably

predict the development of PTE in the rat fluid percussion model of TBI [204]. Excitingly, a recent study showed that increased levels of IL-1β, a proinflammatory cytokine, was associated with increased risk of PTE in humans [205]. While this finding has not yet been developed into an established biomarker and may have caveats, it is an exciting step forward. Perhaps the most interesting development in identifying PTE risk factors is a recent study examining EEG abnormalities seen in the intensive care unit following TBI in humans. Kim and colleagues reported that increased epileptiform abnormalities (including spikes and sharp waves, periodic epileptiform discharges, and rhythmic activity) in the days following TBI indicate elevated risk for developing PTE [206].

Deeper mechanistic insights to link TBI and PTE are still sorely lacking, but will be crucial in developing new biomarkers and therapeutic approaches. For example, does reducing the amount of tissue lost following TBI protect against PTE? What circuit-level changes drive epileptiform activity and epileptogenesis post-injury? How do secondary injury mechanisms, including inflammation, oxidative damage, and apoptosis, contribute to epileptogenesis? These mechanistic questions cannot be easily addressed using clinical studies due to the heterogeneity of human TBI and the ethical and technical limitations of utilizing human subjects. Therefore, we rely on preclinical data to guide our development of translatable clinical approaches. A dizzying array of cellular and molecular changes occur following TBI and may contribute to the development of PTE. Here, we will discuss specific targets which we suspect are especially relevant to epileptogenesis, and will propose how glycolytic inhibitors could be utilized to attenuate these processes.

2.5.3.1 Tissue loss

Because injury severity is related to the risk of post-traumatic epilepsy, it stands to reason that reducing gross and cellular tissue loss after TBI may improve outcomes following injury. Tissue loss can arise from the primary injury [207] and from secondary injury mechanisms that take place later. By the time a patient presents clinically, the initial mechanical force has already occurred and the primary injury cannot be undone. However, evidence supports that much of the tissue loss in TBI occurs due to the second wave of neuronal injury caused by excitotoxicity and ischemic insult [208, 209]. Thus, translatable work should focus on ameliorating secondary injury, as the therapeutic timeline is more clinically feasible. Because 2-DG can acutely decrease hyperexcitability, it may also be able to reduce excitotoxicity. On the other hand, ongoing glucose metabolism provides energy to the system, which may be required to maintain cell health. Perhaps reducing glycolysis will favor glucose flux through the pentose phosphate pathway, which supports replenishment of the antioxidant glutathione (by providing NADPH) and may be protective following injury. Thus, the goal would not be to completely shut down glucose utilization or to starve the tissue, but instead to direct metabolism toward processes which will maximize tissue health. Direct measures of how inhibition of glycolysis may prevent excitotoxicity and cellular loss are sparse, requiring further study to determine if this approach may ameliorate secondary injury and reduce lesion volume after injury. This avenue may prove fruitful however, as the ketogentic diet has been shown to result in reduced cortical tissue loss following CCI [210, 211].

2.5.3.2 Inflammation

TBI induces significant and widespread neuroinflammation [212, 213] which is thought to be involved in the development and progression of epilepsy [214]. Neuroinflammation following injury can include the activation of microglia and astrocytes, invasion of peripheral immune cells, and upregulation of inflammatory signaling cascades. As mentioned above, the presence of inflammatory molecules in the CSF following TBI are indicative of increased risk for developing PTE. Are any of these systems potential targets for metabolic interventions? Interestingly, inhibiting glycolysis using 2-DG led to the death of microglia in culture but a significant increase in neuronal cell loss following hypoxic insult [215]. This suggests that large-scale inhibition of inflammation may not be beneficial following brain insult. *In vivo* manipulations, which are likely more relevant to human TBI, do support using metabolic approaches to minimize inflammation following brain insult. Caloric restriction was shown to reduce microglial activation in the cortical stab model of TBI [216], although caloric restriction occurred before the injury in this experiment. Studies examining the effects of the ketogenic diet on neuroinflammation, however, were not conclusive [208]. Interestingly, inhibiting glycolysis with 2-DG has been shown to reduce disease progression and inflammatory cell infiltration in models of CNS autoimmune disorders [217] and in experimental activation of inflammatory signaling in the brain [218], suggesting a possible neuroprotective role for this approach.

2.5.3.3 Synaptic transmission

From a simplistic viewpoint, the development of PTE is likely due to increased neuronal excitation and decreased neuronal inhibition following TBI. A great deal of

evidence exists for both changes following experimental TBI in animal models. A comprehensive analysis of these changes falls outside of the scope of this discussion, but are reviewed elsewhere [219-221]. Some specific examples of TBI-related changes in synaptic activity include loss of inhibitory interneurons, decreased synaptic inhibition, increased synaptic excitation, and exuberant growth of excitatory synaptic connections [36, 222-224]. Although preclinical studies have failed to demonstrate robust antiepileptogenic effects of the ketogenic diet [225, 226], metabolic approaches may still have potential to restore normal synaptic function following TBI. For example, 2-DG treatment inhibits synaptic vesicle recycling [75], thereby putting the brakes on synaptic activity during the metabolic crisis period following TBI. Additionally, inhibiting glycolysis (but not oxidative phosphorylation) reduces EPSC width and amplitude [82], supporting a role for metabolic manipulation in controlling neuronal excitability and synaptic function. Finally, there is evidence supporting that different neuronal cell types utilize unique metabolic pathways to generate ATP [227]. As compared to excitatory neurons, inhibitory interneurons contain more mitochondria [228], generate a different metabolic response to neuronal activity [64], and express a unique cadre of metabolic enzymes [229]. The differences between energy utilization in different neuronal subtypes may enable cell type-specific metabolic manipulation of neuronal circuit activity through each cell's unique sensitivity to glucose and/or oxygen deprivation. Thus, a metabolic approach may be able to preserve the inhibitory tone of the network by targeting aberrant activity in some neuron types, but not others.

2.5.4 Caveats and Considerations

There are several conceptual concerns that arise when considering glycolytic inhibition as a treatment to prevent PTE following TBI. First, why would one consider reducing energy production in a brain that desperately needs energy to restore cellular and network function after injury? This becomes even more relevant when considering the long-term hypometabolic state that exists following TBI. In fact, there is significant controversy among clinicians as to whether glucose should actually be supplemented for post-TBI patients [230-235]. Additionally, work from Schallert and Hernandez supports the role for acute neuronal/network activity in behavioral recovery after lesional injury, as network inhibition with a short-term GABA agonist results in long-term impairment of behavioral recovery [236]. In response to this concern, it becomes clear that complete starvation or inhibition of metabolic activity is not helpful, particularly in the long term. Metabolic manipulation would likely be most effective in the acute phase, in the first few hours following TBI, and would focus on targeting aberrant, excessive glucose utilization to bring it back down to physiologic levels. Patient stratification using PET scanning or fMRI would help to target this therapy to the patients with the most severe hyperglycolysis, and would ensure that the patient had not already entered the hypometabolic state. Furthermore, the beneficial effects observed with the ketogenic diet may not be mediated by the inhibition of glycolysis, but may be through promoting ketosis [159]. Providing β-hydroxybutyrate, a ketone body metabolized through ketosis, increases ATP levels following TBI [237] and reduces tissue loss following focal ischemia [238], independent of glycolytic inhibition. This suggests that a combined approach of inhibiting glycolysis and supplementing ketosis may have the most

therapeutic efficacy. It is also important to consider the role of oxidative stress after TBI. Oxygen supply is compromised after injury, and preclinical studies support the use of antioxidant treatments (such as N-acetylcysteine) to reduce tissue loss and improve behavioral function after TBI [239]. Further studies are required to understand the relationship between glycolytic activity and oxidative stress in the injured brain. Finally, prolonged treatment with 2-DG may have significant adverse effects, including reported cardiovascular complications [240]. Again, this finding would support a short time course of treatment with glycolytic inhibitors, only to target the increased glucose utilization in the first hours to days following injury.

2.6 In conclusion

The challenges to treating TBI and preventing PTE are extensive. Heterogeneous injury categories, diverse metabolic responses to injury, and difficulty in powering both preclinical and clinical trials for PTE all make this a daunting translational problem. Based on the compelling evidence of metabolic changes following TBI, strong neuroprotective and anticonvulsant properties of the ketogenic diet, and multiple small molecule approaches to manipulate metabolism, we believe that therapeutic opportunities exist to harness metabolic systems to reduce PTE. There are many outstanding questions the field must address, including identifying the cellular sites and types of glucose utilization during normal brain function and after TBI, developing diagnostic tools that provide molecular insight into brain metabolism, understanding how metabolism contributes to post-traumatic epileptogenesis, and identifying biomarkers to stratify the patients at highest risk of developing PTE. We would recommend prioritizing the

development of a quantitative assay to assess changes in glucose utilization in the brain following TBI. This assay could serve as both a prognostic and a predictive biomarker for PTE. Increased glucose utilization may be prognostic as it is likely associated with uncontrolled network activity, consistent with epileptogenesis. It may also serve as a predictive biomarker of which patients would respond best to a metabolically-targeted therapy, such as glycolytic inhibition. This is especially important as hyper-glycolysis may only occur in a brief temporal window and/or in a subset of patients following TBI. Developing new tools and biomarkers is critical, as the clinical needs of TBI patients are clear: to improve long-term quality-of-life and to prevent devastating TBI complications such as PTE. Continued collaboration between basic scientists and clinicians will allow for better understanding of post-TBI pathophysiology and will ultimately advance novel interventional strategies to help these patients.

2.7 Author contributions

JK and CD conceived of and wrote the manuscript.

2.8 Funding

This work was supported by the National Institute of Neurological Disorders and Stroke (R21-NS098009 (CGD) and F31-NS101741 (JBK)) and the Department of Defense (W81XWH-16-ERP-IDA).

2.9 Acknowledgments

We would like to thank Dr. Zin-Juan Klaft for his helpful comments on the manuscript.

Chapter 3 : Glycolytic inhibitor 2-deoxyglucose prevents cortical hyperexcitability following traumatic brain injury[2]

[2] Koenig, JB; Cantu, D; Low, C; Sommer, M; Noubary, F; Croker, D; Whalen, M; Kong, D; Dulla, CG. In revision at *JCI Insight*, 3/20/2019.

3.1 Introduction

Traumatic brain injury (TBI) is a leading cause of death and disability worldwide and can lead to motor, behavioral, and cognitive losses [241] as well as post-traumatic epilepsy (PTE) [242-244]. Patients who develop PTE show higher mortality than TBI patients without epilepsy, and many PTE patients are refractory to the currently available anticonvulsive therapies [242, 244]. Multiple molecular and cellular changes that occur after TBI may play an important role in the pathophysiology of network dysfunction, PTE, and other TBI-induced pathologies. Aberrant electrical activity [245, 246], indiscriminate release of neurotransmitters [247], and altered cerebral glucose utilization [117, 143] all occur after TBI. Additionally, compromised cerebral blood flow, disruption of the blood-brain-barrier [248, 249], increased oxidative stress, and mitochondrial dysfunction [250] create a complex set of neurometabolic disruptions after injury [241, 242, 251]. Together, these changes can disturb synaptic function, cause hard-wired remodeling of neuronal connectivity, and lead to circuit dysfunction and PTE.

Many studies suggest that a key step in developing network dysfunction after injury is the loss of inhibitory GABAergic interneurons, a diverse group of neurons that powerfully constrain cortical excitation. Disruption of inhibitory network activity can lead to motor dysfunction, cognitive losses, and epilepsy [37, 220, 252-254]. The most abundant subtype of cortical interneurons express the calcium-binding protein parvalbumin (PV), fire action potentials at a high frequency (fast-spiking), and provide perisomatic inhibition of excitatory cortical pyramidal neurons [255]. PV+ interneuron loss, atrophy, and dysfunction have been shown in the controlled cortical impact (CCI) [36], lateral fluid percussion [37], partially isolated neocortex (“undercut”) [256, 257],

and weight drop [38] models of TBI. Importantly, human post-mortem studies also show that PV-expressing interneurons are specifically lost following TBI [39]. The mechanisms by which TBI leads to interneuron loss are largely unknown. Therefore, it has been difficult to develop therapeutic interventions to preserve inhibitory network function following TBI.

We believe that the aberrant neuronal activity that occurs acutely after TBI is a key contributor to long-term cortical network dysfunction. In support of this idea, early seizure activity and other EEG abnormalities are associated with poor clinical outcomes and a higher risk of developing post-traumatic epilepsy [206, 245, 246]. Preclinical data from animal models of epilepsy and brain injury demonstrate that early uncontrolled excitation contributes to later loss of GABAergic interneurons and development of inhibitory circuit dysfunction [258-261]. Following TBI in both humans and animal models, this aberrant electrical activity occurs during periods of abnormally elevated glycolytic activity [15, 132, 142, 150, 262, 263]. We hypothesize that reducing hyper-glycolysis will attenuate injury-induced increases in excitatory synaptic activity, ameliorate losses of PV+ interneurons, and ultimately prevent inhibitory network dysfunction.

2-deoxyglucose (2-DG) is a glucose analog that competitively inhibits hexokinase (the rate-limiting enzyme in glycolysis) [178, 264, 265]. Multiple studies demonstrate that 2-DG can be anticonvulsive in both in vitro and in vivo models of epilepsy [179, 180]. 2-DG pre-treatment also prevents kainic acid-induced hippocampal cell loss in rats [266] and can reduce seizure severity [181, 189]. While 2-DG has been previously

explored as an anticonvulsant therapy, it has not yet been utilized as a disease-modifying agent to prevent epileptogenesis after TBI.

In this study, we tested whether 2-DG reduces TBI-induced hyperexcitation and attenuates the development of inhibitory network dysfunction after TBI. We utilized the controlled cortical impact (CCI) model of focal brain contusion, which results in significant cell loss, network hyperexcitability, and spontaneous behavioral and electrographic seizures [41]. Our study shows that acute 2-DG treatment of cortical brain sections attenuated hyperexcitability in the injured brain. In addition, 2-DG treatment reduced the excitability of excitatory neurons, but not inhibitory interneurons. Finally, in vivo treatment with 2-DG for one week following CCI prevented the development of epileptiform activity and reduced the loss of parvalbumin-expressing interneurons. Together, these studies support the potential application of glycolytic inhibitors to reduce cortical hyperexcitability after TBI.

3.2 Results

3.2.1 In vitro 2-DG treatment decreases the excitability of excitatory neurons, but not inhibitory interneurons

2-DG has been previously shown to attenuate epileptiform activity in multiple in vitro and animal models of epilepsy [179, 180, 183]. Pharmacologic inhibition of glycolysis can directly suppress synaptic transmission, reduce membrane resistance [187], and broaden the action potential (AP) waveform [82]. It is unknown, however, whether glycolytic inhibition has differential effects on the excitability of glutamatergic excitatory neurons and GABAergic inhibitory interneurons. Therefore, we assessed the

effects of 2-DG on both cell types in naïve (uninjured) cortex. Whole-cell recordings were established in acute cortical brain slices from adult (>P28) animals of both sexes. Recordings were performed on layer V pyramidal neurons or fast-spiking PV+ GABAergic interneurons. PV interneurons were identified using the *G42* mouse line, a BAC transgenic line in which >70% of genetically GFP-labeled interneurons are PV+ on immunohistochemistry (Figure 3.1, [267]).

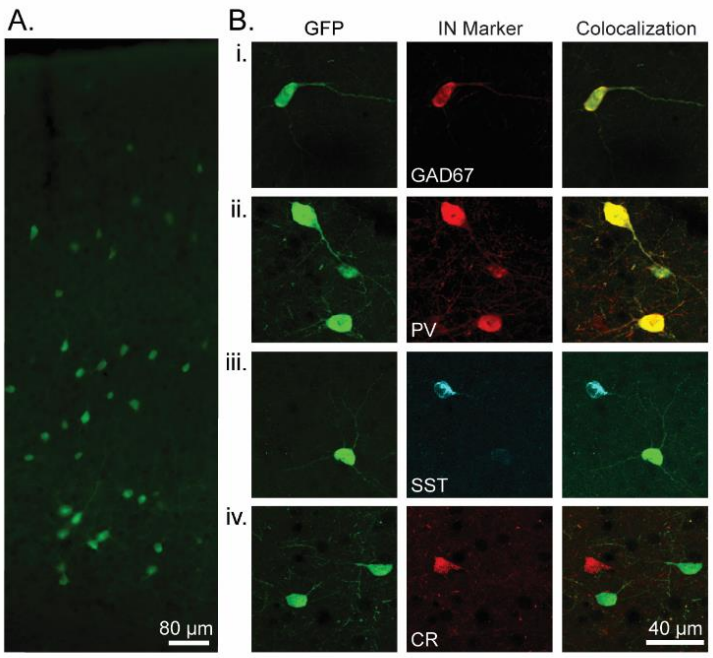

C.

Interneuron Marker	# GFP+ Cells Counted	# GFP+ Cells Co-labeled with IN Marker	Colocalization
GAD67	158	122	77.30%
Parvalbumin (PV)	318	233	73.30%
Somatostatin (SST)	318	0	0.00%
Calretinin (CR)	276	0	0.00%

Figure 3.1: Characterization of G42 mouse line. **A.** Immunohistochemical labeling of genetically-encoded GFP (green) in the somatosensory cortex (SSC) of adult *G42* mice. **B.** Co-labeling of GFP in *G42* mice with markers of inhibitory interneurons in layers V-VI of SSC (i. GAD67, ii. Parvalbumin (PV), iii. Somatostatin (SST), iv. Calretinin (CR)). **C.** Table showing abundant co-labeling of GFP+ cells with PV and GAD67. (n = 4 mice)

In current clamp mode, hyperpolarizing and depolarizing steps were injected in the presence of synaptic receptor blockers (10 μm CPP, 20 μm DNQX, and 10 μm gabazine) and the number of evoked action potentials (APs) was quantified. The results were compared between baseline aCSF (containing 10 mM glucose) and following 10 minutes of slice perfusion with 2-DG-aCSF (8 mM 2-DG, 2 mM glucose). 2-DG-aCSF maintained the same solution osmolarity as baseline aCSF (10 mM total saccharide), while constricting glucose availability to concentrations similar to those present in mouse or human cerebrospinal fluid (2 mM, [268]). In the presence of 2-DG, excitatory layer V pyramidal neurons fired significantly fewer APs at a given level of current injection (Figure 3.2A, 3.2C; see Table 3.1 for all Linear Mixed Model statistical results) while GABAergic interneurons were not affected (Figure 3.2B, 3.2D). Consistent with reduced excitability of glutamatergic excitatory neurons following 2-DG perfusion, rheobase (current injection required to elicit the first AP) was increased in excitatory neurons but was not affected in GABAergic interneurons (Figure 3.2E, H). The decrease in the intrinsic excitability of excitatory neurons was associated with a decrease in membrane resistance which was not observed in GABAergic interneurons (Figure 3.2F, I). No change in resting membrane potential was observed in either cell type upon application of 2-DG (Figure 3.2G, J).

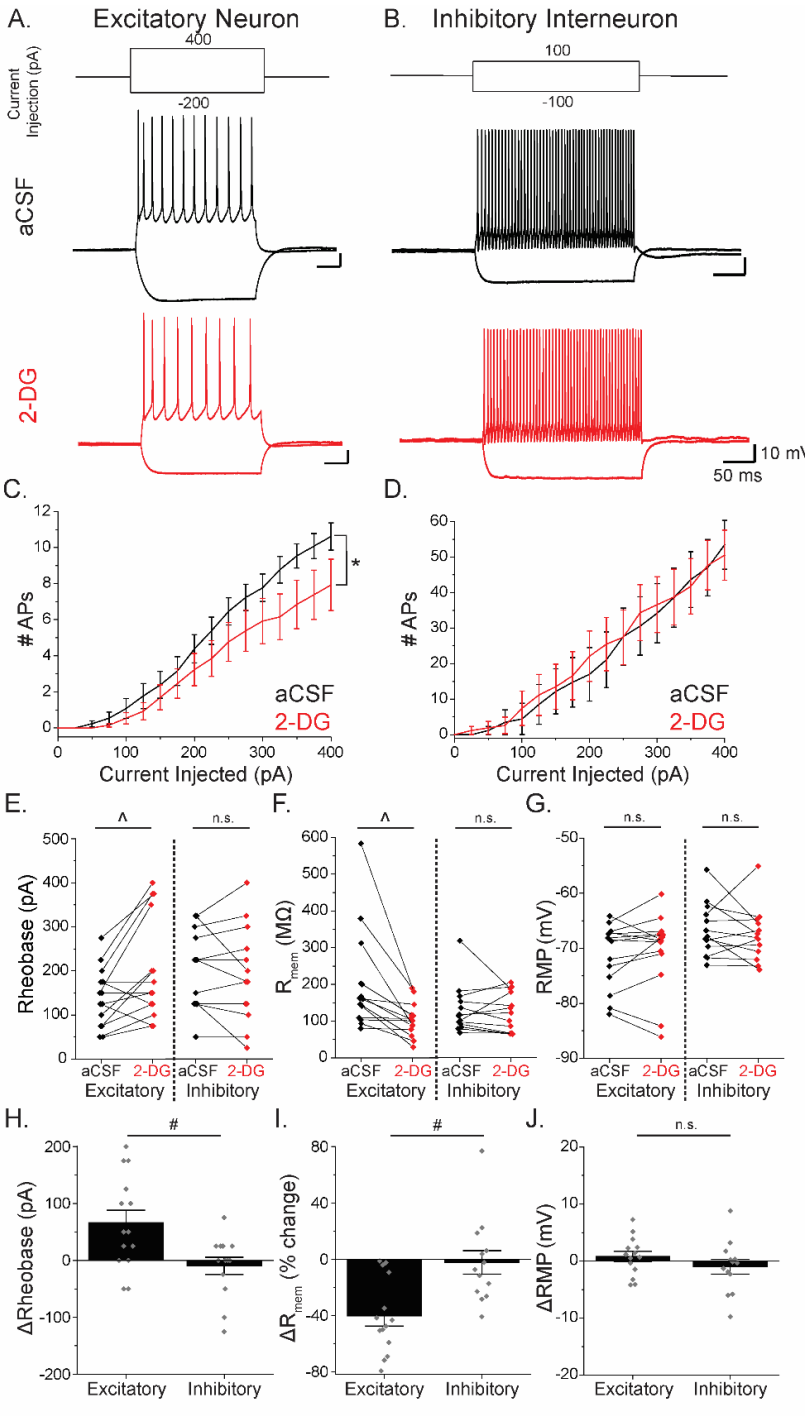

Figure 3.2: In vitro 2-DG treatment decreases the intrinsic excitability of excitatory pyramidal neurons. **A-B.** Representative traces following current injection into layer V cortical excitatory pyramidal neurons **(A)** or interneurons **(B)** before (black) or after (red) treating the cortical slice with 2-DG for 10 minutes. **C-D.** Input-output curves from excitatory pyramidal neurons **(C)** and inhibitory interneurons **(D)**. **E.** Rheobase (current injection required to fire the first action potential) before (black) and after (red) 2-DG

treatment in each cell type. **F.** Membrane resistance before and after 2-DG in each cell type. **G.** Resting membrane potential (RMP) before and after 2-DG treatment in each cell type. **H.** ΔRheobase (rheobase in 2-DG versus baseline) in excitatory neurons and interneurons. **I.** % change in membrane resistance of excitatory neurons and interneurons following 2-DG treatment. **J.** Change in resting membrane potential (RMP) in excitatory neurons and interneurons in 2-DG. (Error bar = SEM. n = 14 excitatory neurons from 9 animals, 13 inhibitory interneurons from 10 animals. LMM: *t > ±1.96, effect: interaction between current injection and 2-DG; #t > ±1.96, effect: cell type. 2-sample t-test: ^p < 0.05. n.s. not significant.)

To control for reduced 2 mM glucose in 2-DG-aCSF, these experiments were repeated in low glucose aCSF (LG-aCSF: 2 mM glucose, 8 mM sucrose (a metabolically inert sugar)). LG-aCSF had no effects on AP firing, input-output curves, or membrane resistance in either excitatory neurons or inhibitory interneurons (Figure 3.3). This demonstrates that simply lowering glucose to 2 mM is not sufficient to alter neuronal excitability. Together, these experiments show that inhibition of glycolysis has cell type-specific effects on neuronal excitability.

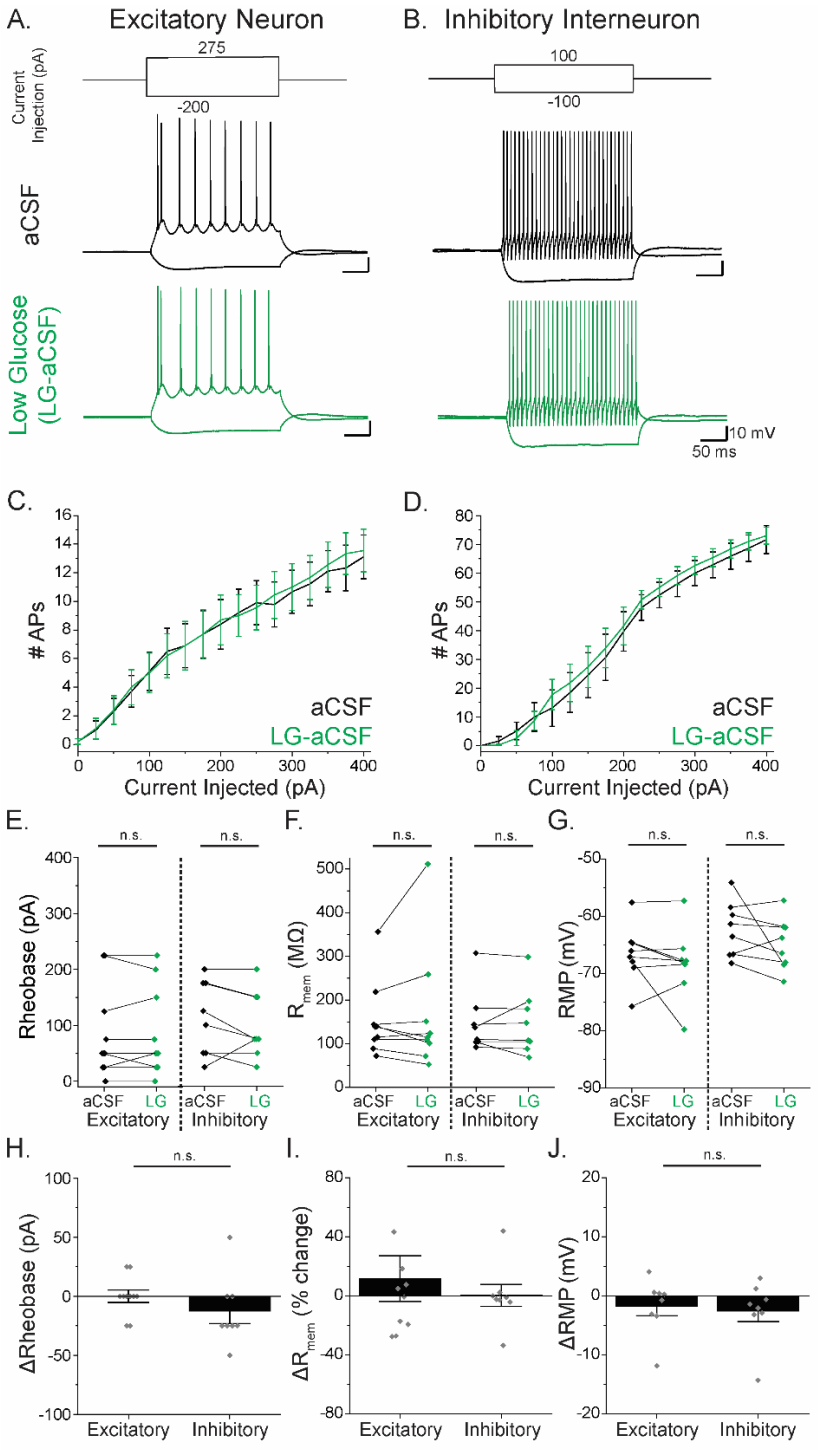

Figure 3.3: Treatment with Low Glucose (LG)-aCSF did not affect the excitability of excitatory or inhibitory neurons. A-B. Representative traces following current injection into layer V cortical excitatory pyramidal neurons (A) or interneurons (B) before (black) or after (green) treating the cortical slice with LG-aCSF for 10 minutes. **C-D.** Input-output curves in excitatory (C) or inhibitory (D) neurons. **E.** Rheobase (current

injection required to fire the first action potential) before (black) and after (green) LG-aCSF treatment in each cell type. **F.** Membrane resistance before and after LG-aCSF in each cell type. **G.** Resting membrane potential (RMP) before and after LG-aCSF treatment in each cell type. **H.** ΔRheobase (rheobase in LG-aCSF versus baseline) in excitatory neurons and interneurons. **I.** % change in membrane resistance of excitatory neurons and interneurons following LG-aCSF treatment. **J.** Change in resting membrane potential (RMP) in excitatory neurons and interneurons in LG-aCSF. (Error bar = SEM. n = 10 excitatory neurons from 5 animals, 8 inhibitory neurons from 5 animals. n.s. not significant.)

3.2.2 2-DG ameliorates CCI-induced increases in synaptic excitation onto GABAergic interneurons

Acutely after TBI, glycolytic activity and neuronal activity are aberrantly increased [15]. We hypothesized that TBI results in increased synaptic excitation of GABAergic interneurons in the peri-injury cortex acutely after injury. If so, this hyperexcitation may contribute to later cell death or dysfunction of PV+ (and other GABAergic) interneurons (see 3.3 Discussion). To test this hypothesis, we utilized controlled cortical impact (CCI) to model focal, contusional TBI in adult male mice. Briefly, a craniectomy was made over left sensorimotor cortex and an impact was delivered to generate a moderate-to-severe injury (3 mm impactor probe diameter, 3.5 m/s velocity, 400 ms dwell time, 1 mm impact depth) [41]. Acute cortical slices were prepared from sham- and CCI-injured brains 3 days following injury and whole-cell recordings were made from fast-spiking GABAergic interneurons within 200 μm of the lateral edge of the CCI lesion. Interneurons were identified with GFP labeling in layer V-VI cortex in *G42* mice, which as above, were primarily PV+ (Figure 3.1). Neurons were voltage-clamped at -70 mV to isolate spontaneous excitatory postsynaptic currents (sEPSCs). Consistent with our hypothesis, there was an increase in the mean frequency of sEPSCs after CCI compared to sham (Figure 3.4B). CCI also resulted in a significant

leftward shift in the sEPSC inter-event interval cumulative distribution (Figure 3.4C). There was a trend towards an increase in sEPSC amplitude, without statistical significance based on LMM or 2-sample Kolmogorov-Smirnov test (Figure 3.4F-G).

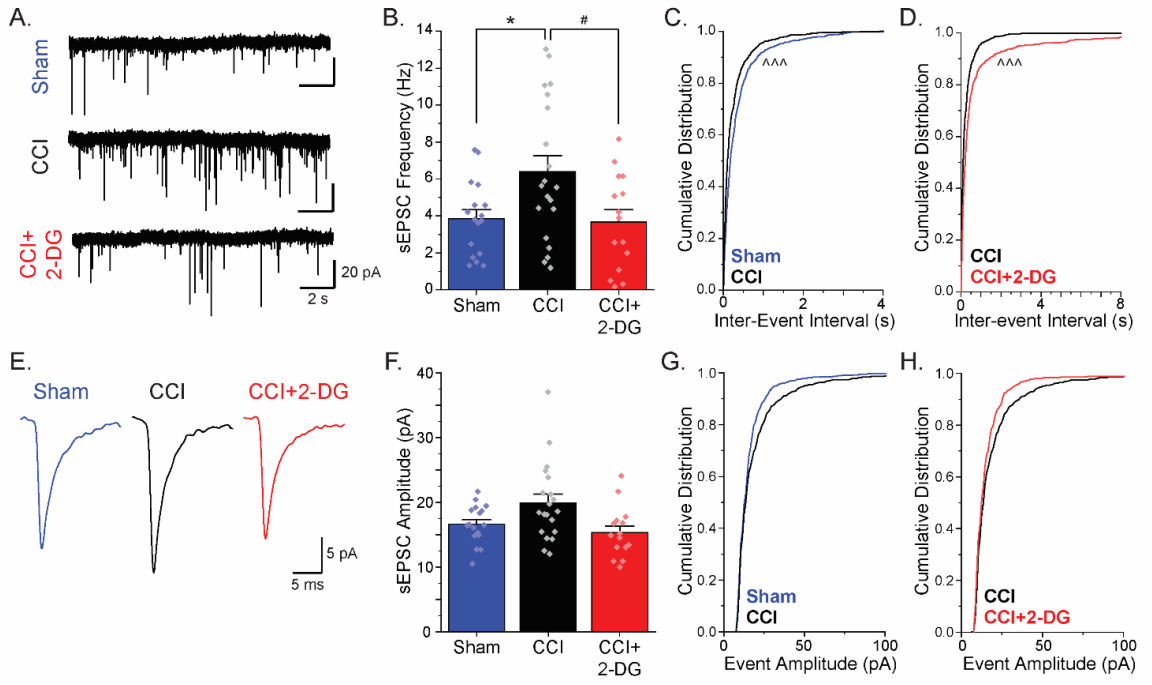

Figure 3.4: In vitro 2-DG attenuates CCI-induced increases of excitatory synaptic activity onto interneurons 3 days after injury. A. Representative sEPSC traces from acute cortical slices from sham animals or CCI-injured animals, and a representative trace from a CCI slice following 10 minutes of 2-DG wash-on. **B.** Mean sEPSC frequencies. **C-D.** Cumulative distributions of inter-event interval generated from 100 random events per recorded cell. **E.** Representative events from each condition, generated by averaging 100 events from a representative trace. **F.** Average event amplitude. **G-H.** Cumulative distributions of event amplitude generated from 100 randomly selected events per cell. (Error bar = SEM. n = 15-20 cells from 4 animals/group. LMM: *t > ±1.96, effect: CCI; #t > ±1.96, effect: interaction between CCI and 2-DG. 2-sample K-S test with correction for multiple comparisons: ^^^p < 1E-5)

Because glucose utilization is elevated acutely after TBI and we had previously observed specific effects of 2-DG on excitatory (but not inhibitory) neuronal activity, we assessed whether 2-DG application to the acute slices would reduce injury-induced

excitation of GABAergic interneurons. When 2-DG-aCSF was applied to acute cortical slices prepared 3 days following CCI, the mean frequency of sEPSCs onto interneurons was reduced to approximately sham levels (Figure 3.4B), corresponding with a rightward shift the sEPSC inter-event interval cumulative distribution (Figure 3.4D). Application of 2-DG to sham tissue did not significantly affect sEPSC frequency. There was, however, a large variability in the response to 2-DG treatment in sham animals and a trend toward more frequent excitatory events (data not shown), demonstrating unique effects of 2-DG in sham versus CCI-injured brain. 2-DG treatment also resulted in a leftward shift of the cumulative event amplitude following CCI (Figure 3.4H), although the comparisons of the mean amplitude by LMM and cumulative distributions by 2-sample Kolmogorov-Smirnov test did not reach statistical significance. Overall, these results suggest that GABAergic interneurons receive increased excitation in the days following TBI and that these effects are attenuated by acute application of 2-DG.

3.2.3 Acute 2-DG treatment attenuates epileptiform activity in cortical brain slices following CCI

Next, we tested whether 2-DG application attenuates network-level cortical hyperexcitability, which is observable in field excitatory postsynaptic potentials (fEPSPs) as early as 2 weeks following TBI [220], and is robustly present by 3-5 weeks following TBI. Brain slices were prepared from mice 3-5 weeks after CCI or sham surgery and electrical stimulation was delivered to ascending cortical inputs to evoke fEPSPs. In sham animals, fEPSPs were brief and low-amplitude. Slices taken 3-5 weeks after CCI, however, exhibited stimulus-evoked fEPSPs with epileptiform activity (increased

amplitude, duration, area, and coastline), consistent with network hyperexcitability ([36], Figure 3.5A). As shown previously in other slice models of epileptiform activity [179], in vitro application of 2-DG markedly reduced the percentage of stimulus-evoked fEPSP traces that exhibited epileptiform activity after CCI from 90% to 18% (Figure 3.5B). Additionally, 2-DG treatment resulted in field potentials with significantly decreased area (Figure 3.5C) and high-frequency activity as measured by fEPSP coastline (Figure 3.5D). In brain slices from sham-injured animals, 2-DG-aCSF did not significantly change the area or coastline of the fEPSPs, or the percentage of epileptiform traces.

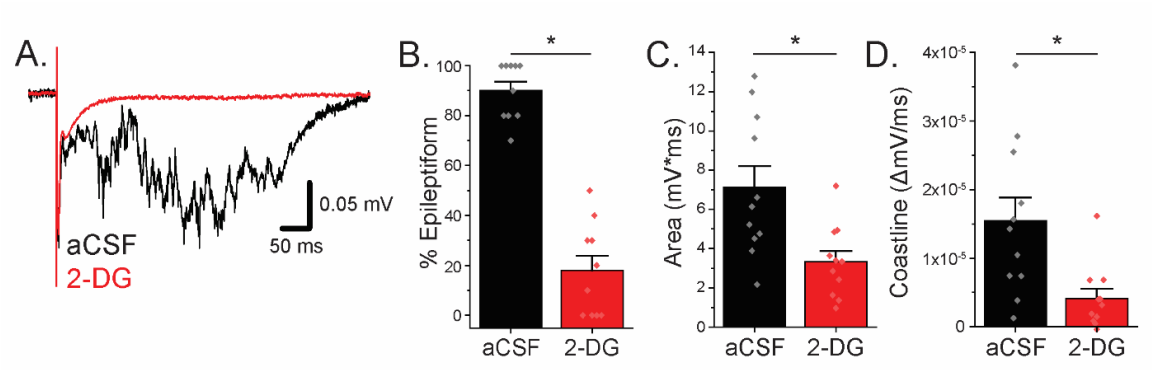

Figure 3.5: Acute 2-DG treatment decreases epileptiform activity in vitro following CCI. A. Representative stimulus-evoked field potentials in an acute cortical slice from a CCI-injured animal before (black) and after (red) local perfusion of 2-DG for 30 minutes. **B.** Percentage of traces with epileptiform activity after CCI. **C-D.** Area (C) and coastline (D) of the field potentials in baseline aCSF and 2-DG-acSF in CCI-injured slices. (Error bar = SEM. n = 10 slices from 6 animals. LMM: *t > ±1.96, effect: interaction between CCI and 2-DG.)

In low glucose conditions (LG-aCSF), post-CCI epileptiform activity was not attenuated (Figure 3.6). These results show that in vitro application of the glycolytic inhibitor 2-DG rapidly attenuates cortical network hyperexcitability 3-5 weeks after TBI.

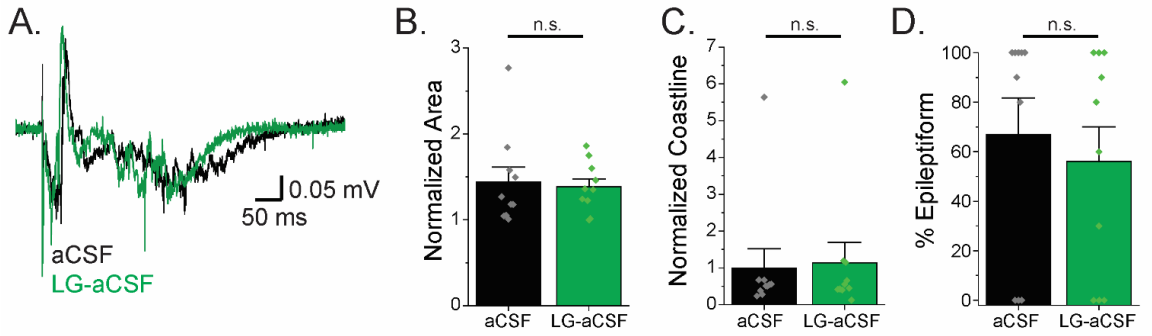

Figure 3.6: Low glucose (LG) conditions do not attenuate epileptiform activity following CCI. A. Representative stimulus-evoked field potentials in an acute cortical slice 3-5 weeks following CCI surgery. **B-C.** Area (B) and coastline (C) measurements from fEPSPs from CCI-injured animals with or without 30 minutes of LG-aCSF. **D.** The percentage of sweeps exhibiting epileptiform activity in slices from CCI animals with or without LG-aCSF treatment. (Error bar = SEM. n = 10 slices from 4 animals. n.s. not significant.)

3.2.4 In vivo 2-DG treatment attenuates epileptiform cortical activity following CCI

We next hypothesized that in vivo 2-DG treatment during a critical period following TBI reduces subsequent cortical hyperexcitability. To test this hypothesis, we treated mice with 2-DG throughout the first week after injury (250 mg/kg or vehicle intraperitoneally, once daily for seven days following CCI or sham surgery) and assessed network hyperexcitability utilizing cortical field recordings. Acute cortical brain slices were prepared 3-5 weeks following the initial surgery (2-4 weeks following the end of 2-DG treatment), when epileptiform activity is expected in the CCI animals [36]. As predicted, sham-injured slices from both treatment groups had normal fEPSPs (Figure 3.7A-B). Consistent with previous studies, acute cortical brain slices from vehicle-treated CCI-injured animals exhibited epileptiform stimulus-evoked fEPSPs (Figure 3.7C).

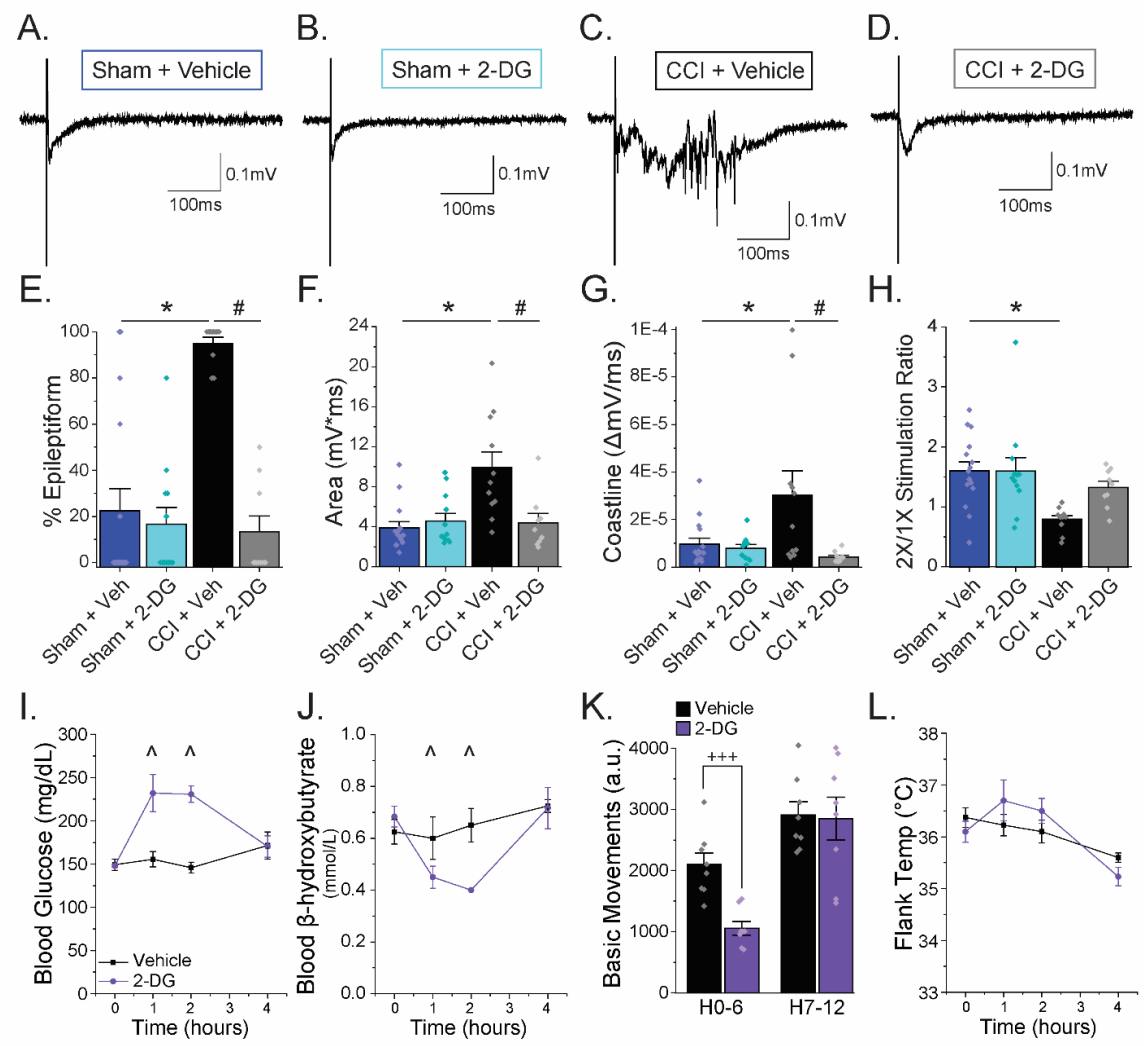

Figure 3.7: In vivo 2-DG treatment following CCI decreases epileptiform activity in acute cortical slices. Animals were given sham or CCI surgery, followed by 1 week of daily intraperitoneal injections of vehicle or 2-DG (250 mg/kg). **A-D.** Representative stimulus-evoked field potentials taken from acute cortical slices 3-5 weeks following sham or CCI surgery, with vehicle or 2-DG treatment. **E.** The percentage of sweeps exhibiting epileptiform activity in sham and CCI-injured animals, with or without 2-DG treatment. **F-G.** Area (F) and coastline (G) of traces taken from sham and CCI-injured animals, with or without 2-DG treatment. **H.** Input-output ratios in each treatment group. **I.** Blood glucose in naïve fasted mice after a single vehicle (black) or 2-DG (purple) injection. **J.** Blood ketone body levels (as measured by β-hydroxybutyrate) after vehicle or 2-DG injection. **K.** Basic locomotor activity in vehicle- or 2-DG-treated animals. **L.** Flank temperature after a single vehicle or 2-DG injection. (Error bar = SEM. n = 9-15 slices from 3 animals/group for field recordings. n = 4 vehicle, 6 2-DG animals for metabolism studies. n = 8 animals/group for locomotor activity. LMM: *t > ±1.96, effect: CCI; #t > ±1.96, effect: interaction between CCI and 2-DG; ^t > ±1.96, effect: 2-DG at each time point. 2-sample t-test: +++p < 0.001)

However, in vivo 2-DG treatment following CCI dramatically attenuated epileptiform fEPSPs (from 95% to 13%) in CCI-injured animals (Figure 3.7D-E). Area and coastline measurements of the evoked fEPSPs following CCI also exhibited significant attenuation with in vivo 2-DG treatment (Figure 3.7F-G).

CCI also disrupts the input/output (I/O) relationship of the cortical network. Cortical I/O responses were assessed by comparing fEPSP area evoked by 1X and 2X threshold stimulation. In the uninjured brain, cortical networks generated graded output in response to increased stimulation. After CCI, however, cortical networks generated all-or-none responses and lacked graded output in response to stimulation (Figure 3.7H). In vivo 2-DG treatment partially restored the disrupted I/O relationship, resulting in graded fEPSP amplitude and area in response to increased stimulation. 2-DG treatment had a large effect size on I/O relationship (0.54 compared to the effect of CCI, -0.81) but did not reach statistical significance by LMM, likely due to the high degree of variability (Figure 3.7H). Together, these experiments show that in vivo 2-DG treatment during the first week after injury attenuates network hyperexcitability and reduces long-term TBI-associated cortical network dysfunction.

3.2.5 In vivo 2-DG treatment transiently affects systemic glucose metabolism, but does not affect body temperature

Since systemic metabolic changes, such as hypothermia, may have independent neuroprotective effects after TBI, we assessed the effects of in vivo 2-DG on whole body metabolism. After a single 2-DG injection (250 mg/kg, intraperitoneal) in fasted animals, blood glucose levels were transiently increased (Figure 3.7I) and β-hydroxybutyrate (a

ketone body) levels were transiently decreased (Figure 3.7J), consistent with decreased glucose utilization and increased ketosis. These changes in blood glucose and β-hydroxybutyrate returned to baseline by 4 hours post-injection. There was also a transient decrease in home cage locomotor activity that resolved to vehicle levels after the first 6 hours post-injection (Figure 3.7K). Importantly, there was no change in flank temperature in 2-DG-injected animals versus vehicle-injected controls (Figure 3.7L), suggesting that hypothermia does not contribute to the neuroprotective effect of 2-DG.

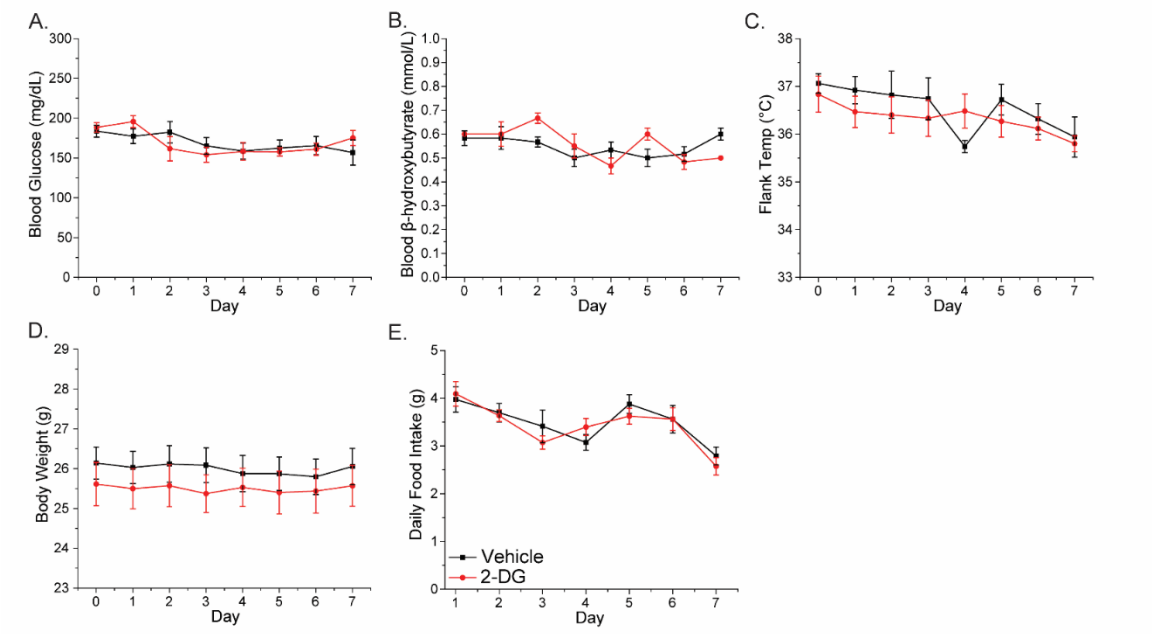

Figure 3.8: 2-DG has no effect on daily blood glucose, blood β-hydroxybutyrate, temperature, body weight, or food intake during a week-long dosing regimen. Animals were injected daily with 2-DG or vehicle. Shown are blood glucose (**A**), β-hydroxybutyrate (**B**), flank temperature (**C**), body weight (**D**), and daily food intake (**E**) measured immediately prior to each daily injection. (Error bar = SEM. n = 6 animals/group.)

Then, daily 2-DG injections were performed in naïve animals for one week to parallel the in vivo dosing regimen post-CCI. Animals were assessed at rest, immediately before their daily 2-DG injection (~24 hours following their most recent injection). There were no changes observed in blood glucose, blood β-hydroxybutyrate, flank temperature, body weight, or daily food intake between vehicle- and 2-DG-treated animals across the entire week of treatment (Figure 3.8). For all experiments reported in this study, in vivo treatment with 2-DG did not affect animal weight or recovery from surgery. These data suggest that there were no significant adaptive metabolic changes across the week-long in vivo 2-DG treatment.

3.2.6 In vivo 2-DG treatment prevents CCI-induced dysregulation of excitatory and inhibitory synaptic activity

TBI causes significant disruption of cortical synaptic activity including increased glutamatergic excitation and reduced GABAergic inhibition of excitatory cortical neurons [36], accordant with network hyperexcitability. Consistent with previous studies, CCI induced a significant increase in mean spontaneous excitatory postsynaptic current (sEPSC) frequency (Figure 3.9A), resulted in a significant leftward shift in the sEPSC inter-event interval cumulative distribution, and had no effect on sEPSC amplitude (Figure 3.9C). Inhibitory synaptic transmission was decreased by CCI, again consistent with previous studies. CCI decreased mean spontaneous inhibitory postsynaptic current (sIPSC) frequency (Figure 3.9G), caused a significant rightward shift in the sIPSC inter-event interval cumulative distribution, and significantly increased mean sIPSC amplitude (Figure 3.9I).

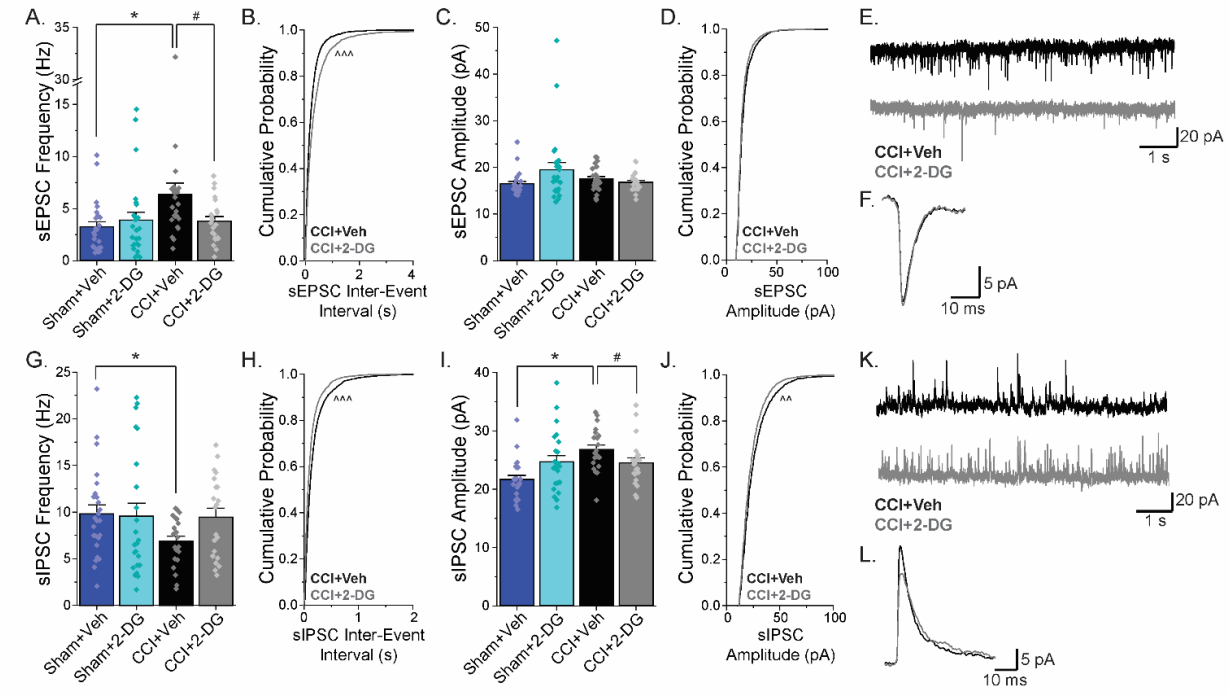

Figure 3.9: In vivo 2-DG treatment attenuates changes in synaptic activity after injury. **A.** Mean sEPSC frequency. **B.** Cumulative distribution of sEPSC inter-event interval. **C.** Mean sEPSC amplitude. **D.** sEPSC amplitude cumulative distribution. **E.** Representative sEPSC traces from vehicle-treated or 2DG-treated CCI brains. **F.** Representative example of sEPSC events (generated by averaging 100 events from a representative trace). **G.** Mean sIPSC frequency. **H.** Cumulative distribution of sIPSC inter-event interval. **I.** Mean sIPSC amplitude. **J.** Cumulative distribution of sIPSC amplitude. **K.** Representative sIPSC traces from vehicle-treated or 2-DG-treated CCI brains. **L.** Representative example of sIPSC events from vehicle-treated or 2-DG-treated CCI brains. (Error bar = SEM. n = 21-26 cells from 5 animals/group. LMM: *t > ±1.96, effect: CCI; #t > ±1.96, effect: interaction between CCI and 2-DG. 2-sample K-S test corrected for multiple comparisons: ^^p < 1E-4; ^^^p < 1E-5)

Consistent with its effects on network hyperexcitability, in vivo 2-DG treatment significantly attenuated CCI-induced increases in excitation. 2-DG treatment reduced mean sEPSC frequency (Figure 3.9A, E) and caused a significant rightward shift in the sEPSC inter-event interval cumulative distribution (Figure 3.9B), with no effect on sEPSC amplitude (Figure 3.9C-D). In vivo treatment with 2-DG also restored inhibitory synaptic transmission after CCI. 2-DG had a large, but not significant, effect on mean

sIPSC frequency (Figure 3.9G), caused a significant leftward shift in the sIPSC inter-event interval cumulative distribution (Figure 3.9H), significantly reduced mean sIPSC amplitude (Figure 3.9I), and caused a leftward shift in the cumulative distribution of sIPSC amplitude (Figure 3.9J). Interestingly, we noted a difference in the distribution of mean sIPSC frequency following CCI; in cells recorded after sham injury, there was consistently a population of neurons (5 out of 25 cells in the Sham+Vehicle group) that received sIPSCs at a high rate (>12 Hz). This population was absent after CCI (0 out of 21 cells in CCI+Vehicle) but was present after in vivo 2-DG treatment (7 out of 21 cells in CCI+2-DG), suggesting that CCI causes a loss of robust network inhibition that is prevented by 2-DG treatment. Together, these data demonstrate that in vivo 2-DG treatment ameliorates network deficits in spontaneous excitatory and inhibitory neurotransmission caused by CCI.

We also examined miniature excitatory and inhibitory postsynaptic currents (mEPSCs or mIPSCs, respectively) following CCI and in vivo 2-DG treatment. Miniature synaptic events were recorded in the presence of tetrodotoxin to block sodium currents (and thus, all action potential firing). There was an increase in the mean frequency and mean amplitude of mEPSCs following CCI (Figure 3.10A, D), although the effect size on mEPSC amplitude was very small. Following in vivo 2-DG treatment, there was a large (but not significant) decrease in mean mEPSC frequency corresponding to a significant rightward shift of the cumulative distribution of the inter-event interval following 2-DG (Figure 3.10A, C). While the interaction between CCI and in vivo 2-DG treatment on mean mEPSC amplitude is statistically significant with LMM, there was no effect of 2-DG on the cumulative distribution of mIPSC amplitude following CCI. These results

suggest that alterations in excitatory synapse number or vesicular release probability (as indicated by the increased mean mEPSC frequency) are attenuated with in vivo 2-DG treatment with minimal effects on mEPSC amplitude (reflecting quantal size).

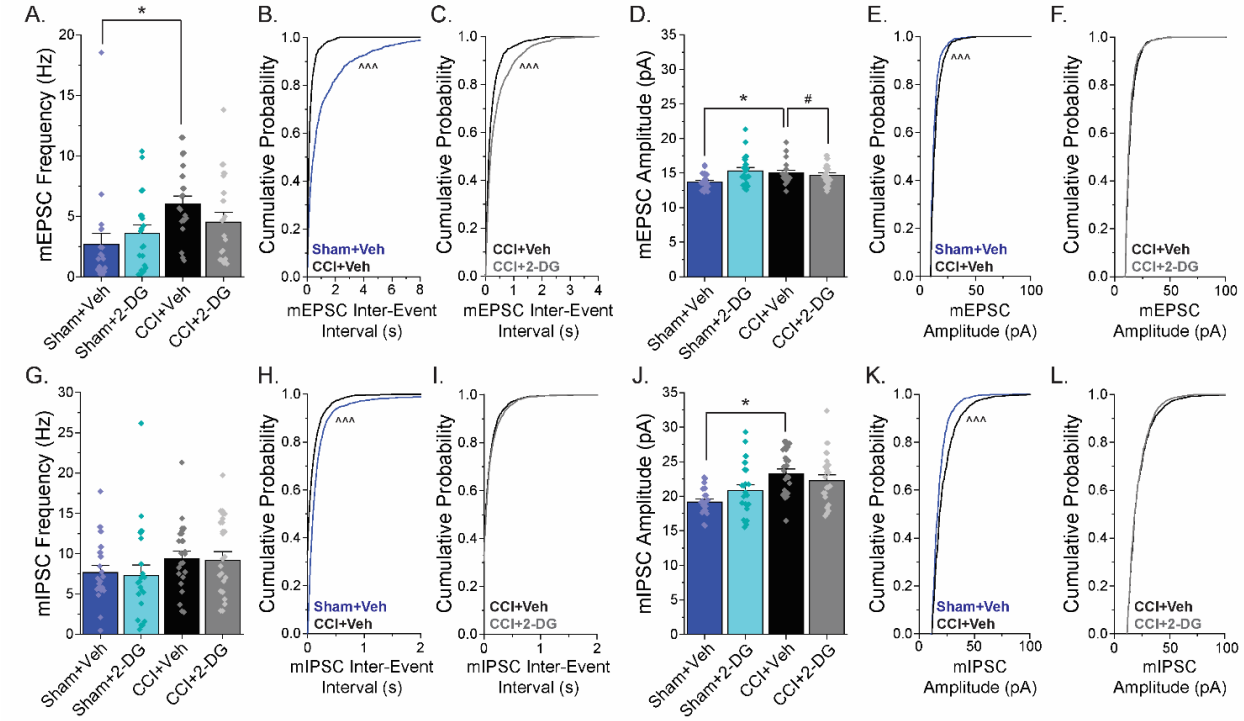

Figure 3.10: CCI and in vivo 2-DG treatment have complex effects on miniature synaptic activity. **A.** Mean mEPSC frequency. **B-C.** Cumulative distributions of mEPSC inter-event interval. **D.** Mean mEPSC amplitude. **E-F.** mEPSC amplitude cumulative distributions. **G.** Mean mIPSC frequency. **H-I.** Cumulative distributions of mIPSC inter-event interval. **J.** Mean mIPSC amplitude. **K-L.** Cumulative distributions of mIPSC amplitude. (Error bar = SEM. n = 19-21 cells from 5 animals/group. LMM: *t > ±1.96, effect: CCI; #t > ±1.96, effect: interaction between CCI and 2-DG. 2-sample K-S test corrected for multiple comparisons: ^^^p < 1E-5)

In contrast, mean mIPSC frequency was not altered by either CCI or in vivo 2-DG treatment (Figure 3.10G). Surprisingly, there was a significant leftward shift in the mIPSC inter-event interval cumulative distribution following CCI, suggesting overall shorter inter-event intervals, and there was no effect of 2-DG on this cumulative

distribution (Figure 3.10H-I). When examining mIPSC amplitude, we observed a significant increase in mean amplitude corresponding to a significant rightward shift in the cumulative distribution of event amplitude after CCI (Figure 3.10J-K). 2-DG treatment had no effect on mIPSC amplitude (Figure 3.10L). In summary, these miniature synaptic activity data indicate that the changes in spontaneous synaptic activity and network hyperexcitability after CCI and 2-DG treatment are not strictly driven by changes in synapse number or synaptic release probability. Not surprisingly, changes in neuronal activity, network organization, and synaptic function all contribute to a complex set of changes that occur following CCI and underly the network-level effects on activity we observe.

3.2.7 In vivo 2-DG treatment attenuates the loss of parvalbumin-expressing interneurons following CCI

Because 2-DG treatment attenuated the development of epileptiform activity and prevented the decrease in sIPSCs after CCI, we hypothesized that it also prevents the loss of parvalbumin-expressing interneurons that had been previously reported [36]. An additional question that we wished to address was whether CCI caused a loss of PV+ cells, or merely a loss of PV protein. To test our hypothesis and address the loss of PV cells versus protein, we used a combination of genetic and immunohistochemical approaches. PV^{Cre} mice, in which Cre-recombinase is expressed under the control of the parvalbumin promoter, were crossed with *Ai9* reporter mice, producing PV^{Cre}*/Ai9* mice which express tdTomato (tdT) in cells containing Cre. This provides a genetic label of PV cells, even if the PV protein itself is lost.

PV^{Cre}*/Ai9* mice underwent CCI or sham surgery and were treated in vivo with 2-DG or vehicle as described above. Brains were prepared for immunohistochemical analysis 3-5 weeks post-CCI. First, lesion volume was approximated across serial sections in CCI animals treated with vehicle or 2-DG. In vivo 2-DG treatment had no significant effect on cavitary lesion volume (2-sample t-test; n = 5 animals/group, p = 0.557). Then, the densities of PV-immunolabeled and tdT-labeled neurons were quantified in five 100-µm-wide rectangular regions of interest (ROIs) in the cortex lateral to the site of CCI injury (or in isotopic cortex in sham animals). Consistent with previous studies [36], the density of PV-immunolabeled cells was significantly reduced in the cortex of vehicle-treated CCI animals relative to sham (Figure 3.11A-E, G). PV+ cell density was significantly reduced in the first 400 µm adjacent to the lesion (Figure 3.11G). A similar result was seen after counting tdT-labeled neurons (Figure 3.11H) although the decrease was significant only in the first 200 µm lateral to the lesion. These results show that CCI causes both a loss of PV cells and a decrease in PV immunoreactivity adjacent to the lesion.

In vivo 2-DG treatment attenuated the loss of PV+ neurons relative to vehicle-treated CCI animals (Figure 3.11F-G). 2-DG prevented PV+ cell loss in the first 300 µm adjacent to the lesion. 2-DG did not globally reduce the loss of tdT+ neurons, although a significant increase in tdT+ neurons was observed in the 100 µm closest to the site of injury (Figure 3.11H), suggesting a focal effect of 2-DG. These results indicate that 2-DG broadly attenuates the loss of PV expression after CCI and focally reduces the loss PV (tdT+) neurons.

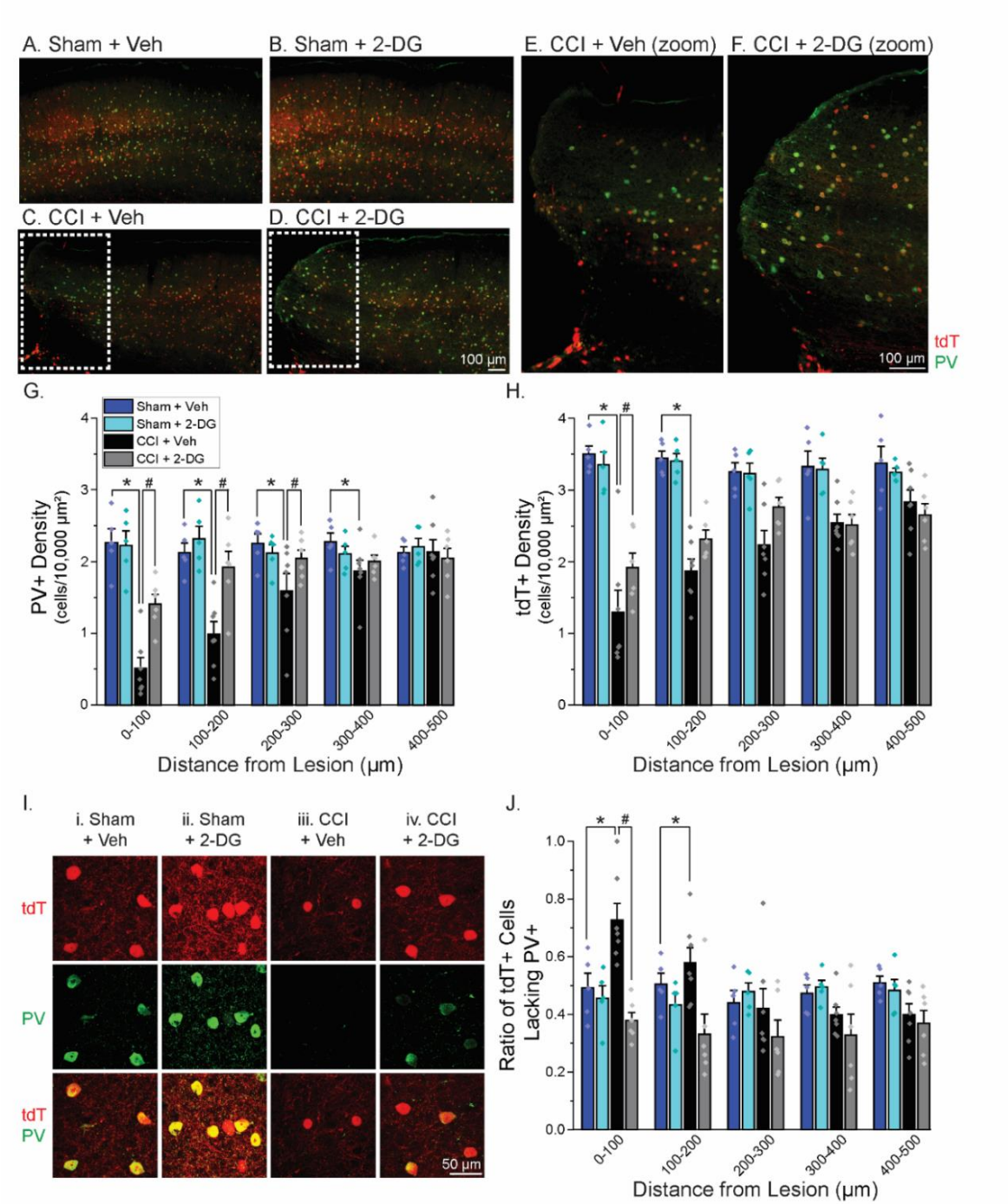

Figure 3.11: In vivo 2-DG treatment attenuates the decrease in PV+ cells in the perilesional cortex. A-D. Representative images with PV (green) and tdT (red – in PV^{Cre} cells) in animals from the different treatment groups, collected 3-5 weeks after sham or CCI surgery. **E-F.** Zoom-in of perilesional area showing loss of colocalized PV+tdT+ cells in the perilesional area after CCI. **G.** Quantification of PV+ cell density in five regions lateral to the CCI cavitary lesion. **H.** Quantification of cells identified with tdT+ in $PV^{Cre}/Ai9$ reporter mice. **I.** Example confocal images of cells in the perilesional

area with genetic tdT expression (red) and PV immunolabel (green). **J.** The density of tdT+ cells not colocalized with PV immunolabel was divided by the total density of tdT+ cells in each ROI to calculate the ratio reported. (Error bar = SEM. n = 5-7 animals/group (3 sections from each animal were analyzed and averaged to generate a single value for each animal). LMM: *t > ±1.96, effect: CCI in each ROI; #t > ±1.96, effect: interaction of CCI and 2-DG in each ROI.)

In order to further examine the effects of CCI and 2-DG on PV cell loss, versus changes in PV protein expression, we assessed the proportion of tdT-labeled neurons that were immune-positive for PV. In sham-injured animals, approximately 50% of tdT-labeled neurons were PV immuno-positive. The abundance of tdT-labeled neurons which lacked PV immunolabeling may be a combination of PV expression below the detection limit of an immunolabeling approach, transient expression of PV during development, and non-specific Cre expression. After CCI, a significantly higher proportion of tdT-labeled neurons lacked PV immunoreactivity (Figure 3.11I-J) with the effect being most prominent in the first 200 μm adjacent to the lesion. This suggests that a sub-set of PV (tdT+) interneurons remain after CCI but lose their expression of PV protein. Because PV is a calcium binding protein that is necessary for physiologic interneuron AP firing, loss of PV expression is consistent with decreased inhibitory function and cortical hyperexcitability [269, 270]. In vivo treatment with 2-DG restored the ratio of PV (tdT+) cells expressing PV to levels seen in sham animals (Figure 3.11J). Together, these results show that CCI causes a loss of PV (tdT+) interneurons and reduces PV expression in remaining PV interneurons. In vivo 2-DG treatment broadly increases PV expression in surviving PV interneurons, consistent with enhanced inhibitory function.

3.3 Discussion

2-DG, a hexokinase inhibitor that reduces glycolytic activity, has been previously explored for its potential neuroprotective, anti-convulsant, and anti-epileptogenic properties, but the mechanisms of its rapid actions on neuronal function are unknown. Here, we demonstrate that 2-DG treatment attenuates excitatory, but not inhibitory, cortical neuron excitability. This provides a potential mechanism by which 2-DG mediates its acute anticonvulsant effects. Furthermore, we show that 2-DG has therapeutic potential to treat traumatic brain injury (TBI). While glycolysis is known to be abnormally elevated acutely following brain injury [119], it is unknown whether early metabolic disruptions contribute to chronic cortical hyperexcitability. Using the CCI model of TBI combined with electrophysiological approaches, we find that excitation onto inhibitory interneurons is elevated 3 days after injury and can be attenuated by acute 2-DG treatment. Finally, in vivo 2-DG treatment during the first week after TBI prevented epileptiform network activity, restored aspects of synaptic function, and reduced parvalbumin-positive inhibitory interneuron loss associated with CCI. Together, our work provides novel insight into acute synaptic dysfunction following TBI, implicates glycolysis in the hyperexcitation of inhibitory interneurons after TBI, and shows that in vivo 2-DG treatment reduces post-traumatic synaptic and network dysfunction.

Our findings, summarized above, demonstrate a complex set of synaptic changes following CCI, in both the acute (Figure 3.4) and chronic (Figure 3.9, 3.10) settings. Acutely after TBI (3 days post-CCI), we observe increased excitation of PV interneurons that we suspect contributes to later inhibitory dysfunction, although our study does not

confirm that interneuron loss and dysfunction occur as a direct result of hyperexcitation. Alternatively, increased excitation of interneurons acutely after CCI may represent a compensatory mechanism to increase inhibitory control of cortical activity in the injured brain. If true, however, one would predict that 2-DG's reduction of IN hyperexcitation would be detrimental to TBI-related outcomes. We did not observe any increases in adverse outcomes, seizures, or mortality during 2-DG treatment in our studies, consistent with 2-DG's known neuroprotective effects and suggesting that acute hyperexcitation of interneurons is, in fact, pathologic.

Next, in the chronic period (3-5 weeks post-CCI), we observed changes in both excitatory and inhibitory synaptic activity that were ameliorated with in vivo 2-DG treatment. Consistent with our previous work [36], CCI increased spontaneous synaptic excitation and decreased spontaneous synaptic inhibiton. Both of these changes were attenauted by in vivo 2-DG treatment, supporting a model in which 2-DG treatment ameliorates synaptic dysfunction after TBI. Miniature excitatory synaptic activity was also elevated following CCI and attenatued by in vivo 2-DG treatment in CCI animals. Interestingly, miniature inhibitory synaptic activity was not affected in our study by either CCI or 2-DG treatment. This is suprising, as we show both decreased sIPSC frequency and loss of PV+ interneurons in the perilesional area. A number of possible mechanisms may be involved. First, sIPSCs and mIPSCs assess all inhibitory inputs, not just those from PV+ interneurons. Thus, compensation by other interneuron subtypes may occur. Second, PV expression is decreased in many remaining PV interneurons after injury. Loss of parvalbumin expression can cause inhibitory dysfunction, hyperexcitability, and worsened seizure phenotype [269, 271, 272], independent of loss

of inhibitory synapses. It is also possible that remaining PV+ interneurons increase their number of synapses to compensate for interneuron cell loss. Finally, a diverse set of other inhibitory changes occur after TBI, including altered chloride transport (reduced KCC2/increased NKCC1 expression [273-277]) and changes in GABA receptor subunit composition and density [278-281]. These mechanisms, among others, could contribute to altered inhibitory circuit function and the complex changes in synaptic and network activity we observe.

Although the exact synaptic mechanisms that mediate network dysfunction after TBI are still incompletely defined, our results demonstrate that in vivo 2-DG treatment significantly ameliorates many of the effects of CCI on synaptic activity. Our study also strongly supports that modulation of metabolism in the injured brain may have therapeutic potential to improve patient outcomes by maintaining proper network function after injury. Further work is required to clarify how early changes in interneuron excitation relate to and may result in long-term network pathology. Specifically, further studies are needed to determine how aberrant excitation of interneurons contributes to changes in parvalbumin expression, altered interneuron function and synaptic output, and interneuron cell loss. In addition, we do not directly demonstrate that in vivo 2-DG treatment reduces brain glycolysis after TBI. 2-DG is well-established as an inhibitor of glycolysis [282] across multiple organ systems, animal models, and disease states [176, 283-289]. We observe acute changes in blood glucose and ketone body levels (Figure 3.7I-J) upon administration of 2-DG, consistent with 2-DG's ability to inhibit glycolysis and decrease glucose utilization. While a recent publication suggests that systemic delivery of 2-DG does not result in appreciable changes in brain hexokinase activity

[184], multiple studies demonstrate that 2-DG treatment broadly inhibits glycolysis in whole brain and brain slices [178-180, 290]. Systemic delivery of 2-DG has been shown to result in transcriptional changes consistent with reduced glycolysis in the brain, including reductions in hexokinase, PGK-1, and LDH-A expression in the rat hippocampus [180]. Furthermore, TBI-associated breach of the blood-brain-barrier [115] may allow greater penetration of 2-DG into the brain, resulting in improved inhibition of brain glycolysis. While we observe robust CNS effects after delivering 2-DG post-CCI, it is possible that they are mediated through a peripheral effect of 2-DG or through a mechanism not directly related to hexokinase inhibition.

From a translational standpoint, the therapeutic rationale to reduce glycolysis after TBI is well-founded on both preclinical and clinical literature [15]. Using PET scanning, studies report that a majority of patients exhibit increased cerebral glucose utilization following severe TBI [119, 120] that later develops into a chronic, hypometabolic state [124, 125, 127]. Additionally, patients with aberrant glucose utilization and network activity during the first week post-TBI have worsened outcomes 6 months later [122]. Preclinical work from multiple animal models of TBI shows early increases in glucose utilization [142, 144, 145, 153, 154] which are activity-dependent [150]. Consistent with focal hyper-glycolysis and network dysfunction, our previous studies show heightened glutamate signaling and PV+ interneuron loss in the peri-injury cortex. Finally, there is abundant evidence supporting the use of the ketogenic diet (which results in decreased glycolysis and increased ketosis) as a strategy to manipulate neural network activity in animals and humans (reviewed in [54, 162-167]). While dietary approaches and glycolytic inhibition have shown efficacy in controlling seizure activity, manipulations of

glucose metabolism have not yet been harnessed effectively in the context of TBI. In our studies, we did not find evidence of chronic changes in animal health, systemic metabolism, or body temperature (Figure 3.8) over the course of 2-DG treatment. This is important as long-term exposure to 2-DG (>2 weeks) has been previously associated with cardiotoxicity [240, 291] and hypothermia alone may neuroprotective after TBI [13, 197, 292]. 2-DG is already in use clinically to limit tumor growth in cancer patients (based on the Warburg effect, which describes increased glycolytic activity in neoplastic cells), and short-term treatments are well-tolerated in humans [176]. This underscores that short-term use of 2-DG as a disease-modifying agent is a feasible clinical strategy.

A particularly important finding of our study is the cell type-specific coupling of metabolism to neuronal excitability. Our results are concordant with published studies showing that GABAergic interneurons have unique energetic requirements and are known to be enriched with mitochondria for energy production via oxidative phosphorylation (reviewed in [293]). Our findings suggest that glutamatergic pyramidal neurons rely on glycolysis to maintain their intrinsic excitability. While glycolysis is traditionally thought to occur mainly in astrocytes (astrocyte-neuron lactate shuttle model [294]), there is significant evidence that glycolysis also occurs in neurons. Multiple glycolytic enzymes are enriched in neurons relative to astrocytes [50, 73] and recent work implicates increased neuronal glycolysis in conditions of heightened energy need [80, 81]. Thus, increased energetic requirements, glycolytic flux, and cell type-specific neuronal activity may all be interdependent during the acute period following TBI, and deserve further investigation. In future studies, we hope to explore the molecular mechanisms of decreased excitability in excitatory neurons in the presence of 2-DG. We

found that decreased excitability in excitatory neurons was associated with significantly decreased membrane resistance, suggesting that the opening of specific ion channels may underly the change in excitability. A possible candidate for this mechanism is an ATP-dependent potassium channel, as K_{ATP} channels have been previously shown to link neuronal energy status with excitability [86, 188, 191] and have been implicated in network hyperexcitability and epilepsy [189, 295]. A deeper understanding of metabolic demands following TBI and how different CNS cells utilize energy will aid in the development of metabolic approaches to manipulate neural network activity with greater precision.

In summary, we report that in vitro and in vivo 2-DG treatments attenuate multiple pathologic cellular and network changes following CCI in mice. Future work is needed to investigate the use of 2-DG to prevent injury pathology, including in diffuse or concussive mechanisms of TBI, in larger animal models, and in pilot clinical trials. Additionally, studies are needed to explore whether reducing cortical hyperexcitability is sufficient to ameliorate patient-oriented outcomes including mortality, seizure frequency/severity in post-traumatic epilepsy, and cognitive/behavioral outcomes. Finally, improving our understanding of the specific energy demands of the neuronal activity, hemodynamic response, and inflammation that occur after TBI will enable us to harness metabolic manipulations to reduce brain injury-associated pathologies.

3.4 Materials and Methods

3.4.1 Study Design

3.4.1.1 Basic Design

All experiments were hypothesis-driven, rigorously designed, and performed in a controlled laboratory environment. Sample size was set based on power analysis calculations using GPower to provide power > 0.80 for $\alpha = 0.05$ for most experiments. We also utilized standards in the field, i.e. ≥3 animals per group, to ensure proper statistical power.

3.4.1.2 Randomization and blinding

Mice were randomized to groups within each experiment (sham vs. CCI; vehicle vs. 2-DG). All studies were blinded at the level of data analysis. Data was numerically encoded and analyzed by a trained experimenter blinded to condition. To further prevent bias during analysis, automated analysis approaches were utilized for all synaptic data sets (Figures 3.9, 3.10). After initial analysis was finalized, the blinding was lifted to compare data across groups. Because CCI lesions are easily discernable from sham and in vitro drug applications cannot be reasonably blinded, blinding during data collection of electrophysiological experiments was not feasible (Figures 3.2, 3.4, 3.5). Due to constraints of animal tracking, blinding was not performed during in vivo drug injections (Figures 3.7, 3.11). Immunohistochemical and anatomical experiments were blinded throughout the data collection process (Figure 3.11).

3.4.1.3 Exclusion criteria and statistical approach

Each experiment had one primary endpoint based on the experimental design. We did not define rules for stopping data collection outside of humane endpoints based on

animal protocols. Data was excluded based on quality control of whole-cell recordings (recordings were excluded when access resistance changed more than 20% during an experiment). Outliers were removed in the context of fEPSP recordings due to inherent variability in the responses evoked with this technique (Figures 3.5, 3.7). Outliers were defined as slices with response area > 2 standard deviations from the group mean and were excluded from the subsequent analysis. The number of experimental replicates is included in the figure captions and in Table 3.1. The number of individual animals, cells, or slices were factored into our analysis using a linear mixed model approach. This approach includes terms to account for inter- and intra-animal variability.

3.4.2 Animals

All animal procedures were performed in accordance with the Tufts University School of Medicine's Institutional Animal Care and Use Committee. All experiments were performed on adult mice. C57/BL6 were obtained from Jackson Labs (Strain #000664), Charles River Laboratories (Strain #027), or bred in-house. PV^{Cre} (Stock #017320), *Ai9* (Stock #07909), and *G42* (Stock #007677) mice were obtained from Jackson Laboratories. Animals were kept on a standard 12-hour light cycle and fed *ad libitum* with regular chow diet and water. Male mice were used for all experiments, unless noted.

3.4.3 Controlled cortical impact

Traumatic brain injury was modeled with controlled cortical impact (CCI), as previously described [36, 296]. Briefly, 10-14-week-old male mice were anesthetized using inhaled isoflurane in oxygen (4% for induction, 2% for maintenance). Following

placement in a Kopf stereotaxic frame, the surgical area was sterilized and a vertical, midline skin incision was made. A 5 mm craniectomy was performed lateral to midline, between bregma and lambda (over the left somatosensory cortex) and the skull flap was removed. The surgical field was flushed with sterile saline throughout the procedure to cool the surgical area during the craniectomy drilling. Impact was performed with a Leica Benchmark Stereotaxic Impactor, using a 3 mm diameter piston, 3.5 m/s velocity, 400 ms dwell time, and 1 mm depth. After the CCI procedure, sutures were used to close the incision. The bone flap was not replaced in order to accommodate swelling after the procedure and to prevent pressure-induced damage to the injury site. Sham animals received the anesthesia and craniotomy drilling, but did not receive the CCI. Animals were singly housed following surgery until time of sacrifice.

3.4.4 In vivo 2-DG treatment

Animals were injected intraperitoneally (I.P.) with 250 mg/kg 2-DG dissolved in sterile saline to a final injection volume of 200 µL per dose. Vehicle injections consisted of 200 µL of sterile saline per dose. For the in vivo 2-DG treatment paradigm, the first dose was administered ~20 minutes after CCI or sham surgery, and the doses were continued daily for 7 days at the same time of day. Animal weight was recorded daily to monitor animal health.

3.4.5 Acute brain slice preparation

Brain slices were prepared as previously described [36, 297]. Briefly, mice were anesthetized in an isoflurane chamber and then decapitated by guillotine. Brains were rapidly removed and placed in chilled slicing solution (in mM: 234 sucrose, 11 glucose,

24 $NaHCO_3$, 2.5 KCl, 1.25 NaH_2PO_4, 10 $MgSO_4$, 0.5 $CaCl_2$) equilibrated with 95% O_2/5% CO_2. The brain was then glued to the slicing stage of a Leica VT1200S vibratome and the slicing chamber was filled with chilled slicing solution, again equilibrated with 95% O_2/5% CO_2. Coronal slices (300 or 400 μm-thick) were taken at 0.05 mm/s and hemisected. The slices were placed in a chamber filled with artificial cerebrospinal fluid (aCSF, in mM: 126 NaCl, 26 $NaHCO_3$, 3 KCl, 1.25 NaH_2PO_4, 2 $MgCl_2$, 2 $CaCl_2$, 10 glucose) equilibrated with 95% O_2/5% CO_2. The chamber with the acute cortical slices was incubated in a water bath at 34°C for one hour, and then stored at room temperature until recording.

3.4.6 In vitro treatment of acute cortical slices with 2-DG

For 2-DG wash-on experiments, 2-DG-aCSF solution was prepared by adding 8 mM 2-DG and removing 8 mM glucose from the standard aCSF recipe (to maintain solution osmolarity, for a final concentration of 2 mM glucose, 8 mM 2-DG). Baseline field or whole-cell recordings were obtained, and then the regular aCSF perfusate was replaced with 2-DG-aCSF for the remaining recordings. For low glucose wash-on experiments, aCSF containing 2 mM glucose and 8 mM sucrose (an inert sugar) was prepared (LG-aCSF), and LG-aCSF was washed on following baseline field or whole-cell recording collection.

3.4.7 Whole-cell recordings

Acute cortical slices were placed in a submersion recording chamber of an Olympus BX51 microscope with continuous perfusion of oxygenated aCSF at 32°C. Layer V pyramidal neurons were visually identified with infrared differential interference contrast microscopy, and fast-spiking parvalbumin-positive cortical interneurons were

identified based on GFP expression in *G42* mice (Jax Stock #007677). Whole-cell recording mode was achieved with a borosilicate glass electrode (3-5 MΩ) filled with internal solution optimized for each experiment (described below). Access resistance, membrane resistance, and capacitance were monitored throughout each experiment. Cells with >20% change in access resistance during the experiment were excluded from analysis. Data were collected using an Axon Multiclamp 700B amplifier, Digidata 1440A digitizer, and pClamp software.

For recordings of synaptic activity, the internal utilized was, in mM: 140 CsMs, 10 HEPES, 5 NaCl, 0.2 EGTA, 5 QX314, 1.8 MgATP, 0.3 NaGTP, pH = 7.25, mOsm = 290. The recording electrode was placed within 200 μm of the lateral edge of the cavitary cortical lesion. Spontaneous EPSCs and IPSCs were recorded by voltage-clamping the cell at -70 and 0 mV, respectively, for 2 minutes. Synaptic activity analysis was performed using MiniAnalysis (SynaptoSoft) with the experimenter blinded to experimental group.

For current injection experiments, the internal utilized was, in mM: 120 KGluconate, 11 KCl, 10 HEPES, 10 EGTA, 2 $MgCl_2$, 2 MgATP, 0.3 NaGTP, pH = 7.3, mOsm = 290. The perfused aCSF also included DNQX (20 μM), CPP (10 μM), and gabazine (10 μM) to block synaptic activity. Current injection steps were applied to each cell (ranging from -200 → 400 pA in 25 pA steps) and cell type was confirmed using AP shape and firing rate.

3.4.8 Field recordings

Brain slices were placed in an interface chamber perfused with 34°C, oxygenated aCSF at a rate of 2 mL/min. A tungsten stimulating electrode was placed at the layer VI-

white matter boundary to stimulate ascending white matter tracts. A borosilicate glass micropipette (pulled to a resistance of ~1 MΩ) was filled with aCSF and placed in the corresponding area of layer V cortex directly above the stimulating electrode. Recordings were performed in the perilesional cortex (within 100 μm of the injury site) or in isotopic cortex in sham animals. Electrical stimulus (8-25 μA, 100 μs pulse length) was delivered using a stimulus isolator (World Precision Instruments) at 30 second intervals. The signal was amplified with a Multiclamp 700A amplifier, digitized with a Digidata 1322A digitizer (sampling rate = 20 kHz), and recorded with pClamp software (Molecular Devices). Threshold stimulus intensity was defined as the minimal required stimulus to obtain a detectable field response (≥ 0.05 mV). "2X threshold" was defined by doubling the threshold stimulus intensity for a given slice.

3.4.9 Analysis of field recordings

Evoked field potentials were analyzed using pClamp software and MATLAB. First, traces were adjusted by subtracting the baseline (the average amplitude directly before the stimulus), imposing a low-pass filter (Bessel 8-pole, 1000 Hz cutoff), and filtering for electrical 60 Hz noise. The area of the field potential was measured by integrating the charge transfer in the first 250 ms following the stimulus. Coastline measurements describe the relative amount of high-frequency activity in the field response and were measured by summing the distance between each point taken every 50 μs over a 250 ms time window following the stimulus. The percentage of epileptiform sweeps for a given slice was determined by counting the number of field potentials that exhibited epileptiform activity (prolonged, high frequency, and high amplitude) out of 10 total sweeps (over a 5 minute period).

3.4.10 Immunohistochemistry

Animals were transcardially perfused with 100 mL of phosphate-buffered saline (PBS) followed by 100 mL of 4% paraformaldehyde (PFA) in 0.4 M phosphate buffer (PB). Brains were dissected out, placed in 4% PFA in PB overnight, and then moved to a 30% sucrose solution for 3 days. Forty μm thick coronal slices were taken on a Thermo Fisher Microm HM 525 cryostat. For CCI or sham animals, the brains were serial sectioned, so that each collection well contained a representative set of coronal sections throughout the entire CCI lesion, with each section 400 μm apart from the next. Slices were washed with PBS and then incubated in blocking buffer (10% normal goat serum (NGS), 5% bovine serum albumin (BSA) in PBS with 0.2% Triton X-100 (PBS-T)) at room temperature for 1 hour. The slices were incubated overnight at 4°C with primary antibody in PBS-T with 5% NGS/1% BSA. The primary antibodies used were as follows: parvalbumin (PV; mouse; Swant PV235; 1:1000 for Figure 3.11, 1:2000 for Figure 3.1), Green Fluorescent Protein (GFP; chicken; Abcam Ab13970; 1:1000), Glutamate decarboxylase 67 (GAD67; mouse; Millipore MAB5406; 1:10000), Somatostatin (SST; rat; Millipore MAB354; 1:100), and Calretinin (CR; mouse; Swant 6B3; 1:5000). Then slices were washed with PBS and incubated with secondary antibody (anti- mouse, rat, or chicken antibodies tagged with Alexa 488, Cy3, or 647, applied at 1:500) in PBS-T with 5% NGS/1% BSA for 2 hours at room temperature. Finally, slices were rinsed with PBS and mounted, in anatomical order, onto slides using Vectashield with DAPI.

Imaging for cell counting was performed using a Keyence epifluorescence microscope with a 10x or 20x optical zoom. Additional images for Figure 3.11 were taken on a Leica SPE confocal microscope with a 63x oil objective; additional images for

Figure 3.1 were taken on a Nikon A1R confocal microscope with a 40x oil objective (Olympus). For each experiment, identical laser and capture parameters were utilized across all experimental groups.

3.4.11 Analysis of imaging data

Image analysis was performed using Fiji/ImageJ software. For Figure 3.11, 5 regions of interest (ROIs) were drawn lateral to the edge of the cavitary CCI lesion, with each ROI 100 µm wide. PV+ and tdTomato (tdT)+ cells were counted independently, by an experimenter blinded to treatment group. The cell counts were then divided by the area of the selected region to find the cell density. The number of PV+tdT+ colocalized cells was determined by comparing the locations of cell bodies selected in the individual PV+ and tdT+ counting phases. Three sections from each brain (representing the same anatomical regions across all subjects) were quantified and averaged to obtain a single cell density value per cell type in each ROI in each animal. For Figure 3.1, GFP+ cells were identified manually in layer V-VI cortex of sections from *G42* mice, and then examined for their co-labeling with PV, GAD67, SST, or CR immunolabels.

Lesion volume was evaluated in >10 serial sections from each animal, mounted and imaged in anatomical order. A blinded experimenter traced the size of the cavitary lesion in each section and the area of missing tissue was recorded. Each area was multiplied by 400 µm (the distance between the serial sections) to estimate the lesion volume.

3.4.12 Metabolic studies

Blood glucose was measured using a OneTouch glucose meter and blood β-hydroxybutyrate was measured using a PrecisionXtra Ketone Monitor with blood taken

from the tail. Flank temperature was measured using a subcutaneous temperature probe (BioMedic Data Systems Implantable Electronic ID Transponders IPTT-300). Food intake was measured by subtracting the final weight from the initial weight of the chow during the indicated study period. Home cage locomotor activity was measured utilizing a photobeam-break system (Tufts Behavior Core). Animals were fasted for 16-18 hours before acute measurements following 2-DG injection (Figure 3.6).

3.4.13 Statistical analysis

Most experiments used a 2 X 2 factorial design. To assay the statistical significance of each factor (fixed effect) and the interaction between factors, we performed linear mixed model (LMM) analysis (see Table 3.1 and Supplementary Methods, [298]). For comparison of cumulative distributions of inter-event interval or amplitude of synaptic events, we utilized a 2-sample Kolmogorov-Smirnov test with α level corrected for multiple comparisons. For analyzing home cage locomotor activity and lesion volume, we used a 2-sample Student's t-test (2-tailed) with $\alpha = 0.05$.

3.4.14 Study approval

All animal procedures were performed in accordance with (and approved by) the Tufts University School of Medicine's Institutional Animal Care and Use Committee. No human subjects or tissues were used in this study.

3.4.15 Drugs and reagents

Salts were obtained from Sigma-Aldrich or Fisher Scientific. Glucose was obtained from Fisher Scientific. 2-deoxy-D-glucose and DNQX were obtained from Sigma-Aldrich. CPP was obtained from Abcam. Gabazine was obtained from Tocris.

3.5 Author Contributions

CD and JK conceived of and designed experiments examining 2-DG's effects on neuronal excitability and synaptic activity. CD, DC, and JK conceived of and designed experiments examining 2-DG's effects on epileptiform activity and interneuron density. CD, JK, CL, and DK conceived of and designed experiments examining effects of 2-DG on metabolism. JK performed experiments and analyzed the data for Figures 3.2, 3.4, 3.9, 3.11, 3.3, 3.6, and 3.10. DC performed experiments for Figures 3.5 and 3.7A-H; DC and JK analyzed the data for Figures 3.5 and 3.7A-H. JK and CL performed metabolic experiments and analyzed the data for Figures 3.7I-L and 3.8. MS performed experiments and analyzed the data for Figure 3.1. FN performed all LMM statistical analysis (Tables 3.1-2). JK and CD wrote first draft of manuscript; comments from all authors were incorporated into the final draft.

3.6 Acknowledgments

We would like to thank Dr. Christian Bjorbaek for his helpful feedback on the manuscript and Dr. Maribel Rios and Dr. Jamie Maguire for their helpful comments. We would also like to thank Dominique Ameroso for her assistance with confocal imaging for Figure 3.11.

3.6.1 Funding

This work was supported by the National Institute of Neurological Disorders and Stroke [R21-NS098009 (CD) and F31-NS101741(JK)] and the United States Department of Defense (W81XWH-16-ERP-IDA).

3.6.2 Competing interests

There are no competing interests to declare.

3.7 Supplementary Methods

3.7.1 Linear mixed model analysis

For most of the statistical analysis, we utilized linear mixed model (LMM) analysis. This approach estimates the effect size of each factor while accounting for intra- and inter-animal variability. LMMs were fitted with random intercepts to assess for the correlation between repeated measurements on the same mouse, and experiment-specific effects were analyzed for statistical significance. t values > 1.96 and < −1.96 were considered to be statistically significant and corresponded to 95% confidence intervals that did not cross zero. Each LMM examined both main fixed effects and interactions between the effects.

Experiments with a traditional 2 X 2 factorial design (including those for Figures 3.5, 3.7, and 3.9) used LMM to examine fixed effects of CCI, 2-DG treatment, and the interaction between these two effects. To compare input-output curves in Figure 3.2, the fixed effects were current injection, 2-DG treatment, and the interaction between the two effects. LMM was also utilized to compare excitatory and inhibitory neurons in Figure 3.2, by examining cell type as the fixed effect.

In Figure 3.4, the statistical approach also paralleled the experimental design. The primary experimental question was whether synaptic activity onto interneurons was altered acutely after CCI (as this had not been shown previously); thus “Stage 1” of the

statistical approach was to examine CCI as the solitary fixed effect. Then, in "Stage 2" of the experiment and statistical analysis, we examined the effects of in vitro 2-DG wash-on to slices taken from either CCI or sham animals (and thus used both CCI and 2-DG as fixed effects).

In Figure 3.11, there was another fixed effect (ROI), introduced as a categorical variable. We performed LMM with fixed effects of CCI, 2-DG, ROI, and interactions between each of these. Comparisons were made with ROI5 (the furthest region from the CCI lesion) as the reference point. To further interpret these complex results, we utilized LMM with the Type III analysis of variance (ANOVA) test with Satterthwaite's method to assess the global significance of "ROI" as a single factor instead of each ROI as an independent factor relative to ROI5. Thus, the Type III ANOVA reports global effects across all ROIs (Table 3.2).

3.7.2 Cumulative distribution generation

Cumulative distributions were generated by randomly selecting 100 events from each recording to ensure that data from more active cells were not more heavily weighted than data from cells with fewer events. Random event selection was accomplished using a custom-written MATLAB script. Within each treatment group, randomly selected events from each cell were pooled to generate a single cumulative distribution, and distributions were compared using a 2-sample Kolmogorov-Smirnov (K-S) test. To account for the large degrees of freedom associated with comparing distributions and to prevent false positives, we decreased α to 0.001. We further corrected for repeated comparisons when doing multiple 2-sample K-S tests on the same data set by dividing α by 6 possible comparisons across the four treatment groups (final α = 1.67E-4).

Linear Mixed Model Effects											
Figure	**N**	**Fixed effect**	**Coefficient**	**SE**	**t value**	**Significant**	**Fixed effect**	**Coefficient**	**SE**	**t value**	**Significant**
1	**Excitatory:** n=14 cells from 9 animals **Inhibitory:** n=13 cells from 10 animals	**Excitatory Neuron Input/Output** Units: # APs					**Inhibitory Interneuron Input/Output** Units: # APs				
		Current Injection	0.03133	0.001336	23.451	*	Current Injection	0.14475	0.008215	17.62	*
		2-DG *(in vitro)*	0.273077	0.456739	0.598		2-DG *(in vitro)*	2.522917	2.808498	0.898	
		Interaction Current/2-DG	-0.007801	0.001889	-4.129	*	Interaction Current/2-DG	-0.005598	0.011618	-0.482	
		ΔRheobase (excitatory versus inhibitory) Units: pA					**%ΔR$_{mem}$ (excitatory versus inhibitory)** Units: % change				
		Cell Type	75.687	26.982	2.805	*	Cell Type	-38.62%	11.14%	-3.468	*
		ΔRMP (excitatory versus inhibitory) Units: mV									
		Cell Type	1.827	1.542	1.184						
2	**Sham+aCSF:** n=17 cells **Sham+2-DG:** n=11 cells **CCI+aCSF:** n=20 cells **CCI+2-DG:** n=15 cells **4 animals/group**	**Frequency - sEPSCs onto INs (PID3)** Units: Hz					**Amplitude - sEPSCs onto INs (PID3)** Units: pA				
		Stage 1: CCI only	2.559	1.0263	2.493	*	*Stage 1: CCI only*	3.144	1.773	1.773	
		Stage 2: CCI + 2-DG Effects					*Stage 2: CCI + 2-DG Effects*				
		CCI	2.559	1.619	1.581		CCI	2.653	2.251	1.178	
		2-DG *(in vitro)*	2.387	1.272	1.877		2-DG *(in vitro)*	-1.709	1.619	-1.056	
		Interaction CCI/2-DG	-5.148	1.696	-3.036	*	Interaction CCI/2-DG	-2.815	2.158	-1.304	
3	**Sham:** n=6 slices from 3 animals **CCI:** n=10 slices from 6 animals	**fEPSP % Epileptiform - *In vitro* 2-DG treatment** Units: % sweeps					**fEPSP Area - *In vitro* 2-DG treatment** Units: mV*ms				
		CCI	90.20%	7.27%	12.412	*	CCI	3.1432	1.4637	2.147	*
		2-DG *(in vitro)*	-2.36E-16	6.45%	0		2-DG *(in vitro)*	0.8189	1.2192	0.672	
		Interaction CCI/2-DG	-72.00%	8.16%	-8.825	*	Interaction CCI/2-DG	-4.6187	1.5157	-3.047	*
		fEPSP Coastline - *In vitro* 2-DG treatment Units: ΔmV/ms									
		CCI	1.23E-05	4.05E-06	3.034	*					
		2-DG *(in vitro)*	5.36E-06	3.48E-06	1.542						
		Interaction CCI/2-DG	-1.67E-05	4.32E-06	-3.859	*					
4	**Sham+Veh:** n=15 slices **Sham+2-DG:** n=12 slices **CCI+Veh:** n=10 slices **CCI+2-DG:** n=9 slices **3 animals/group**	**fEPSP % Epileptiform - *In vivo* 2-DG treatment** Units: % sweeps					**fEPSP Area - *In vivo* 2-DG treatment** Units: mV*ms				
		CCI	67.50%	12.13%	5.566	*	CCI	6.0403	1.3315	4.537	*
		2-DG *(in vivo)*	-5.83%	11.83%	-0.493		2-DG *(in vivo)*	0.6882	1.2991	0.53	
		Interaction CCI/2-DG	-59.72%	18.26%	-3.27	*	Interaction CCI/2-DG	-6.2079	1.9901	-3.119	*
		fEPSP Coastline - *In vivo* 2-DG treatment Units: ΔmV/ms					**fEPSP Input/Output - *In vivo* 2-DG treatment** Units: ratio				
		CCI	2.05E-05	7.58E-06	2.701	*	CCI	-0.81373	0.23292	-3.494	*
		2-DG *(in vivo)*	-1.97E-06	7.65E-06	-0.258		2-DG *(in vivo)*	-0.01304	0.23067	-0.057	
		Interaction CCI/2-DG	-2.39E-05	1.14E-05	-2.102	*	Interaction CCI/2-DG	0.5443	0.34703	1.568	
	Vehicle: n=4 animals **2-DG:** n=6 animals	**Blood Glucose - single 2-DG injection** Units: mg/dL					**Blood β-hydroxybutyrate - single 2-DG injection** Units: mmol/L				
		Interaction (Hour 1)/2-DG	78.083	26.131	2.988	*	Interaction (Hour 1)/2-DG	-0.20833	0.08598	-2.423	*
		Interaction (Hour 2)/2-DG	86.5	26.131	3.31	*	Interaction (Hour 2)/2-DG	-0.30833	0.08598	-3.586	*
		Interaction (Hour 4)/2-DG	0.25	26.131	0.01		Interaction (Hour 4)/2-DG	-0.06667	0.08598	-0.775	
		Flank Temperature - single 2-DG injection Units: °C									
		Interaction (Hour 1)/2-DG	0.75	0.50827	1.476						
		Interaction (Hour 2)/2-DG	0.675	0.50827	1.328						
		Interaction (Hour 4)/2-DG	-0.09167	0.50827	-0.18						
5	**sEPSCs:** n=22-26 cells/group from 5 animals/group **sIPSCs:** n=21-25 cells/group from 5 animals/group	**Frequency - sEPSCs onto pyramidal neurons (PID21-35)** Units: Hz					**Amplitude - sEPSCs onto pyramidal neurons (PID21-35)** Units: pA				
		CCI	3.0884	1.0952	2.82	*	CCI	1.151	1.551	0.742	
		2-DG *(in vivo)*	0.654	1.1057	0.591		2-DG *(in vivo)*	3.066	1.555	1.972	*
		Interaction CCI/2-DG	-3.1991	1.5744	-2.032	*	Interaction CCI/2-DG	-3.902	2.215	-1.762	
		Frequency - sIPSCs onto pyramidal neurons (PID21-35) Units: Hz					**Amplitude - sIPSCs onto pyramidal neurons (PID21-35)** Units: pA				
		CCI	-2.9437	1.4551	-2.023	*	CCI	5.504	1.56	3.528	*
		2-DG *(in vivo)*	-0.258	1.4203	-0.182		2-DG *(in vivo)*	2.97	1.533	1.938	
		Interaction CCI/2-DG	2.8493	2.0781	1.371		Interaction CCI/2-DG	-5.487	2.21	-2.483	*
6	3 slices analyzed to generate 1 average value per animal **Sham+Veh:** 5 animals **Sham+2-DG:** 5 animals **CCI+Veh:** 7 animals **CCI+2-DG:** 6 animals	**PV+ Density** Units: cells/10,000 μm^2					**tdT+ Density** Units: cells/10,000 μm^2				
		Interaction CCI/ROI1	-1.771	0.2083	-8.501	*	Interaction CCI/ROI1	-1.665	0.2567	-6.487	*
		Interaction CCI/ROI2	-1.148	0.2083	-5.513	*	Interaction CCI/ROI2	-1.027	0.2567	-4	*
		Interaction CCI/ROI3	-0.6815	0.2083	-3.271	*	Interaction CCI/ROI3	-0.4762	0.2567	-1.855	
		Interaction CCI/ROI4	-0.4185	0.2083	-2.009	*	Interaction CCI/ROI4	-0.2377	0.2567	-0.926	
		Interaction CCI/2-DG/ROI1	1.111	0.2997	3.707	*	Interaction CCI/2-DG/ROI1	0.8247	0.3693	2.233	*
		Interaction CCI/2-DG/ROI2	0.9103	0.2997	3.037	*	Interaction CCI/2-DG/ROI2	0.532	0.3693	1.44	
		Interaction CCI/2-DG/ROI3	0.7652	0.2997	2.553	*	Interaction CCI/2-DG/ROI3	0.6053	0.3693	1.639	
		Interaction CCI/2-DG/ROI4	0.4751	0.2997	1.585		Interaction CCI/2-DG/ROI4	0.5779	0.3693	0.156	
		PV+ tdT+ Colocalized Density Units: cells/10,000 μm^2					**Ratio of tdT+ Cells Lacking PV+** Units: ratio				
		Interaction CCI/ROI1	-1.393	0.1829	-7.614	*	Interaction CCI/ROI1	0.364877	0.05684	6.419	*
		Interaction CCI/ROI2	-0.9167	0.1829	-5.011	*	Interaction CCI/ROI2	0.191243	0.05684	3.365	*
		Interaction CCI/ROI3	-0.5225	0.1829	-2.856	*	Interaction CCI/ROI3	0.091818	0.05684	1.615	
		Interaction CCI/ROI4	-0.248	0.1829	-1.356		Interaction CCI/ROI4	0.027345	0.05684	0.481	
		Interaction CCI/2-DG/ROI1	0.761	0.2632	2.892	*	Interaction CCI/2-DG/ROI1	-0.336425	0.081767	-4.114	*
		Interaction CCI/2-DG/ROI2	0.5429	0.2632	2.063	*	Interaction CCI/2-DG/ROI2	-0.157418	0.081767	-1.925	
		Interaction CCI/2-DG/ROI3	0.6884	0.2632	2.616	*	Interaction CCI/2-DG/ROI3	-0.139133	0.081767	-1.702	
		Interaction CCI/2-DG/ROI4	0.2361	0.2632	0.897		Interaction CCI/2-DG/ROI4	-0.087048	0.081767	-1.065	

Table 3.1: Linear mixed model results, organized by figure.

Type III Analysis of Variance with Satterthwaite's Method			
Data	**Effect/Interaction**	**p value**	**Signficant**
PV+ Density	CCI	1.83E-04	*
	2-DG	0.074809	
	ROI	1.27E-11	*
	CCI/ROI	5.83E-15	*
	2-DG/ROI	1.21E-04	*
	CCI/2-DG	0.058903	
	CCI/2-DG/ROI	0.002792	*
tdT+ Density	CCI	6.07E-09	*
	2-DG	0.35164	
	ROI	1.02E-06	*
	CCI/ROI	1.48E-11	*
	2-DG/ROI	0.09617	
	CCI/2-DG	0.10985	
	CCI/2-DG/ROI	0.11161	
PV+ tdT+ Colocalized Density	CCI	0.0037177	*
	2-DG	0.0729436	
	ROI	9.72E-09	*
	CCI/ROI	7.91E-15	*
	2-DG/ROI	2.34E-04	*
	CCI/2-DG	0.101366	
	CCI/2-DG/ROI	0.0202878	*
Ratio of tdT+ Lacking PV+	CCI	0.307487	
	2-DG	0.067198	
	ROI	1.58E-06	*
	CCI/ROI	2.78E-06	*
	2-DG/ROI	1.34E-06	*
	CCI/2-DG	0.127384	
	CCI/2-DG/ROI	0.001373	*

Table 3.2: Type III ANOVA results.

Chapter 4 : Discussion

In the past two chapters, I have outlined the rationale behind using a glycolytic inhibitor to prevent brain dysfunction after TBI and have experimentally confirmed that 2-DG attenuates several cortical pathologies after CCI in mice. Specifically, I showed that *in vivo* 2-DG treatment attenuates epileptiform activity, changes in spontaneous excitatory and inhibitory synaptic activity, and loss of parvalbumin-expressing cells near the lesion after CCI. At a more basic level, I showed that acute 2-DG treatment ameliorates epileptiform activity in cortical slices, perhaps through a cell type-specific mechanism of reducing the excitability of excitatory neurons but not inhibitory interneurons. In section 3.3, I provided a basic discussion of the complexities and implications of our findings. In the following chapter, I will discuss a few of our key results in greater depth and will propose future studies to extend our understanding in those areas. Finally, I will outline the potential to apply our results to human TBI patients, including the possible challenges we may encounter during translation.

4.1 Why the PV cells?

Parvalbumin (PV) is a calcium-binding protein that is expressed in an important type of GABAergic neurons developmentally derived from the medial ganglionic eminence [299]. PV+ cells can be characterized by their electrophysiological properties, as they have a short AP duration and are fast-spiking (can fire APs >100 Hz). PV basket cells (which are more abundant in the cortex than axo-axonic chandelier cells) synapse onto neuronal somata and provide inhibitory constraint to cortical networks [255]. They are also known to generate key network oscillations in the brain (specifically gamma oscillations at 30-100 Hz). Changes in PV interneuron function and density have been

implicated in many different neurologic and psychiatric disorders, including epilepsy, autism, and schizophrenia [271, 300, 301].

PV interneurons seem to be specifically susceptible to cell death after brain insult, including after TBI, seizures, and stroke [37, 259, 302, 303]. The loss of PV interneurons has been reported in multiple models of TBI, including CCI [36], fluid percussion injury [37], weight drop [38], and cortical "undercut" [256]. In human postmortem tissue after TBI, there is also a selective reduction in the density of parvalbumin cells [39]. Importantly, most of these studies (including prior work from our lab) utilize immune-based approaches to locate and quantify parvalbumin protein, and often will report this as synonymous with parvalbumin cell density. However, recent work has shown that expression levels of parvalbumin can be variable, and further, that the presence/concentration of the parvalbumin protein correlates to electrophysiologic properties. For example, a recent study utilizing RNA-sequencing in combination with whole-cell recording (PatchSeq), found that normalized *Pvalb* gene expression was correlated to the AP half-width and maximum firing frequency of PV+ interneurons, such that neurons that expressed more PV were faster-spiking [272]. To further complicate the analysis of PV interneurons after injury, it has also been shown that the perineuronal net (an extracellular matrix surrounding PV cells) is important in maintaining inhibitory function, and that loss of the perineuronal net after TBI may occur before the loss of PV protein [224].

Since the expression level of parvalbumin is an important factor in determining a neuron's function and effects *in vivo*, we decided to combine genetic and immunohistochemical approaches to assess the effects of CCI and 2-DG treatment on

both PV cell density *and* PV expression. After CCI, we found a reduction in the density of tdT+ (genetically labeled in $PV^{Cre}/Ai9$ mice) and PV+ (labeled with an immunohistochemical approach) cells near the lesion (Figure 3.11). This finding parallels a recent study from the Anderson lab examining CCI in young mice [304]. Further, we found that *in vivo* 2-DG treatment after CCI attenuates the loss of parvalbumin-expressing interneurons and restores the ratio of PV (tdT+) cells that express the PV protein. While 2-DG had a focal effect on the density of PV (tdT+) cells, its broader effect was on restoring/maintaining PV expression in surviving tdT+ cells. Importantly, the rescue of PV-expressing cells follows with the increased frequency of sIPSCs with 2-DG treatment after CCI. As mentioned in Section 3.3, the observed effects of 2-DG on sIPSC but not mIPSC frequency points to the fact that 2-DG may have broader effects on cortical inhibitory function, beyond just rescuing the density of PV-expressing cells.

Our findings also raise many questions about the regulation of the parvalbumin protein, particularly in the context of TBI. How do aberrant excitation, metabolic activity, and other secondary injury mechanisms contribute to reductions in PV expression and loss of PV cells? Are these two changes driven by a similar mechanism? Does damage to, or degradation of, the peri-neuronal nets surrounding PV cells contribute to their loss or dysfunction? Which of these targets should we focus on as we design therapeutic interventions?

In our model (Figure 1.1), we hypothesize that aberrant excitation of PV interneurons acutely after TBI (as shown in Figure 3.4) contributes to their loss and dysfunction. However, our studies do not establish a causal link between hyperexcitation and changes in PV expression and PV+ cell density. While decreased PV density is

commonly observed in the setting of seizures, it is unclear whether changes in PV cells are a cause or result of hyperexcitability (or both). Thus, an important future study will examine whether increased excitation of PV interneurons is sufficient to induce reductions in PV expression. This could be tested using a chemogenetic approach (perhaps with a G_q DREADD injected into somatosensory cortex of a *CamKIIa*^{Cre} mouse line) to increase activity in cortical pyramidal neurons in a specific region. Following this activation, immunohistochemistry for PV near the site of viral injection could determine whether the increased neuronal activation resulted in changes in PV expression.

A caveat: While our model implicates the loss/dysfunction of PV-expressing neurons as a key component of hyperexcitability after TBI, it is important to note that we observed robust effects of CCI and *in vivo* 2-DG treatment on *excitatory* synaptic activity as well. In fact, while we observed no effect of CCI or 2-DG on miniature IPSC frequency, both of these factors had a significant effect on miniature EPSC frequency, suggesting that there might be direct effects on the excitatory component of the network. While excitatory and inhibitory changes in the network are interdependent and difficult to analyze separately, our complex (and somewhat surprising) synaptic activity data warrants further investigation, and perhaps, an expansion of our model to include changes in excitation.

4.2 Determining a mechanism of action for 2-DG

In addition to examining the effects of *in vivo* 2-DG treatment on parvalbumin expression and interneuron density after CCI, we also sought to determine the effect of *in vitro* 2-DG on interneurons. It had been previously shown that inhibition of glycolysis,

but not oxidative phosphorylation, broadened the action potential waveform in excitatory neurons in the Calyx of Held [82]. Glycolytic inhibition with 2-DG has also been shown to reduce the input resistance of hippocampal excitatory neurons, which was attributed in one study to increased potassium conductance secondary to adenosine release [187]. Additionally, as a potential anticonvulsant mechanism of action, 2-DG has been shown to induce current flow through K_{ATP} channels and lead to activation of extrasynaptic $GABA_A$ receptors by increasing neurosteroidogenesis in hippocampal granule cells [188]. However, the effects of 2-DG on inhibitory GABAergic neurons has not been previously explored.

Utilizing whole-cell recording of cortical pyramidal neurons and GFP-labeled interneurons in acute cortical slices from *G42* mice, we found that acute 2-DG treatment specifically reduces the intrinsic excitability and membrane resistance of excitatory neurons, but not inhibitory interneurons. Initially, this was a surprising finding to us, as one might assume that interneurons rely heavily on rapid glycolytic ATP production to maintain their fast firing rates. In fact, the increased susceptibility of PV interneurons to cell death after brain injury has often been attributed to their presumed increased metabolic need relative to other neuron subtypes. On closer examination, many studies demonstrate that interneurons rely heavily on oxidative phosphorylation to power their activity, as they are heavily enriched in mitochondria (reviewed in [293]). Thus, hypoxic conditions, mitochondrial damage, and oxidative stress in the context of TBI may be important contributors to interneuron toxicity, as opposed to an energy crisis resulting from low glucose and reduced ATP concentrations. On the other hand, it has been shown that excitatory neuron populations rely on the generation of a "glycolytic metabolon" and

dynamically increase their utilization of glucose to support increased neuronal activity [77, 80]. Thus, our findings indicate a cell type-specific coupling of metabolism to neuronal excitability, such that glycolysis is required to maintain the activity of pyramidal neurons but not inhibitory interneurons.

An important caveat of our studies is that we utilized the *G42* mouse line to identify interneurons. In this reporter line, >70% of labeled cortical cells are PV+, and 0% of labeled cells are SST+ or CR+ (Figure 3.1). In order to fully explore the cell type-specificity of the effects of 2-DG, these experiments should be repeated to examine other subtypes of interneurons. This can be accomplished using other interneuron reporter mouse lines (such as a *SST^{Cre}/Ai9* line to identify SST+ cells). This experiment would establish whether PV cells are unique in their ability to maintain firing in the presence of a glycolytic inhibitor, or whether this is a property generalizable to all GABAergic inhibitory cells.

4.2.1 Possible cell type-specific targets

In future studies, we hope to identify the specific cellular or molecular targets that differentiate the responses of excitatory and inhibitory neurons to 2-DG. As mentioned in section 3.3, a possible mediator of the reduced membrane resistance and excitability of pyramidal neurons could be the K_{ATP} channel, which opens in response to local decreases in ATP concentration. 2-DG has been previously shown to increase potassium flux through K_{ATP} channels in excitatory neurons [188] and to increase the expression of K_{ATP} channel subunits Kir6.1 and Kir6.2 after seizures [189]. Our findings would suggest that K_{ATP} channels are differentially regulated, localized, or activated in excitatory neurons

compared to interneurons, such that 2-DG only exerts its effects to reduce membrane resistance and excitability in the former subtype.

Importantly, our *in vitro* studies do not determine the primary cell type affected by 2-DG application. While our observed effects were on neuronal excitability and membrane resistance, it is possible that these effects were mediated through glycolytic inhibition in astrocytes instead of neurons. If this were to be true, the neuron subtype-specific effects of 2-DG on excitability could result from differential coupling of astrocytes to different types of neurons. The astrocyte-neuron lactate shuttle (ANLS) model proposes that glycolysis occurs mainly in astrocytes, and that lactate is then delivered to neurons for further metabolism [61]. This process relies on lactate dehydrogenase (LDH, which facilitates conversion between lactate and glycolytic end-product pyruvate) as well as monocarboxylate transporters (MCTs) which transport lactate between astrocytes and neurons. Thus, we can probe whether the ANLS contributes to 2-DG's effects by utilizing pharmacologic blockade of LDH and/or MCT. If 2-DG still reduces the excitability of excitatory neurons in the presence of an MCT blocker to inhibit the ANLS, then we could conclude that 2-DG acts directly on neurons, as opposed to acting indirectly through glycolytic inhibition in astrocytes.

I hypothesize that 2-DG acts through glycolytic inhibition in neurons, especially in the context of TBI, given its rapid effects *in vitro* and the large body of evidence that neurons increase glycolytic flux in settings of increased energetic need. However, a study by Sada et al. found that LDH inhibition in the substantia nigra hyperpolarized neurons and affected their activity [190], suggesting that metabolic products from the ANLS do contribute to maintaining neuronal function at baseline in some brain regions. In this

same study, Sada and colleagues also found that the anticonvulsant stiripentol exerts its effects through LDH inhibition. Thus, manipulations of either astrocytic *or* neuronal glycolysis may be effective in controlling network function, depending on the target region and the physiologic range of neuronal activity in that area.

Further, I did observe effects of *in vivo* 2-DG treatment on astrocytes after CCI. In addition to their central importance as modulators of neurotransmission at the tripartite synapse and their role in brain metabolism, astrocytes are important contributors to the neuroinflammatory response after injury. In line with this, I found increased glial fibrillary acidic protein (GFAP) immunoreactivity near the CCI lesion 3-5 weeks after injury, indicative of chronic reactive astrocytosis (Figure 5.1 in the Appendix). Interestingly, *in vivo* 2-DG treatment for one week after CCI attenuated the chronic astrocytic response in the perilesional area, although this effect was not statistically significant by 2-way ANOVA.

4.2.2 Potential systemic effects of 2-DG

In our experiments, we have focused our attention on the effects of 2-DG on neuronal and network activity after TBI. However, the broad impact of manipulating glycolysis should not be underestimated, particularly in the complex landscape of pathophysiological changes post-TBI. Acutely after 2-DG administration, glycolytic flux is reduced, resulting in a transient elevation in blood glucose concentration (Figure 3.7I). As a result of reduced glucose breakdown via glycolysis, other sources of fuel, such as ketone bodies, are mobilized and catabolized as an alternative energy source. Thus, there is also a transient decrease in blood ketone body levels (Figure 3.7J). Interestingly, although we originally utilized 2-DG as a mimic of the ketogenic diet (KD), these acute

findings are actually opposite of what is observed in patients chronically maintained on KD [305]. Further, unlike KD patients that have low blood glucose and high ketone body levels, we did not observe persistent changes in either of these measures across our week-long 2-DG dosing regimen (Figure 3.8).

Our studies do not fully characterize the systemic metabolic changes that may result from 2-DG treatment. For instance, changes in liver glycogenolysis, gluconeogenesis, or ketosis may have far-reaching effects that we did not evaluate. Additionally, cell types with high metabolic requirements may be affected by systemic 2-DG treatment. As an example, macrophages have been shown to be susceptible to morphologic changes, and even cell death in culture, when metabolism is constricted [215]. As macrophages are central players in the neuroinflammatory response after TBI, alteration of their activation, recruitment, morphology, or function by 2-DG could have far-reaching neurological consequences. 2-DG treatment has also been shown to increase cerebral blood flow [306] which could independently affect secondary injury mechanisms after TBI (perhaps via altered immune cell, cytokine, or nutrient delivery). These findings underscore the far-reaching effects of systemic delivery of a glycolytic inhibitor. Future studies should further examine the effects of 2-DG on neuroinflammatory processes and compare the effects of 2-DG to the KD in order to better understand its underlying cellular and systemic mechanisms of action.

4.3 How 2-DG's effects on cortical dysfunction relate to post-TBI complications

In the studies presented above, I showed that *in vivo* 2-DG treatment attenuates many changes in cortical function after CCI, including reducing epileptiform activity,

restoring cortical input-output relationship, ameliorating changes in spontaneous excitatory and inhibitory synaptic activity, and increasing the density of parvalbumin-expressing interneurons near the lesion. However, we have not yet shown whether 2-DG can affect behavioral or seizure phenotypes associated with post-TBI complications. Ultimately, if this treatment were to be translated into human patients, we would hope to observe improvements in patient-oriented outcomes including the incidence of post-TBI behavioral deficits, seizure activity, or mortality.

4.3.1 2-DG's effects on animal behavior

In the Appendix, I report data from a behavioral battery I performed following CCI and *in vivo* 2-DG treatment (Figure 5.2). Published data from multiple groups show behavioral deficits after CCI and other mouse models of TBI, including motor dysfunction on the Rotarod and wire grip assays [137, 139] and learning deficits assessed in the Morris Water Maze (MWM) [137]. Some groups also report affective changes including increased depressive-like behavior in the forced swim test (FST) [137] and reduced anxiety in the elevated plus maze (EPM) [307]. Unfortunately, these studies vary widely and utilize a broad range of injury types, severities, and time points. Thus, I designed a behavioral battery unique to our needs (Figure 5.2A), with the hopes of capturing early motor changes (as motor recovery is reported after 1-2 weeks in many CCI studies) and assessing behavioral changes at our key 3-5 week time frame (when we observe cortical dysfunction).

In this behavioral battery, we did not observe post-CCI deficits in MWM, FST, or EPM outcomes 3-5 weeks after injury, and therefore, could not assess whether *in vivo* 2-DG had ameliorative effects on these behaviors. During the first week after CCI, we

observed a significant reduction in motor coordination on the Rotarod assay, evidenced by shorter latencies to falling off the rod in the CCI animals relative to sham. In this study, *in vivo* 2-DG treatment did not significantly affect Rotarod performance. Both vehicle-treated and 2-DG-treated CCI mice recovered at similar rates and returned to approximately sham levels by 14 days after injury.

Importantly, while we did not elicit behavioral rescue with 2-DG, animals treated with *in vivo* 2-DG did not have worsened performance in any of the assays we assessed. It was somewhat surprising that CCI did not result in greater behavioral deficits in our hands, but it is possible that our specific injury paradigm did not damage certain cortical circuits to the same degree as protocols used by other labs. For example, we did not observe a deficit on the MWM, however, our CCI parameters result in a lesion largely located in the cortex and only a subset of our animals exhibit hippocampal involvement. Other models of TBI result in more hippocampal damage, which may explain the worsened behavioral phenotypes on hippocampal-dependent tasks reported by other labs. Additionally, even subtle changes in how behavioral experiments are performed (such as the gender of the experimenter or the strain of mouse) can affect the results, and may explain why our assays did not recapitulate findings published by other groups.

4.3.2 Understanding 2-DG's effects on seizure phenotypes

As the long-term goal of our work is to determine whether 2-DG has therapeutic potential to reduce post-traumatic epilepsy, future studies need to examine its effects on seizure phenotypes. The data presented above lends support to 2-DG's potential as a post-TBI therapeutic, as we report that both *in vitro* and *in vivo* 2-DG treatment attenuates cortical hyperexcitability after CCI. Here, I propose two additional studies that should be

performed to continue our investigation of 2-DG's effects on PTE and associated phenotypes.

First, we can assess whether *in vivo* 2-DG treatment reduces seizure susceptibility after TBI. It has been previously shown that CCI reduces seizure threshold, such that animals have decreased latency to seizure induced by pentylenetetrazole (PTZ) injection. Using PTZ or another convulsive agent (such as kainic acid) in combination with EEG recordings, we will assess whether 2-DG attenuates the increased seizure susceptibility found after injury. An important advantage to this study is that it can be performed at the same time point across animals and at the same time point as our other electrophysiological studies (3-5 weeks after injury), before spontaneous behavioral seizures develop.

The primary PTE experiment will assess whether *in vivo* 2-DG treatment acutely after injury decreases the percentage of animals that go on to develop spontaneous seizures after CCI or decreases the seizure frequency/severity among animals with PTE. After CCI, ~5-30% of animals develop spontaneous seizures by 12 weeks after injury. The incidence of seizure activity after CCI seems to be dependent on mouse strain (with CD-1 mice exhibiting higher rates of PTE than C57s), injury severity, and time point examined. Importantly, the proportion of mice that develop spontaneous seizures after CCI resembles the incidence of PTE in humans after severe TBI. However, because of the relatively low incidence of PTE after CCI, this experiment will require very large sample sizes to achieve adequate statistical power to determine whether 2-DG exhibited a therapeutic effect.

4.4 Translating 2-DG as a TBI therapeutic: opportunities and challenges

Currently, there are no disease-modifying therapies approved to prevent the development of long-term complications after TBI in humans. Unfortunately, as in other CNS disorders, attempts to translate preclinical ideas have not been effective. In this section, I will reiterate the factors in support of translating 2-DG as a clinical TBI treatment (as discussed in Chapter 2 and 3.3) and will outline some key steps and challenges we will need to overcome for successful translation.

2-DG is already used clinically as a cancer therapeutic and is well-tolerated in humans. As a competitive hexokinase inhibitor, 2-DG exerts the greatest effects in the most metabolically active cells in a cancer patient, which via the Warburg effect, are usually the dividing neoplastic cells. In our case after TBI, 2-DG would likely target the zones of increased glycolytic activity in the brain, as uptake of both glucose and 2-DG would be increased in parallel. Additionally, compromise of the BBB after TBI [115, 308] would further aid in the delivery of 2-deoxyglucose to the brain parenchyma. The therapeutic rationale behind utilizing 2-DG after TBI is well-founded on both preclinical and clinical literature (see Chapter 2).

One of the key challenges in successfully translating a PTE therapeutic is based on the epidemiology of the disease. Because only a small portion of TBI patients will go on to develop PTE and patients can develop seizures months to years following their initial TBI, clinical studies require very large sample sizes and long follow-up. As a field, we need to focus on finding novel biomarkers that can effectively stratify patients based on their likelihood of developing PTE. In a clinical study, if we first deliver the therapeutic (in this case, 2-DG) to the patients at highest risk, then we are more likely to

observe a drug effect if it exists. Delivering 2-DG to a high-risk group would increase the baseline incidence in the vehicle-treated patients, and thus, the sample sizes could be smaller and still be of sufficient power to see an effect of 2-DG. Further, it would reduce the "number needed to treat" (NNT) to see a positive effect, as the NNT increases as the study population becomes more diverse and less likely to benefit from an intervention. Once a drug is found to be safe and effective, its use can be gradually expanded to larger patient populations.

There have been some important advances in the TBI biomarker field that will hopefully aid in the successful translation of new TBI therapeutics. For example, a recent publication identified specific EEG abnormalities (including epileptiform activity and interictal spikes) within the first week after TBI that conferred a higher risk of being diagnosed with PTE within 2 years [206]. While this study only indicated certain factors as increasing the risk of later seizures, as opposed to being fully predictive of epileptogenesis, it provides an important first step in patient stratification. Additionally, it suggests that more rigorous studies of EEG abnormalities throughout the first week after TBI (instead of the limited, short-term recordings the authors had access to) are warranted and may reveal more effective PTE biomarkers.

Another use of biomarkers is to identify which patients are most likely to benefit from a specific therapeutic approach. For our proposed intervention (limiting glucose utilization after injury), we can utilize metabolic imaging to stratify patients. Specifically, TBI patients that show the most aberrantly increased glucose uptake and glycolytic activity on PET scan may be most likely to benefit from intervention with a glycolytic inhibitor. On the other hand, PET scanning may be utilized to identify patients that would

be poor candidates for 2-DG – we would not want to deliver a glycolytic inhibitor to a patient that has pronounced hypometabolism, as this could worsen their condition. Finally, PET scanning could help us determine the ideal dosing schedule for 2-DG to restore physiologic levels of glucose utilization after TBI. In our preclinical studies, we only experimented with one 2-DG dosing regimen, which involved one daily intraperitoneal injection of 250 mg/kg 2-DG for seven days following CCI. Future studies must determine the "critical window" to garner the benefits of 2-DG – specifically whether delayed initiation of 2-DG treatment (such as might occur while a patient is transferred to a larger hospital for TBI care) can still attenuate changes in cortical pathology. Further, the ideal dose and timing must be established in order to maximize beneficial effects in the brain while minimizing adverse peripheral effects.

One additional challenge to translating 2-DG into TBI patients is getting appropriate patient consent for a clinical study. As the risk of PTE increases with injury severity, our high-risk cohorts are likely to have significantly impaired consciousness when they arrive to the hospital after TBI. TBI patient outcomes are also worsened if the patient has consumed alcohol, but an intoxicated patient is often not legally competent to give consent. While this challenge can be overcome in an IRB protocol by having another individual (next of kin) give consent, it is an important consideration when designing a study with a time-sensitive treatment for a population that may not have adequate mental capacity for medical decision-making.

4.5 Conclusion

In this thesis, I have examined the therapeutic potential of the glycolytic inhibitor 2-deoxyglucose to preserve brain function after TBI. Through *in vitro* and *in vivo* studies, I have shown that 2-DG attenuates hyperexcitability and pathologic cortical changes after controlled cortical impact in mice. Further, I identified a novel neuron subtype-specific coupling of metabolism to excitability. I reviewed the preclinical and clinical literature that provide therapeutic rationale for our approach and have discussed the future experiments and considerations that must be addressed to successfully translate 2-DG from the bench to the bedside. This work lends support for the use of metabolic therapies to manipulate neuronal network function, and specifically points to hyper-glycolysis as a promising target of disease-modifying therapy following traumatic brain injury.

Chapter 5 : Appendix

5.1 The effects of 2-DG on post-CCI astrocytosis

Following CCI and *in vivo* 2-DG treatment, we assessed chronic reactive astrocytosis using glial fibrillary acidic protein (GFAP) immunoreactivity 3-5 weeks after injury. There was minimal GFAP reactivity in brains from the sham animals. However, following CCI, there was robust GFAP reactivity, particularly in the perilesional cortex. *In vivo* 2-DG treatment resulted in a partial attenuation of the GFAP+ area in the first 2 ROIs near the CCI lesion, although this was nonsignificant via 2-way ANOVA.

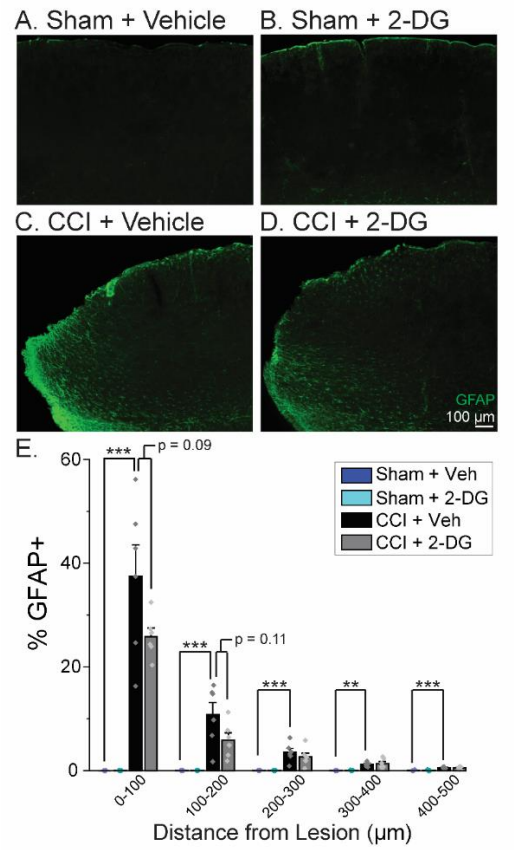

Figure 5.1 Effects of CCI and 2-DG treatment on chronic reactive astrocytosis. Animals underwent sham or CCI surgery and one week of vehicle or 2-DG treatment. Immunohistochemical GFAP reactivity was quantified in serial coronal sections 3-5 weeks after CCI. **A-D.** Representative images from each experimental group. GFAP immunoreactivity in green. **E.** Quantification of % positive pixels after GFAP immunohistochemistry in 5 regions lateral to the CCI lesion. (n = 6 animals/group; 3 sections/animal analyzed to generate a single average value for each animal. 2-way ANOVA: **$p < 0.01$; ***$p < 0.001$)

5.2 In vivo 2-DG treatment does not reduce lesion volume or improve behavioral outcomes following CCI

As CCI results in a large cavitary lesion associated with significant tissue loss, we compared lesion volume to determine whether *in vivo* 2-DG treatment had gross tissue-sparing effects. By serial sectioning brains after CCI and tracing the size of the cavitation in each section, we estimated overall lesion volume. I*n vivo* 2-DG treatment had no significant effect on cavitation size (Figure 5.2B).

We also sought to assess whether 2-DG had any effect (either beneficial or adverse) on behavioral outcomes following CCI. First, there were no significant differences between the four treatment groups on the open field assay, suggesting that the general locomotor behavior was similar across subjects (Figure 5.2C). Next, we utilized the Rotarod assay to assess motor performance during the first week after injury. There was a significant deficit in CCI-injured animals relative to sham animals, as the CCI animals spent a significantly lower time on the accelerating Rotarod before falling off (Figure 5.2D). *In vivo* 2-DG treatment did not have any effect on the performance of the animals on this assay. By 14 days and 28 days post-CCI, animals that had received either vehicle or 2-DG both recovered to the levels of performance of the sham animals.

We also performed the Morris Water Maze (MWM) to assess spatial learning, elevated plus maze (EPM) to assess anxiety-like behavior, and the forced swim test (FST) to assess depressive-like behavior.

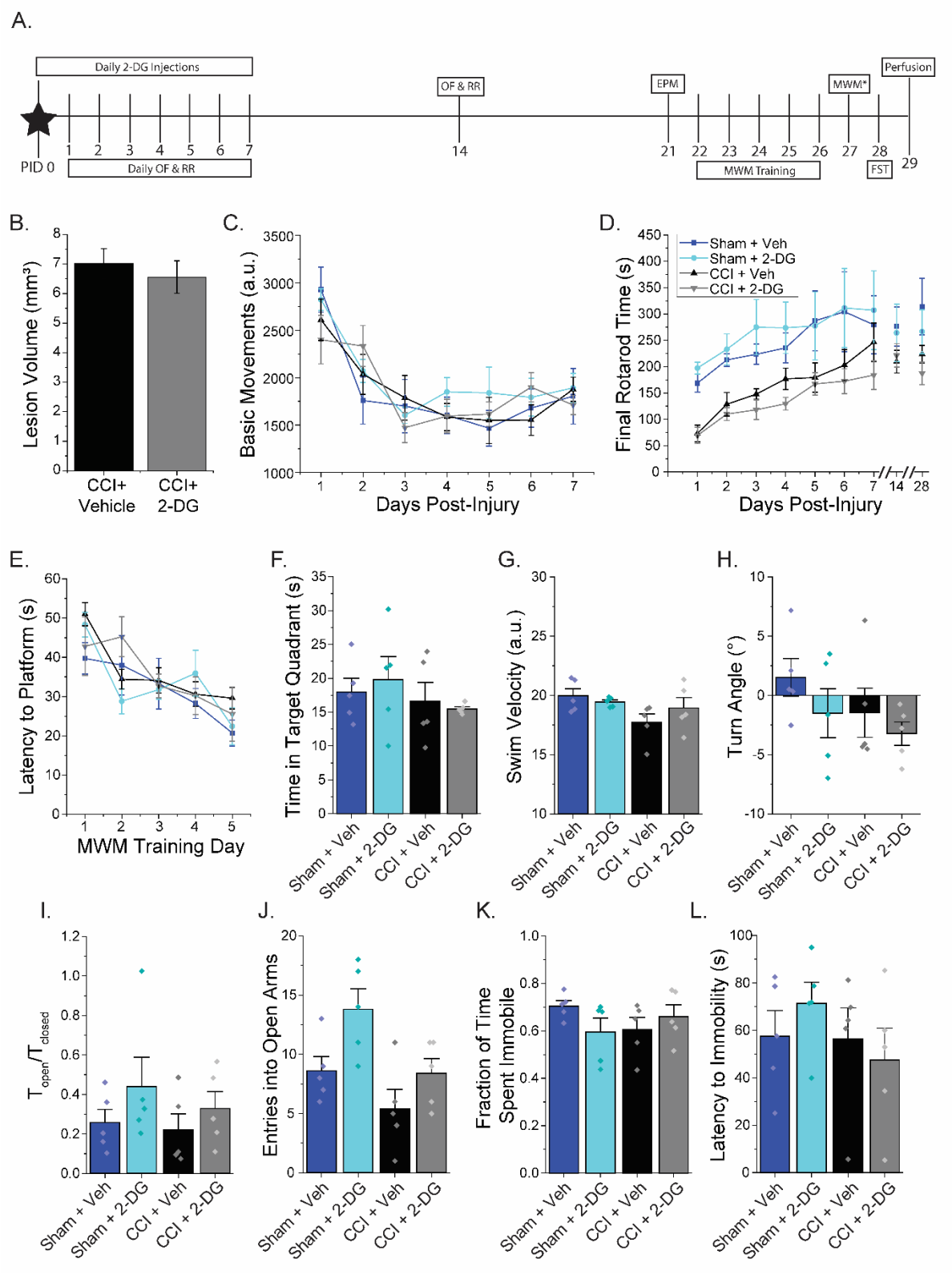

Figure 5.2 2-DG treatment does not affect behavior on Rotarod, MWM, EPM, or FST. A. Timeline of the behavioral testing paradigm. C57 male mice underwent sham or CCI surgery and one week of daily vehicle or 2-DG injections. Mice were tested on open

field (OF), Rotarod (RR), elevated plus maze (EPM), Morris water maze (MWM) with probe test (MWM*), and forced swim test (FST) on the indicated post-injury day (PID). Animals were sacrificed on PID 29. **B.** Lesion volume was estimated by tracing the CCI lesion on serial sections throughout the entire cavitation. **C.** Basic movements assessed during 10-minute sessions in an open field arena. **D.** Animals were assessed on the Rotarod at PID 1-7, PID 14, and PID 28. Final Rotarod time refers to the latency until the mouse fell off the accelerating rod. CCI caused a transient motor deficit that recovered by PID 14; *in vivo* 2-DG treatment did not affect Rotarod performance. **E.** Latency to finding the target platform during MWM training. **F-H.** Assessment of the MWM probe trial, including time spent in the target quadrant (F), swimming speed (G), and average turn angle throughout the trial (H). **I-J.** Assessment of the EPM assay, including the ratio of time spent in the open arms versus closed arms (I) and the number of entries into the open arms (J). **K-L.** Assessment of the FST, including the fraction of time spent immobile in the tank (versus actively swimming) (K) and the latency to becoming immobile (L).

On these three assays, we did not observe differences between the four experimental groups. We were somewhat surprised that CCI did not result in deficits in spatial learning, since this had been previously reported by other groups. Further, in the MWM probe trial, we did not observe an effect of CCI on the animal's swimming velocity or on their turn angle (as may be expected with a unilateral lesion to the sensorimotor cortex). In the EPM and FST, we did not observe increased anxiety or depressive-like behavior following CCI. This is in line with the literature, which reports a mix of both positive and negative findings on these two tests. Overall, our behavioral battery did not reveal any significant therapeutic (or importantly, adverse) effects of *in vivo* 2-DG treatment after CCI.

5.2.1 Behavioral methods

For all behavioral tests, the experimenter was blinded to the experimental group. Animals were group housed and allowed to acclimate to the testing room for at least 30 minutes before each test. When testing was performed on Day 1-7 following injury,

animals were assessed prior to their daily 2-DG injection. Open field assessment was performed by placing each animal individually into an open arena (40X40 cm) equipped with a photobeam-break system connected to MotorMonitor software for data collection. Basic movements (measured with arbitrary units) were recorded by summing all movement during a 10-minute test period.

Rotarod was performed using a 5-laned treadmill (MedAssociates Model ENV-577M). The rod was accelerated from 4 to 40 rpm over 5 minutes. We report the time each animal was able to stay on the rod without falling off, averaged across five trials per testing day. Each animal was allowed adequate rest (>10 minutes) between trials.

The elevated plus maze (EPM) consisted of one 5 minute trial for each animal. At the beginning of the trial, animals were placed in the center of the maze with their nose facing an open arm. Each trial was assessed using a photobeam-break system connected to MotorMonitor software for data collection. The time spent in the open arms, time spent in the closed arms, and number of entries into each arm were quantified and compared across groups.

The Morris water maze (MWM) consisted of 5 days of training (4 trials/day) and 2 probe trials on the sixth day. A large tank was filled with water (kept at 20-21°C) mixed with white tempera paint to make it opaque. During training, a clear platform was placed ~1 inch beneath the surface of the water in the northeast quadrant of the tank. Mice were given 60 seconds per training trial to find the platform. If the mouse did not find the platform during that time, it was guided to the platform and kept there for 15 seconds before removal from the tank. The platform was removed for the probe trials,

which were each 60 seconds in length. After each trial, mice were placed into a clean cage with a heating pad to recover. Data was collected using Ethovision software.

The forced swim test was performed in a small acrylic tank, 2/3 full with water at 23-25°C. Animals were placed into the water for a single six minute trial. Trials were recorded with a video camera and were later analyzed by a blinded experimenter using the Boris behavioral software.

Chapter 6 : Bibliography

1. The CDC, N., DoD, and VA Leadership Panel, *Report to Congress on Traumatic Brain Injury in the United States: Understanding the Public Health Problem among Current and Former Military Personnel.*, t.N.I.o.H.N. Centers for Disease Control and Prevention (CDC), the Department of Defense (DoD), and the Department of Veterans Affairs (VA), Editor. 2013.
2. Rajajee, V., *Management of acute severe traumatic brain injury*, in *UpToDate*, J. Wilterdink, Editor.
3. Najem, D., et al., *Traumatic brain injury: classification, models, and markers.* Biochem Cell Biol, 2018. **96**(4): p. 391-406.
4. Merchant-Borna, K., et al., *Novel Method of Weighting Cumulative Helmet Impacts Improves Correlation with Brain White Matter Changes After One Football Season of Sub-concussive Head Blows.* Ann Biomed Eng, 2016. **44**(12): p. 3679-3692.
5. Killam, C., R.L. Cautin, and A.C. Santucci, *Assessing the enduring residual neuropsychological effects of head trauma in college athletes who participate in contact sports.* Arch Clin Neuropsychol, 2005. **20**(5): p. 599-611.
6. Bazarian, J.J., et al., *Persistent, long-term cerebral white matter changes after sports-related repetitive head impacts.* PLoS One, 2014. **9**(4): p. e94734.
7. Prevention, C.f.D.C.a., *Report to Congress on Traumatic Brain Injury in the United States: Epidemiology and Rehabilitation.*, N.C.f.I.P.a.C.D.o.U.I. Prevention., Editor. 2015: Atlanta, GA.
8. Faul, M. and V. Coronado, *Epidemiology of traumatic brain injury.* Handb Clin Neurol, 2015. **127**: p. 3-13.
9. Brenner, L.A., et al., *Traumatic brain injury, posttraumatic stress disorder, and postconcussive symptom reporting among troops returning from iraq.* J Head Trauma Rehabil, 2010. **25**(5): p. 307-12.
10. Maas, A.I., et al., *Prediction of outcome in traumatic brain injury with computed tomographic characteristics: a comparison between the computed tomographic classification and combinations of computed tomographic predictors.* Neurosurgery, 2005. **57**(6): p. 1173-82; discussion 1173-82.
11. Rovlias, A. and S. Kotsou, *The influence of hyperglycemia on neurological outcome in patients with severe head injury.* Neurosurgery, 2000. **46**(2): p. 335-42; discussion 342-3.
12. Jeremitsky, E., et al., *The impact of hyperglycemia on patients with severe brain injury.* J Trauma, 2005. **58**(1): p. 47-50.
13. Lewis, S.R., et al., *Hypothermia for traumatic brain injury.* Cochrane Database Syst Rev, 2017. **9**: p. CD001048.
14. Klein, P., et al., *Commonalities in epileptogenic processes from different acute brain insults: Do they translate?* Epilepsia, 2018. **59**(1): p. 37-66.
15. Koenig, J.B. and C.G. Dulla, *Dysregulated Glucose Metabolism as a Therapeutic Target to Reduce Post-traumatic Epilepsy.* Front Cell Neurosci, 2018. **12**: p. 350.
16. Menon, D.K., et al., *Position statement: definition of traumatic brain injury.* Arch Phys Med Rehabil, 2010. **91**(11): p. 1637-40.
17. Evans, R.W., *Postconcussion syndrome*, in *UpToDate*, J. Wilterdink, Editor.

18. Zaloshnja, E., et al., *Prevalence of long-term disability from traumatic brain injury in the civilian population of the United States, 2005.* J Head Trauma Rehabil, 2008. **23**(6): p. 394-400.
19. Wilson, L., et al., *The chronic and evolving neurological consequences of traumatic brain injury.* Lancet Neurol, 2017. **16**(10): p. 813-825.
20. Collins-Praino, L.E. and F. Corrigan, *Does neuroinflammation drive the relationship between tau hyperphosphorylation and dementia development following traumatic brain injury?* Brain Behav Immun, 2017. **60**: p. 369-382.
21. Ikonomovic, M.D., et al., *Alzheimer's pathology in human temporal cortex surgically excised after severe brain injury.* Exp. Neurol, 2004. **190**(1): p. 192-203.
22. Shively, S., et al., *Dementia resulting from traumatic brain injury: what is the pathology?* Arch Neurol, 2012. **69**(10): p. 1245-51.
23. Evans, R.W., *Sequelae of mild traumatic brain injury*, in *UpToDate*, J.L. Wilterdink, Editor.
24. Mez, J., et al., *Clinicopathological Evaluation of Chronic Traumatic Encephalopathy in Players of American Football.* JAMA, 2017. **318**(4): p. 360-370.
25. Randolph W Evans, S.C.S., *Post-traumatic seizures and epilepsy*, in *UpToDate*, J.F. Dashe, Editor.
26. Tubi, M.A., et al., *Early seizures and temporal lobe trauma predict post-traumatic epilepsy: A longitudinal study.* Neurobiol Dis, 2018.
27. Salazar, A.M., et al., *Epilepsy after penetrating head injury. I. Clinical correlates: a report of the Vietnam Head Injury Study.* Neurology, 1985. **35**(10): p. 1406-1414.
28. Haltiner, A.M., N.R. Temkin, and S.S. Dikmen, *Risk of seizure recurrence after the first late posttraumatic seizure.* Arch Phys Med Rehabil, 1997. **78**(8): p. 835-40.
29. Schachter, S.C., *Antiseizure drugs: Mechanism of action, pharmacology, and adverse effects*, in *UpToDate*, J.F. Dashe, Editor.
30. Thompson, K., et al., *Pharmacological treatments for preventing epilepsy following traumatic head injury.* Cochrane Database Syst Rev, 2015(8): p. CD009900.
31. Temkin, N.R., et al., *Magnesium sulfate for neuroprotection after traumatic brain injury: a randomised controlled trial.* Lancet Neurol, 2007. **6**(1): p. 29-38.
32. Xiong, Y., A. Mahmood, and M. Chopp, *Animal models of traumatic brain injury.* Nat Rev Neurosci, 2013. **14**(2): p. 128-42.
33. Dolle, J.P., et al., *Newfound sex differences in axonal structure underlie differential outcomes from in vitro traumatic axonal injury.* Exp Neurol, 2018. **300**: p. 121-134.
34. Manley, G.T., et al., *Controlled cortical impact in swine: pathophysiology and biomechanics.* J Neurotrauma, 2006. **23**(2): p. 128-39.
35. Wolf, J.A., et al., *Concussion Induces Hippocampal Circuitry Disruption in Swine.* J Neurotrauma, 2017. **34**(14): p. 2303-2314.
36. Cantu, D., et al., *Traumatic Brain Injury Increases Cortical Glutamate Network Activity by Compromising GABAergic Control.* Cereb. Cortex, 2014.
37. Huusko, N., et al., *Loss of hippocampal interneurons and epileptogenesis: a comparison of two animal models of acquired epilepsy.* Brain Struct Funct, 2015. **220**(1): p. 153-91.

38. Carron, S.F., et al., *Differential susceptibility of cortical and sub-cortical inhibitory neurons and astrocytes in the long term following diffuse traumatic brain injury.* J Comp Neurol, 2016.
39. Buritica, E., et al., *Changes in calcium-binding protein expression in human cortical contusion tissue.* J Neurotrauma, 2009. **26**(12): p. 2145-55.
40. Bolkvadze, T. and A. Pikaennen, *Development of post-traumatic epilepsy after controlled cortical impact and lateral fluid-percussion-induced brain injury in the mouse.* Journal of neurotrauma, 2012. **29**(5): p. 789-812.
41. Hunt, R.F., S.W. Scheff, and B.N. Smith, *Posttraumatic epilepsy after controlled cortical impact injury in mice.* Exp. Neurol, 2009. **215**(2): p. 243-252.
42. Dulla, C., et al., *Imaging of glutamate in brain slices using FRET sensors.* J. Neurosci. Methods, 2008. **168**(2): p. 306-319.
43. Rolfe, D.F. and G.C. Brown, *Cellular energy utilization and molecular origin of standard metabolic rate in mammals.* Physiol Rev, 1997. **77**(3): p. 731-58.
44. Alle, H., A. Roth, and J.R. Geiger, *Energy-efficient action potentials in hippocampal mossy fibers.* Science, 2009. **325**(5946): p. 1405-8.
45. Rangaraju, V., N. Calloway, and T.A. Ryan, *Activity-driven local ATP synthesis is required for synaptic function.* Cell, 2014. **156**(4): p. 825-35.
46. Beland-Millar, A., et al., *Effects of Systemic Metabolic Fuels on Glucose and Lactate Levels in the Brain Extracellular Compartment of the Mouse.* Front Neurosci, 2017. **11**: p. 7.
47. Herculano-Houzel, S., *The glia/neuron ratio: how it varies uniformly across brain structures and species and what that means for brain physiology and evolution.* Glia, 2014. **62**(9): p. 1377-91.
48. Magistretti, P.J., et al., *Neurotransmitters regulate energy metabolism in astrocytes: implications for the metabolic trafficking between neural cells.* Dev Neurosci, 1993. **15**(3-5): p. 306-12.
49. Hui, S., et al., *Glucose feeds the TCA cycle via circulating lactate.* Nature, 2017. **551**(7678): p. 115-118.
50. Yellen, G., *Fueling thought: Management of glycolysis and oxidative phosphorylation in neuronal metabolism.* J Cell Biol, 2018.
51. Tantama, M., et al., *Imaging energy status in live cells with a fluorescent biosensor of the intracellular ATP-to-ADP ratio.* Nat Commun, 2013. **4**: p. 2550.
52. Hung, Y.P. and G. Yellen, *Live-cell imaging of cytosolic NADH-NAD+ redox state using a genetically encoded fluorescent biosensor.* Methods Mol Biol, 2014. **1071**: p. 83-95.
53. Bernardinelli, Y., P.J. Magistretti, and J.Y. Chatton, *Astrocytes generate Na+-mediated metabolic waves.* Proc Natl Acad Sci U S A, 2004. **101**(41): p. 14937-42.
54. Rogawski, M.A., W. Loscher, and J.M. Rho, *Mechanisms of Action of Antiseizure Drugs and the Ketogenic Diet.* Cold Spring Harb Perspect Med, 2016. **6**(5).
55. Lin, A.L., et al., *Nonlinear coupling between cerebral blood flow, oxygen consumption, and ATP production in human visual cortex.* Proc Natl Acad Sci U S A, 2010. **107**(18): p. 8446-51.
56. Buxton, R.B., *Interpreting oxygenation-based neuroimaging signals: the importance and the challenge of understanding brain oxygen metabolism.* Front Neuroenergetics, 2010. **2**: p. 8.

57. Genoud, C., et al., *Plasticity of astrocytic coverage and glutamate transporter expression in adult mouse cortex.* PLoS Biol, 2006. **4**(11): p. e343.
58. Pinky, N.F., et al., *Region- and activity-dependent regulation of extracellular glutamate.* J Neurosci, 2018.
59. Armbruster, M., E. Hanson, and C.G. Dulla, *Glutamate Clearance Is Locally Modulated by Presynaptic Neuronal Activity in the Cerebral Cortex.* J Neurosci, 2016. **36**(40): p. 10404-10415.
60. Magistretti, P.J. and J.Y. Chatton, *Relationship between L-glutamate-regulated intracellular Na+ dynamics and ATP hydrolysis in astrocytes.* J Neural Transm (Vienna), 2005. **112**(1): p. 77-85.
61. Pellerin, L. and P.J. Magistretti, *Glutamate uptake into astrocytes stimulates aerobic glycolysis: a mechanism coupling neuronal activity to glucose utilization.* Proc Natl Acad Sci U S A, 1994. **91**(22): p. 10625-9.
62. Voutsinos-Porche, B., et al., *Glial glutamate transporters mediate a functional metabolic crosstalk between neurons and astrocytes in the mouse developing cortex.* Neuron, 2003. **37**(2): p. 275-86.
63. Azarias, G., et al., *Glutamate transport decreases mitochondrial pH and modulates oxidative metabolism in astrocytes.* J Neurosci, 2011. **31**(10): p. 3550-9.
64. Peng, L., X. Zhang, and L. Hertz, *High extracellular potassium concentrations stimulate oxidative metabolism in a glutamatergic neuronal culture and glycolysis in cultured astrocytes but have no stimulatory effect in a GABAergic neuronal culture.* Brain Res, 1994. **663**(1): p. 168-172.
65. Bittner, C.X., et al., *Fast and reversible stimulation of astrocytic glycolysis by K+ and a delayed and persistent effect of glutamate.* J Neurosci, 2011. **31**(12): p. 4709-13.
66. Ruminot, I., et al., *NBCe1 mediates the acute stimulation of astrocytic glycolysis by extracellular K+.* J Neurosci, 2011. **31**(40): p. 14264-71.
67. Yu, N., et al., *Arachidonic acid stimulates glucose uptake in cerebral cortical astrocytes.* Proc Natl Acad Sci U S A, 1993. **90**(9): p. 4042-6.
68. Hutchinson, D.S., R.J. Summers, and M.E. Gibbs, *Beta2- and beta3-adrenoceptors activate glucose uptake in chick astrocytes by distinct mechanisms: a mechanism for memory enhancement?* J Neurochem, 2007. **103**(3): p. 997-1008.
69. Hof, P.R., E. Pascale, and P.J. Magistretti, *K+ at concentrations reached in the extracellular space during neuronal activity promotes a Ca2+-dependent glycogen hydrolysis in mouse cerebral cortex.* J Neurosci, 1988. **8**(6): p. 1922-8.
70. Sorg, O. and P.J. Magistretti, *Characterization of the glycogenolysis elicited by vasoactive intestinal peptide, noradrenaline and adenosine in primary cultures of mouse cerebral cortical astrocytes.* Brain Res, 1991. **563**(1-2): p. 227-33.
71. Sorg, O., et al., *Adenosine triphosphate and arachidonic acid stimulate glycogenolysis in primary cultures of mouse cerebral cortical astrocytes.* Neurosci Lett, 1995. **188**(2): p. 109-12.
72. Ashrafi, G. and T.A. Ryan, *Glucose metabolism in nerve terminals.* Curr Opin Neurobiol, 2017. **45**: p. 156-161.
73. Lundgaard, I., et al., *Direct neuronal glucose uptake Heralds activity-dependent increases in cerebral metabolism.* Nat. Commun, 2015. **6**: p. 6807.

74. Ferreira, J.M., A.L. Burnett, and G.A. Rameau, *Activity-dependent regulation of surface glucose transporter-3.* J Neurosci, 2011. **31**(6): p. 1991-9.
75. Ashrafi, G., et al., *GLUT4 Mobilization Supports Energetic Demands of Active Synapses.* Neuron, 2017. **93**(3): p. 606-615 e3.
76. Bak, L.K., et al., *Neuronal glucose but not lactate utilization is positively correlated with NMDA-induced neurotransmission and fluctuations in cytosolic Ca2+ levels.* J Neurochem, 2009. **109 Suppl 1**: p. 87-93.
77. Diaz-Garcia, C.M., et al., *Neuronal Stimulation Triggers Neuronal Glycolysis and Not Lactate Uptake.* Cell Metab, 2017. **26**(2): p. 361-374 e4.
78. Hall, C.N., et al., *Oxidative phosphorylation, not glycolysis, powers presynaptic and postsynaptic mechanisms underlying brain information processing.* J Neurosci, 2012. **32**(26): p. 8940-51.
79. Sobieski, C., M.J. Fitzpatrick, and S.J. Mennerick, *Differential Presynaptic ATP Supply for Basal and High-Demand Transmission.* J Neurosci, 2017. **37**(7): p. 1888-1899.
80. Jang, S., et al., *Glycolytic Enzymes Localize to Synapses under Energy Stress to Support Synaptic Function.* Neuron, 2016. **90**(2): p. 278-91.
81. Bas-Orth, C., et al., *Synaptic Activity Drives a Genomic Program That Promotes a Neuronal Warburg Effect.* J Biol Chem, 2017. **292**(13): p. 5183-5194.
82. Lujan, B., et al., *Glycolysis selectively shapes the presynaptic action potential waveform.* J Neurophysiol, 2016. **116**(6): p. 2523-2540.
83. Galow, L.V., et al., *Energy substrates that fuel fast neuronal network oscillations.* Front Neurosci, 2014. **8**: p. 398.
84. Tanner, G.R., et al., *Single K ATP channel opening in response to action potential firing in mouse dentate granule neurons.* J Neurosci, 2011. **31**(23): p. 8689-96.
85. Lemak, M.S., et al., *KATP channels modulate intrinsic firing activity of immature entorhinal cortex layer III neurons.* Front Cell Neurosci, 2014. **8**: p. 255.
86. Lutas, A., L. Birnbaumer, and G. Yellen, *Metabolism regulates the spontaneous firing of substantia nigra pars reticulata neurons via KATP and nonselective cation channels.* J Neurosci, 2014. **34**(49): p. 16336-47.
87. Pearson, T., et al., *A depletable pool of adenosine in area CA1 of the rat hippocampus.* J. Neurosci, 2001. **21**(7): p. 2298-2307.
88. Rau, A.R., O.J. Ariwodola, and J.L. Weiner, *Postsynaptic adenosine A2A receptors modulate intrinsic excitability of pyramidal cells in the rat basolateral amygdala.* Int J Neuropsychopharmacol, 2015. **18**(6).
89. Sacktor, B., J.E. Wilson, and C.G. Tiekert, *Regulation of glycolysis in brain, in situ, during convulsions.* J Biol Chem, 1966. **241**(21): p. 5071-5.
90. Wasterlain, C.G., et al., *Pathophysiological mechanisms of brain damage from status epilepticus.* Epilepsia, 1993. **34 Suppl 1**: p. S37-53.
91. Chugani, H.T., et al., *Interictal and postictal focal hypermetabolism on positron emission tomography.* Pediatr Neurol, 1993. **9**(1): p. 10-5.
92. Bansal, L., et al., *PET hypermetabolism in medically resistant childhood epilepsy: Incidence, associations, and surgical outcome.* Epilepsia, 2016. **57**(3): p. 436-44.
93. Namer, I.J., et al., *Hypermetabolism during resting-state FDG-PET suggesting intrinsic epileptogenicity in focal cortical dysplasia.* Clin Nucl Med, 2014. **39**(11): p. 993-5.

94. Alkonyi, B., H.T. Chugani, and C. Juhasz, *Transient focal cortical increase of interictal glucose metabolism in Sturge-Weber syndrome: implications for epileptogenesis.* Epilepsia, 2011. **52**(7): p. 1265-72.
95. De Tiege, X., et al., *Regional cerebral glucose metabolism in epilepsies with continuous spikes and waves during sleep.* Neurology, 2004. **63**(5): p. 853-7.
96. Radtke, R.A., et al., *Temporal lobe hypometabolism on PET: predictor of seizure control after temporal lobectomy.* Neurology, 1993. **43**(6): p. 1088-92.
97. Vielhaber, S., et al., *Correlation of hippocampal glucose oxidation capacity and interictal FDG-PET in temporal lobe epilepsy.* Epilepsia, 2003. **44**(2): p. 193-9.
98. Jeong, J.W., et al., *Objective 3D surface evaluation of intracranial electrophysiologic correlates of cerebral glucose metabolic abnormalities in children with focal epilepsy.* Hum Brain Mapp, 2017. **38**(6): p. 3098-3112.
99. Diehl, B., et al., *Cerebral hemodynamic response to generalized spike-wave discharges.* Epilepsia, 1998. **39**(12): p. 1284-9.
100. Zhao, M., et al., *Focal increases in perfusion and decreases in hemoglobin oxygenation precede seizure onset in spontaneous human epilepsy.* Epilepsia, 2007. **48**(11): p. 2059-67.
101. Federico, P., et al., *Functional MRI of the pre-ictal state.* Brain, 2005. **128**(Pt 8): p. 1811-7.
102. Vezzani, A., B. Lang, and E. Aronica, *Immunity and Inflammation in Epilepsy.* Cold Spring Harb Perspect Med, 2015. **6**(2): p. a022699.
103. Ingvar, M., *Cerebral blood flow and metabolic rate during seizures. Relationship to epileptic brain damage.* Ann N Y Acad Sci, 1986. **462**: p. 194-206.
104. Pereira de Vasconcelos, A., A. Ferrandon, and A. Nehlig, *Local cerebral blood flow during lithium-pilocarpine seizures in the developing and adult rat: role of coupling between blood flow and metabolism in the genesis of neuronal damage.* J Cereb Blood Flow Metab, 2002. **22**(2): p. 196-205.
105. Ingvar, M. and B.K. Siesjo, *Local blood flow and glucose consumption in the rat brain during sustained bicuculline-induced seizures.* Acta Neurol Scand, 1983. **68**(3): p. 129-44.
106. Alvestad, S., et al., *Limbic structures show altered glial-neuronal metabolism in the chronic phase of kainate induced epilepsy.* Neurochem Res, 2008. **33**(2): p. 257-66.
107. Guo, Y., et al., *In vivo mapping of temporospatial changes in glucose utilization in rat brain during epileptogenesis: an 18F-fluorodeoxyglucose-small animal positron emission tomography study.* Neuroscience, 2009. **162**(4): p. 972-9.
108. Jupp, B., et al., *Hypometabolism precedes limbic atrophy and spontaneous recurrent seizures in a rat model of TLE.* Epilepsia, 2012. **53**(7): p. 1233-44.
109. Folbergrova, J., M. Ingvar, and B.K. Siesjo, *Metabolic changes in cerebral cortex, hippocampus, and cerebellum during sustained bicuculline-induced seizures.* J Neurochem, 1981. **37**(5): p. 1228-38.
110. McDonald, T.S. and K. Borges, *Impaired hippocampal glucose metabolism during and after flurothyl-induced seizures in mice: Reduced phosphorylation coincides with reduced activity of pyruvate dehydrogenase.* Epilepsia, 2017. **58**(7): p. 1172-1180.

111. Wasterlain, C.G., et al., *Brain energy metabolism during experimental neonatal seizures.* Neurochem Res, 2010. **35**(12): p. 2193-8.
112. Neppl, R., et al., *In vivo detection of postictal perturbations of cerebral metabolism by use of proton MR spectroscopy: preliminary results in a canine model of prolonged generalized seizures.* AJNR Am J Neuroradiol, 2001. **22**(10): p. 1933-43.
113. Ivanov, A.I., C. Bernard, and D.A. Turner, *Metabolic responses differentiate between interictal, ictal and persistent epileptiform activity in intact, immature hippocampus in vitro.* Neurobiol Dis, 2015. **75**: p. 1-14.
114. Walls, A.B., et al., *A subconvulsive dose of kainate selectively compromises astrocytic metabolism in the mouse brain in vivo.* J Cereb Blood Flow Metab, 2014. **34**(8): p. 1340-6.
115. Shlosberg, D., et al., *Blood-brain barrier breakdown as a therapeutic target in traumatic brain injury.* Nat Rev Neurol, 2010. **6**(7): p. 393-403.
116. Dulla, C.G., D.A. Coulter, and J. Ziburkus, *From Molecular Circuit Dysfunction to Disease: Case Studies in Epilepsy, Traumatic Brain Injury, and Alzheimer's Disease.* Neuroscientist, 2016. **22**(3): p. 295-312.
117. Prins, M., et al., *The pathophysiology of traumatic brain injury at a glance.* Dis Model Mech, 2013. **6**(6): p. 1307-15.
118. Stovell, M.G., et al., *Assessing Metabolism and Injury in Acute Human Traumatic Brain Injury with Magnetic Resonance Spectroscopy: Current and Future Applications.* Front Neurol, 2017. **8**: p. 426.
119. Bergsneider, M., et al., *Cerebral hyperglycolysis following severe traumatic brain injury in humans: a positron emission tomography study.* J Neurosurg, 1997. **86**(2): p. 241-51.
120. Bergsneider, M., et al., *Dissociation of cerebral glucose metabolism and level of consciousness during the period of metabolic depression following human traumatic brain injury.* J Neurotrauma, 2000. **17**(5): p. 389-401.
121. Wu, H.M., et al., *Subcortical white matter metabolic changes remote from focal hemorrhagic lesions suggest diffuse injury after human traumatic brain injury.* Neurosurgery, 2004. **55**(6): p. 1306-15; discussio 1316-7.
122. Vespa, P.M., et al., *Persistently low extracellular glucose correlates with poor outcome 6 months after human traumatic brain injury despite a lack of increased lactate: a microdialysis study.* J Cereb Blood Flow Metab, 2003. **23**(7): p. 865-77.
123. Wu, H.M., et al., *Selective metabolic reduction in gray matter acutely following human traumatic brain injury.* J Neurotrauma, 2004. **21**(2): p. 149-61.
124. Kawai, N., et al., *Metabolic disturbance without brain ischemia in traumatic brain injury: a positron emission tomography study.* Acta Neurochir Suppl, 2008. **102**: p. 241-5.
125. Shiga, T., et al., *Loss of neuronal integrity: a cause of hypometabolism in patients with traumatic brain injury without MRI abnormality in the chronic stage.* Eur J Nucl Med Mol Imaging, 2006. **33**(7): p. 817-22.
126. Sakamoto, S., et al., *Prediction of seizure outcome following epilepsy surgery: asymmetry of thalamic glucose metabolism and cerebral neural activity in temporal lobe epilepsy.* Seizure, 2009. **18**(1): p. 1-6.

127. Nakayama, N., et al., *Relationship between regional cerebral metabolism and consciousness disturbance in traumatic diffuse brain injury without large focal lesions: an FDG-PET study with statistical parametric mapping analysis.* J Neurol Neurosurg Psychiatry, 2006. **77**(7): p. 856-62.
128. Hattori, N., et al., *Correlation of regional metabolic rates of glucose with glasgow coma scale after traumatic brain injury.* J Nucl Med, 2003. **44**(11): p. 1709-16.
129. Kato, T., et al., *Statistical image analysis of cerebral glucose metabolism in patients with cognitive impairment following diffuse traumatic brain injury.* J Neurotrauma, 2007. **24**(6): p. 919-26.
130. Carpenter, K.L., et al., *(13)C-labelled microdialysis studies of cerebral metabolism in TBI patients.* Eur J Pharm Sci, 2014. **57**: p. 87-97.
131. Dusick, J.R., et al., *Increased pentose phosphate pathway flux after clinical traumatic brain injury: a [1,2-13C2]glucose labeling study in humans.* J Cereb Blood Flow Metab, 2007. **27**(9): p. 1593-602.
132. Jalloh, I., et al., *Glycolysis and the pentose phosphate pathway after human traumatic brain injury: microdialysis studies using 1,2-(13)C2 glucose.* J Cereb Blood Flow Metab, 2015. **35**(1): p. 111-20.
133. Hutchinson, P.J., et al., *A combined microdialysis and FDG-PET study of glucose metabolism in head injury.* Acta Neurochir (Wien), 2009. **151**(1): p. 51-61; discussion 61.
134. Vespa, P., et al., *Metabolic crisis occurs with seizures and periodic discharges after brain trauma.* Ann Neurol, 2016. **79**(4): p. 579-90.
135. Van Horn, J.D., A. Bhattrai, and A. Irimia, *Multimodal Imaging of Neurometabolic Pathology due to Traumatic Brain Injury.* Trends Neurosci, 2017. **40**(1): p. 39-59.
136. Guglielmetti, C., et al., *In vivo metabolic imaging of Traumatic Brain Injury.* Sci Rep, 2017. **7**(1): p. 17525.
137. Zhao, Z., et al., *Comparing the predictive value of multiple cognitive, affective, and motor tasks after rodent traumatic brain injury.* J Neurotrauma, 2012. **29**(15): p. 2475-89.
138. Chauhan, N.B., R. Gatto, and M.B. Chauhan, *Neuroanatomical correlation of behavioral deficits in the CCI model of TBI.* J Neurosci Methods, 2010. **190**(1): p. 1-9.
139. Fox, G.B., R.A. LeVasseur, and A.I. Faden, *Behavioral responses of C57BL/6, FVB/N, and 129/SvEMS mouse strains to traumatic brain injury: implications for gene targeting approaches to neurotrauma.* J Neurotrauma, 1999. **16**(5): p. 377-89.
140. Bolkvadze, T., N. Puhakka, and A. Pitkanen, *Epileptogenesis after traumatic brain injury in Plaur-deficient mice.* Epilepsy Behav, 2016. **60**: p. 187-96.
141. Bolkvadze, T. and A. Pitkanen, *Development of post-traumatic epilepsy after controlled cortical impact and lateral fluid-percussion-induced brain injury in the mouse.* J Neurotrauma, 2012. **29**(5): p. 789-812.
142. Andersen, B.J. and A. Marmarou, *Post-traumatic selective stimulation of glycolysis.* Brain Res, 1992. **585**(1-2): p. 184-9.
143. Yoshino, A., et al., *Dynamic changes in local cerebral glucose utilization following cerebral conclusion in rats: evidence of a hyper- and subsequent hypometabolic state.* Brain Res, 1991. **561**(1): p. 106-119.

144. Thomas, S., et al., *Cerebral metabolic response to traumatic brain injury sustained early in development: a 2-deoxy-D-glucose autoradiographic study.* J Neurotrauma, 2000. **17**(8): p. 649-65.
145. Casey, P.A., et al., *Early and sustained alterations in cerebral metabolism after traumatic brain injury in immature rats.* J Neurotrauma, 2008. **25**(6): p. 603-14.
146. Deng-Bryant, Y., et al., *Ketogenic diet prevents alterations in brain metabolism in young but not adult rats after traumatic brain injury.* J Neurotrauma, 2011. **28**(9): p. 1813-25.
147. Vallez Garcia, D., et al., *Three Month Follow-Up of Rat Mild Traumatic Brain Injury: A Combined [(18)F]FDG and [(11)C]PK11195 Positron Emission Study.* J Neurotrauma, 2016. **33**(20): p. 1855-1865.
148. Shultz, S.R., et al., *Can structural or functional changes following traumatic brain injury in the rat predict epileptic outcome?* Epilepsia, 2013. **54**(7): p. 1240-50.
149. Brabazon, F., et al., *[(18)F]FDG-PET Combined with MRI Elucidates the Pathophysiology of Traumatic Brain Injury in Rats.* J Neurotrauma, 2017. **34**(5): p. 1074-1085.
150. Kawamata, T., et al., *Administration of excitatory amino acid antagonists via microdialysis attenuates the increase in glucose utilization seen following concussive brain injury.* J. Cereb. Blood Flow Metab, 1992. **12**(1): p. 12-24.
151. Ip, E.Y., et al., *Metabolic, neurochemical, and histologic responses to vibrissa motor cortex stimulation after traumatic brain injury.* J Cereb Blood Flow Metab, 2003. **23**(8): p. 900-10.
152. Selwyn, R.G., et al., *Outcome after Repetitive Mild Traumatic Brain Injury Is Temporally Related to Glucose Uptake Profile at Time of Second Injury.* J Neurotrauma, 2016. **33**(16): p. 1479-91.
153. Zhou, J., et al., *Temporal Changes in Cortical and Hippocampal Expression of Genes Important for Brain Glucose Metabolism Following Controlled Cortical Impact Injury in Mice.* Front Endocrinol (Lausanne), 2017. **8**: p. 231.
154. Amorini, A.M., et al., *Metabolic, enzymatic and gene involvement in cerebral glucose dysmetabolism after traumatic brain injury.* Biochim Biophys Acta, 2016. **1862**(4): p. 679-687.
155. Hamlin, G.P., et al., *Increased expression of neuronal glucose transporter 3 but not glial glucose transporter 1 following severe diffuse traumatic brain injury in rats.* J Neurotrauma, 2001. **18**(10): p. 1011-8.
156. Bartnik-Olson, B.L., et al., *Astrocyte oxidative metabolism and metabolite trafficking after fluid percussion brain injury in adult rats.* J Neurotrauma, 2010. **27**(12): p. 2191-202.
157. Moro, N., et al., *Pyruvate treatment attenuates cerebral metabolic depression and neuronal loss after experimental traumatic brain injury.* Brain Res, 2016. **1642**: p. 270-277.
158. Moro, N., et al., *Delayed sodium pyruvate treatment improves working memory following experimental traumatic brain injury.* Neurosci Lett, 2011. **491**(2): p. 158-62.
159. Prins, M.L. and J.H. Matsumoto, *The collective therapeutic potential of cerebral ketone metabolism in traumatic brain injury.* J Lipid Res, 2014. **55**(12): p. 2450-7.

160. Hu, Z.G., et al., *Ketogenic diet reduces cytochrome c release and cellular apoptosis following traumatic brain injury in juvenile rats.* Ann Clin Lab Sci, 2009. **39**(1): p. 76-83.
161. Hu, Z.G., et al., *The protective effect of the ketogenic diet on traumatic brain injury-induced cell death in juvenile rats.* Brain Inj, 2009. **23**(5): p. 459-65.
162. Yellen, G., *Ketone bodies, glycolysis, and KATP channels in the mechanism of the ketogenic diet.* Epilepsia, 2008. **49 Suppl 8**: p. 80-2.
163. Milder, J. and M. Patel, *Modulation of oxidative stress and mitochondrial function by the ketogenic diet.* Epilepsy Res, 2012. **100**(3): p. 295-303.
164. Rho, J.M., *How does the ketogenic diet induce anti-seizure effects?* Neurosci Lett, 2017. **637**: p. 4-10.
165. Boison, D., *New insights into the mechanisms of the ketogenic diet.* Curr Opin Neurol, 2017. **30**(2): p. 187-192.
166. Simeone, T.A., et al., *Do ketone bodies mediate the anti-seizure effects of the ketogenic diet?* Neuropharmacology, 2018. **133**: p. 233-241.
167. Paoli, A., et al., *Ketogenic diet in neuromuscular and neurodegenerative diseases.* Biomed Res Int, 2014. **2014**: p. 474296.
168. Bostock, E.C., K.C. Kirkby, and B.V. Taylor, *The Current Status of the Ketogenic Diet in Psychiatry.* Front Psychiatry, 2017. **8**: p. 43.
169. Valdebenito, R., et al., *Targeting of astrocytic glucose metabolism by beta-hydroxybutyrate.* J Cereb Blood Flow Metab, 2016. **36**(10): p. 1813-1822.
170. Meidenbauer, J.J., J.G. Mantis, and T.N. Seyfried, *The EL mouse: a natural model of autism and epilepsy.* Epilepsia, 2011. **52**(2): p. 347-57.
171. Meidenbauer, J.J. and M.F. Roberts, *Reduced glucose utilization underlies seizure protection with dietary therapy in epileptic EL mice.* Epilepsy Behav, 2014. **39**: p. 48-54.
172. Ghosh, S., P. Gupta, and E. Sen, *TNFalpha driven HIF-1alpha-hexokinase II axis regulates MHC-I cluster stability through actin cytoskeleton.* Exp Cell Res, 2016. **340**(1): p. 116-24.
173. Liu, X., et al., *Dual mechanisms for glucose 6-phosphate inhibition of human brain hexokinase.* J Biol Chem, 1999. **274**(44): p. 31155-9.
174. Schmidt, M.M. and R. Dringen, *Differential effects of iodoacetamide and iodoacetate on glycolysis and glutathione metabolism of cultured astrocytes.* Front Neuroenergetics, 2009. **1**: p. 1.
175. Wu, C.L., et al., *Mushroom body glycolysis is required for olfactory memory in Drosophila.* Neurobiol Learn Mem, 2018. **150**: p. 13-19.
176. Zhang, D., et al., *2-Deoxy-D-glucose targeting of glucose metabolism in cancer cells as a potential therapy.* Cancer Lett, 2014. **355**(2): p. 176-83.
177. Ockuly, J.C., et al., *Behavioral, cognitive, and safety profile of 2-deoxy-2-glucose (2DG) in adult rats.* Epilepsy Res, 2012. **101**(3): p. 246-52.
178. Stafstrom, C.E., A. Roopra, and T.P. Sutula, *Seizure suppression via glycolysis inhibition with 2-deoxy-D-glucose (2DG).* Epilepsia, 2008. **49 Suppl 8**: p. 97-100.
179. Stafstrom, C.E., et al., *Anticonvulsant and antiepileptic actions of 2-deoxy-D-glucose in epilepsy models.* Ann. Neurol, 2009. **65**(4): p. 435-447.

180. Garriga-Canut, M., et al., *2-Deoxy-D-glucose reduces epilepsy progression by NRSF-CtBP-dependent metabolic regulation of chromatin structure.* Nat. Neurosci, 2006. **9**(11): p. 1382-1387.
181. Lian, X.Y., F.A. Khan, and J.L. Stringer, *Fructose-1,6-bisphosphate has anticonvulsant activity in models of acute seizures in adult rats.* J Neurosci, 2007. **27**(44): p. 12007-11.
182. Gasior, M., et al., *Anticonvulsant and proconvulsant actions of 2-deoxy-D-glucose.* Epilepsia, 2010. **51**(8): p. 1385-94.
183. Shao, L.R. and C.E. Stafstrom, *Glycolytic inhibition by 2-deoxy-d-glucose abolishes both neuronal and network bursts in an in vitro seizure model.* J Neurophysiol, 2017. **118**(1): p. 103-113.
184. Samokhina, E., et al., *Chronic inhibition of brain glycolysis initiates epileptogenesis.* J Neurosci Res, 2017. **95**(11): p. 2195-2206.
185. Loscher, W., *Preclinical assessment of proconvulsant drug activity and its relevance for predicting adverse events in humans.* Eur J Pharmacol, 2009. **610**(1-3): p. 1-11.
186. Nedergaard, S. and M. Andreasen, *Opposing effects of 2-deoxy-d-glucose on interictal- and ictal-like activity when K(+) currents and GABAA receptors are blocked in rat hippocampus in vitro.* J Neurophysiol, 2018. **119**(5): p. 1912-1923.
187. Zhao, Y.T., S. Tekkok, and K. Krnjevic, *2-Deoxy-D-glucose-induced changes in membrane potential, input resistance, and excitatory postsynaptic potentials of CA1 hippocampal neurons.* Can J Physiol Pharmacol, 1997. **75**(5): p. 368-74.
188. Forte, N., et al., *2-Deoxy-d-glucose enhances tonic inhibition through the neurosteroid-mediated activation of extrasynaptic GABAA receptors.* Epilepsia, 2016. **57**(12): p. 1987-2000.
189. Yang, H., et al., *The antiepileptic effect of the glycolytic inhibitor 2-deoxy-D-glucose is mediated by upregulation of K(ATP) channel subunits Kir6.1 and Kir6.2.* Neurochem Res, 2013. **38**(4): p. 677-85.
190. Sada, N., et al., *Epilepsy treatment. Targeting LDH enzymes with a stiripentol analog to treat epilepsy.* Science, 2015. **347**(6228): p. 1362-7.
191. Martinez-Francois, J.R., et al., *BAD and KATP channels regulate neuron excitability and epileptiform activity.* Elife, 2018. **7**.
192. Stringer, J.L. and K. Xu, *Possible mechanisms for the anticonvulsant activity of fructose-1,6-diphosphate.* Epilepsia, 2008. **49 Suppl 8**: p. 101-3.
193. Ding, Y., et al., *Fructose-1,6-diphosphate protects against epileptogenesis by modifying cation-chloride co-transporters in a model of amygdaloid-kindling temporal epilepticus.* Brain Res, 2013. **1539**: p. 87-94.
194. Chang, B.S., D.H. Lowenstein, and N. Quality Standards Subcommittee of the American Academy of, *Practice parameter: antiepileptic drug prophylaxis in severe traumatic brain injury: report of the Quality Standards Subcommittee of the American Academy of Neurology.* Neurology, 2003. **60**(1): p. 10-6.
195. Kirmani, B.F., et al., *Role of Anticonvulsants in the Management of Posttraumatic Epilepsy.* Front Neurol, 2016. **7**: p. 32.
196. Trinka, E. and F. Brigo, *Antiepileptogenesis in humans: disappointing clinical evidence and ways to move forward.* Curr Opin Neurol, 2014. **27**(2): p. 227-35.

197. Crompton, E.M., et al., *Meta-Analysis of Therapeutic Hypothermia for Traumatic Brain Injury in Adult and Pediatric Patients.* Crit Care Med, 2017. **45**(4): p. 575-583.
198. Maas, A. and N. Stocchetti, *Hypothermia and the complexity of trials in patients with traumatic brain injury.* Lancet Neurol, 2011. **10**(2): p. 111-3.
199. Andrews, P.J., B.A. Harris, and G.D. Murray, *Hypothermia for Intracranial Hypertension after Traumatic Brain Injury.* N Engl J Med, 2016. **374**(14): p. 1385.
200. Gajavelli, S., et al., *Glucose and oxygen metabolism after penetrating ballistic-like brain injury.* J Cereb Blood Flow Metab, 2015. **35**(5): p. 773-80.
201. Annegers, J.F., et al., *A population-based study of seizures after traumatic brain injuries.* N. Engl. J. Med, 1998. **338**(1): p. 20-24.
202. Ritter, A.C., et al., *Incidence and risk factors of posttraumatic seizures following traumatic brain injury: A Traumatic Brain Injury Model Systems Study.* Epilepsia, 2016. **57**(12): p. 1968-1977.
203. Piccenna, L., G. Shears, and T.J. O'Brien, *Management of post-traumatic epilepsy: An evidence review over the last 5 years and future directions.* Epilepsia Open, 2017. **2**(2): p. 123-144.
204. Liu, Y.R., et al., *Progressive metabolic and structural cerebral perturbations after traumatic brain injury: an in vivo imaging study in the rat.* J Nucl Med, 2010. **51**(11): p. 1788-95.
205. Diamond, M.L., et al., *IL-1beta associations with posttraumatic epilepsy development: a genetics and biomarker cohort study.* Epilepsia, 2014. **55**(7): p. 1109-19.
206. Kim, J.A., et al., *Epileptiform activity in traumatic brain injury predicts post-traumatic epilepsy.* Ann Neurol, 2018. **83**(4): p. 858-862.
207. Hemphill, M.A., et al., *Traumatic brain injury and the neuronal microenvironment: a potential role for neuropathological mechanotransduction.* Neuron, 2015. **85**(6): p. 1177-92.
208. Gasior, M., M.A. Rogawski, and A.L. Hartman, *Neuroprotective and disease-modifying effects of the ketogenic diet.* Behav Pharmacol, 2006. **17**(5-6): p. 431-9.
209. McIntosh, T.K., et al., *The Dorothy Russell Memorial Lecture. The molecular and cellular sequelae of experimental traumatic brain injury: pathogenetic mechanisms.* Neuropathol Appl Neurobiol, 1998. **24**(4): p. 251-67.
210. Appelberg, K.S., D.A. Hovda, and M.L. Prins, *The effects of a ketogenic diet on behavioral outcome after controlled cortical impact injury in the juvenile and adult rat.* J Neurotrauma, 2009. **26**(4): p. 497-506.
211. Prins, M.L., L.S. Fujima, and D.A. Hovda, *Age-dependent reduction of cortical contusion volume by ketones after traumatic brain injury.* J Neurosci Res, 2005. **82**(3): p. 413-20.
212. Corps, K.N., T.L. Roth, and D.B. McGavern, *Inflammation and neuroprotection in traumatic brain injury.* JAMA Neurol, 2015. **72**(3): p. 355-62.
213. Gadani, S.P., et al., *Dealing with Danger in the CNS: The Response of the Immune System to Injury.* Neuron, 2015. **87**(1): p. 47-62.
214. Vezzani, A., et al., *The role of inflammation in epilepsy.* Nat Rev Neurol, 2011. **7**(1): p. 31-40.

215. Vilalta, A. and G.C. Brown, *Deoxyglucose prevents neurodegeneration in culture by eliminating microglia.* J Neuroinflammation, 2014. **11**: p. 58.
216. Loncarevic-Vasiljkovic, N., et al., *Caloric restriction suppresses microglial activation and prevents neuroapoptosis following cortical injury in rats.* PLoS One, 2012. **7**(5): p. e37215.
217. Liu, R.T., et al., *Enhanced glycolysis contributes to the pathogenesis of experimental autoimmune neuritis.* J Neuroinflammation, 2018. **15**(1): p. 51.
218. Tannahill, G.M., et al., *Succinate is an inflammatory signal that induces IL-1beta through HIF-1alpha.* Nature, 2013. **496**(7444): p. 238-42.
219. Park, K. and T. Biederer, *Neuronal adhesion and synapse organization in recovery after brain injury.* Future. Neurol, 2013. **8**(5): p. 555-567.
220. Hunt, R.F., J.A. Boychuk, and B.N. Smith, *Neural circuit mechanisms of post-traumatic epilepsy.* Front Cell Neurosci, 2013. **7**: p. 89.
221. Guerriero, R.M., C.C. Giza, and A. Rotenberg, *Glutamate and GABA imbalance following traumatic brain injury.* Curr Neurol Neurosci Rep, 2015. **15**(5): p. 27.
222. Hunt, R.F., S.W. Scheff, and B.N. Smith, *Synaptic reorganization of inhibitory hilar interneuron circuitry after traumatic brain injury in mice.* J Neurosci, 2011. **31**(18): p. 6880-90.
223. Hunt, R.F., S.W. Scheff, and B.N. Smith, *Regionally localized recurrent excitation in the dentate gyrus of a cortical contusion model of posttraumatic epilepsy.* J Neurophysiol, 2010. **103**(3): p. 1490-500.
224. Hsieh, T.H., et al., *Trajectory of Parvalbumin Cell Impairment and Loss of Cortical Inhibition in Traumatic Brain Injury.* Cereb Cortex, 2017. **27**(12): p. 5509-5524.
225. Schwartzkroin, P.A., et al., *Does ketogenic diet alter seizure sensitivity and cell loss following fluid percussion injury?* Epilepsy Res, 2010. **92**(1): p. 74-84.
226. McDougall, A., M. Bayley, and S.E. Munce, *The ketogenic diet as a treatment for traumatic brain injury: a scoping review.* Brain Inj, 2018. **32**(4): p. 416-422.
227. Kann, O., I.E. Papageorgiou, and A. Draguhn, *Highly energized inhibitory interneurons are a central element for information processing in cortical networks.* J Cereb Blood Flow Metab, 2014. **34**(8): p. 1270-82.
228. Gulyas, A.I., et al., *Populations of hippocampal inhibitory neurons express different levels of cytochrome c.* Eur J Neurosci, 2006. **23**(10): p. 2581-94.
229. Zeisel, A., et al., *Brain structure. Cell types in the mouse cortex and hippocampus revealed by single-cell RNA-seq.* Science, 2015. **347**(6226): p. 1138-42.
230. Arlotta, P., et al., *Ctip2 controls the differentiation of medium spiny neurons and the establishment of the cellular architecture of the striatum.* J Neurosci, 2008. **28**(3): p. 622-32.
231. Moro, N., et al., *Glucose administration after traumatic brain injury improves cerebral metabolism and reduces secondary neuronal injury.* Brain Res, 2013. **1535**: p. 124-36.
232. Shi, J., et al., *Review: Traumatic brain injury and hyperglycemia, a potentially modifiable risk factor.* Oncotarget, 2016.
233. Shijo, K., et al., *Glucose administration after traumatic brain injury exerts some benefits and no adverse effects on behavioral and histological outcomes.* Brain Res, 2015. **1614**: p. 94-104.

234. Pecha, T., et al., *Hyperglycemia during craniotomy for adult traumatic brain injury.* Anesth Analg, 2011. **113**(2): p. 336-42.
235. Zhao, Q.J., X.G. Zhang, and L.X. Wang, *Mild hypothermia therapy reduces blood glucose and lactate and improves neurologic outcomes in patients with severe traumatic brain injury.* J Crit Care, 2011. **26**(3): p. 311-5.
236. Hernandez, T.D. and T. Schallert, *Long-term impairment of behavioral recovery from cortical damage can be produced by short-term GABA-agonist infusion into adjacent cortex.* Restor Neurol Neurosci, 1990. **1**(5): p. 323-30.
237. Prins, M.L., et al., *Increased cerebral uptake and oxidation of exogenous betaHB improves ATP following traumatic brain injury in adult rats.* J Neurochem, 2004. **90**(3): p. 666-72.
238. Suzuki, M., et al., *Beta-hydroxybutyrate, a cerebral function improving agent, protects rat brain against ischemic damage caused by permanent and transient focal cerebral ischemia.* Jpn J Pharmacol, 2002. **89**(1): p. 36-43.
239. Bhatti, J., et al., *Systematic Review of Human and Animal Studies Examining the Efficacy and Safety of N-Acetylcysteine (NAC) and N-Acetylcysteine Amide (NACA) in Traumatic Brain Injury: Impact on Neurofunctional Outcome and Biomarkers of Oxidative Stress and Inflammation.* Front Neurol, 2017. **8**: p. 744.
240. Terse, P.S., et al., *2-Deoxy-d-Glucose (2-DG)-Induced Cardiac Toxicity in Rat: NT-proBNP and BNP as Potential Early Cardiac Safety Biomarkers.* Int J Toxicol, 2016. **35**(3): p. 284-93.
241. Arciniegas, D.B., K. Held, and P. Wagner, *Cognitive Impairment Following Traumatic Brain Injury.* Curr Treat Options Neurol, 2002. **4**(1): p. 43-57.
242. Frey, L.C., *Epidemiology of posttraumatic epilepsy: a critical review.* Epilepsia, 2003. **44 Suppl 10**: p. 11-7.
243. Gupta, P.K., et al., *Subtypes of post-traumatic epilepsy: clinical, electrophysiological, and imaging features.* J Neurotrauma, 2014. **31**(16): p. 1439-43.
244. Schierhout, G. and I. Roberts, *Prophylactic antiepileptic agents after head injury: a systematic review.* J Neurol Neurosurg Psychiatry, 1998. **64**(1): p. 108-12.
245. Jennett, W.B. and W. Lewin, *Traumatic epilepsy after closed head injuries.* J Neurol Neurosurg Psychiatry, 1960. **23**: p. 295-301.
246. Chiaretti, A., et al., *Early post-traumatic seizures in children with head injury.* Childs Nerv Syst, 2000. **16**(12): p. 862-6.
247. Katayama, Y., et al., *Massive increases in extracellular potassium and the indiscriminate release of glutamate following concussive brain injury.* J Neurosurg, 1990. **73**(6): p. 889-900.
248. Golding, E.M., C.S. Robertson, and R.M. Bryan, Jr., *The consequences of traumatic brain injury on cerebral blood flow and autoregulation: a review.* Clin Exp Hypertens, 1999. **21**(4): p. 299-332.
249. Grundl, P.D., et al., *Early cerebrovascular response to head injury in immature and mature rats.* J Neurotrauma, 1994. **11**(2): p. 135-48.
250. Hiebert, J.B., et al., *Traumatic brain injury and mitochondrial dysfunction.* Am J Med Sci, 2015. **350**(2): p. 132-8.
251. Sharp, D.J., G. Scott, and R. Leech, *Network dysfunction after traumatic brain injury.* Nat. Rev. Neurol, 2014. **10**(3): p. 156-166.

252. Wei, D., et al., *Degeneration and regeneration of GABAergic interneurons in the dentate gyrus of adult mice in experimental models of epilepsy.* CNS Neurosci Ther, 2015. **21**(1): p. 52-60.
253. Toth, K., et al., *Loss and reorganization of calretinin-containing interneurons in the epileptic human hippocampus.* Brain, 2010. **133**(9): p. 2763-77.
254. Staley, K., *Molecular mechanisms of epilepsy.* Nat. Neurosci, 2015. **18**(3): p. 367-372.
255. Hu, H., J. Gan, and P. Jonas, *Interneurons. Fast-spiking, parvalbumin(+) GABAergic interneurons: from cellular design to microcircuit function.* Science, 2014. **345**(6196): p. 1255263.
256. Prince, D.A., et al., *Epilepsy following cortical injury: cellular and molecular mechanisms as targets for potential prophylaxis.* Epilepsia, 2009. **50 Suppl 2**: p. 30-40.
257. Avramescu, S., D.A. Nita, and I. Timofeev, *Neocortical post-traumatic epileptogenesis is associated with loss of GABAergic neurons.* J Neurotrauma, 2009. **26**(5): p. 799-812.
258. Buckmaster, P.S., E. Abrams, and X. Wen, *Seizure frequency correlates with loss of dentate gyrus GABAergic neurons in a mouse model of temporal lobe epilepsy.* J Comp Neurol, 2017. **525**(11): p. 2592-2610.
259. Chen, S., et al., *Pilocarpine-induced status epilepticus causes acute interneuron loss and hyper-excitatory propagation in rat insular cortex.* Neuroscience, 2010. **166**(1): p. 341-53.
260. Epsztein, J., et al., *Ongoing epileptiform activity in the post-ischemic hippocampus is associated with a permanent shift of the excitatory-inhibitory synaptic balance in CA3 pyramidal neurons.* J Neurosci, 2006. **26**(26): p. 7082-92.
261. Kuruba, R., X. Wu, and D.S. Reddy, *Benzodiazepine-refractory status epilepticus, neuroinflammation, and interneuron neurodegeneration after acute organophosphate intoxication.* Biochim Biophys Acta, 2018. **1864**(9 Pt B): p. 2845-2858.
262. Bergsneider, M., et al., *Metabolic recovery following human traumatic brain injury based on FDG-PET: time course and relationship to neurological disability.* J. Head Trauma Rehabil, 2001. **16**(2): p. 135-148.
263. Vespa, P., et al., *Metabolic crisis without brain ischemia is common after traumatic brain injury: a combined microdialysis and positron emission tomography study.* J Cereb Blood Flow Metab, 2005. **25**(6): p. 763-74.
264. Bertoni, J.M., *Competitive inhibition of rat brain hexokinase by 2-deoxyglucose, glucosamine, and metrizamide.* J Neurochem, 1981. **37**(6): p. 1523-8.
265. Cisternas, P., et al., *Modulation of Glucose Metabolism in Hippocampal Neurons by Adiponectin and Resistin.* Mol Neurobiol, 2018.
266. Lee, J., et al., *2-Deoxy-D-glucose protects hippocampal neurons against excitotoxic and oxidative injury: evidence for the involvement of stress proteins.* J Neurosci Res, 1999. **57**(1): p. 48-61.
267. Chattopadhyaya, B., et al., *Experience and activity-dependent maturation of perisomatic GABAergic innervation in primary visual cortex during a postnatal critical period.* J Neurosci, 2004. **24**(43): p. 9598-611.

268. Hegen, H., M. Auer, and F. Deisenhammer, *Serum glucose adjusted cut-off values for normal cerebrospinal fluid/serum glucose ratio: implications for clinical practice.* Clin Chem Lab Med, 2014. **52**(9): p. 1335-40.
269. Schwaller, B., et al., *Parvalbumin deficiency affects network properties resulting in increased susceptibility to epileptic seizures.* Mol Cell Neurosci, 2004. **25**(4): p. 650-63.
270. DeFelipe, J., et al., *Selective changes in the microorganization of the human epileptogenic neocortex revealed by parvalbumin immunoreactivity.* Cereb Cortex, 1993. **3**(1): p. 39-48.
271. Drexel, M., et al., *Selective Silencing of Hippocampal Parvalbumin Interneurons Induces Development of Recurrent Spontaneous Limbic Seizures in Mice.* J Neurosci, 2017. **37**(34): p. 8166-8179.
272. Munoz-Manchado, A.B., et al., *Diversity of Interneurons in the Dorsal Striatum Revealed by Single-Cell RNA Sequencing and PatchSeq.* Cell Rep, 2018. **24**(8): p. 2179-2190 e7.
273. Wu, H., et al., *Melatonin attenuates neuronal apoptosis through up-regulation of K(+) -Cl(-) cotransporter KCC2 expression following traumatic brain injury in rats.* J Pineal Res, 2016. **61**(2): p. 241-50.
274. Bonislawski, D.P., E.P. Schwarzbach, and A.S. Cohen, *Brain injury impairs dentate gyrus inhibitory efficacy.* Neurobiol Dis, 2007. **25**(1): p. 163-9.
275. Hui, H., et al., *Inhibition of Na(+)-K(+)-2Cl(-) Cotransporter-1 attenuates traumatic brain injury-induced neuronal apoptosis via regulation of Erk signaling.* Neurochem Int, 2016. **94**: p. 23-31.
276. Lu, K.T., et al., *Inhibition of the Na+ -K+ -2Cl- -cotransporter in choroid plexus attenuates traumatic brain injury-induced brain edema and neuronal damage.* Eur J Pharmacol, 2006. **548**(1-3): p. 99-105.
277. Wang, F., et al., *NKCC1 up-regulation contributes to early post-traumatic seizures and increased post-traumatic seizure susceptibility.* Brain Struct Funct, 2017. **222**(3): p. 1543-1556.
278. Raible, D.J., et al., *GABA(A) receptor regulation after experimental traumatic brain injury.* J. Neurotrauma, 2012. **29**(16): p. 2548-2554.
279. Drexel, M., et al., *Expression of GABA receptor subunits in the hippocampus and thalamus after experimental traumatic brain injury.* Neuropharmacology, 2015. **88**: p. 122-133.
280. Raible, D.J., et al., *JAK/STAT pathway regulation of GABAA receptor expression after differing severities of experimental TBI.* Exp Neurol, 2015. **271**: p. 445-56.
281. Huusko, N. and A. Pitkanen, *Parvalbumin immunoreactivity and expression of GABAA receptor subunits in the thalamus after experimental TBI.* Neuroscience, 2014. **267**: p. 30-45.
282. Wick, A.N., et al., *Localization of the primary metabolic block produced by 2-deoxyglucose.* J Biol Chem, 1957. **224**(2): p. 963-9.
283. Kalia, V.K., S. Prabhakara, and V. Narayanan, *Modulation of cellular radiation responses by 2-deoxy-D-glucose and other glycolytic inhibitors: implications for cancer therapy.* J Cancer Res Ther, 2009. **5 Suppl 1**: p. S57-60.
284. Miwa, H., et al., *Leukemia cells demonstrate a different metabolic perturbation provoked by 2-deoxyglucose.* Oncol Rep, 2013. **29**(5): p. 2053-7.

285. Wang, A., et al., *Glucose metabolism mediates disease tolerance in cerebral malaria.* Proc Natl Acad Sci U S A, 2018. **115**(43): p. 11042-11047.
286. Shintani, H., et al., *Calorie Restriction Mimetics: Upstream-Type Compounds for Modulating Glucose Metabolism.* Nutrients, 2018. **10**(12).
287. Floberg, J.M. and J.K. Schwarz, *Manipulation of Glucose and Hydroperoxide Metabolism to Improve Radiation Response.* Semin Radiat Oncol, 2019. **29**(1): p. 33-41.
288. Ingram, D.K. and G.S. Roth, *Glycolytic inhibition as a strategy for developing calorie restriction mimetics.* Exp Gerontol, 2011. **46**(2-3): p. 148-54.
289. Kane, A., et al., *Cardioprotective inhibitors of reperfusion injury*, in *Probe Reports from the NIH Molecular Libraries Program*. 2010: Bethesda (MD).
290. Tekkok, S. and K. Krnjevic, *Long-term potentiation in hippocampal slices induced by temporary suppression of glycolysis.* J Neurophysiol, 1995. **74**(6): p. 2763-6.
291. Minor, R.K., et al., *Chronic ingestion of 2-deoxy-D-glucose induces cardiac vacuolization and increases mortality in rats.* Toxicol Appl Pharmacol, 2010. **243**(3): p. 332-9.
292. Ma, H., et al., *Therapeutic hypothermia as a neuroprotective strategy in neonatal hypoxic-ischemic brain injury and traumatic brain injury.* Curr Mol Med, 2012. **12**(10): p. 1282-96.
293. Kann, O., *The interneuron energy hypothesis: Implications for brain disease.* Neurobiol Dis, 2016. **90**: p. 75-85.
294. Pellerin, L., et al., *Evidence supporting the existence of an activity-dependent astrocyte-neuron lactate shuttle.* Dev Neurosci, 1998. **20**(4-5): p. 291-9.
295. Gimenez-Cassina, A., et al., *BAD-dependent regulation of fuel metabolism and K(ATP) channel activity confers resistance to epileptic seizures.* Neuron, 2012. **74**(4): p. 719-730.
296. Mannix, R.C., et al., *Age-dependent effect of apolipoprotein E4 on functional outcome after controlled cortical impact in mice.* J Cereb Blood Flow Metab, 2011. **31**(1): p. 351-61.
297. Hanson, E., et al., *Astrocytic glutamate uptake is slow and does not limit neuronal NMDA receptor activation in the neonatal neocortex.* Glia, 2015.
298. Aarts, E., et al., *A solution to dependency: using multilevel analysis to accommodate nested data.* Nat Neurosci, 2014. **17**(4): p. 491-6.
299. Lim, L., et al., *Development and Functional Diversification of Cortical Interneurons.* Neuron, 2018. **100**(2): p. 294-313.
300. Lewis, D.A., et al., *Cortical parvalbumin interneurons and cognitive dysfunction in schizophrenia.* Trends Neurosci, 2012. **35**(1): p. 57-67.
301. Ferguson, B.R. and W.J. Gao, *PV Interneurons: Critical Regulators of E/I Balance for Prefrontal Cortex-Dependent Behavior and Psychiatric Disorders.* Front Neural Circuits, 2018. **12**: p. 37.
302. Xie, Y., et al., *Prolonged deficits in parvalbumin neuron stimulation-evoked network activity despite recovery of dendritic structure and excitability in the somatosensory cortex following global ischemia in mice.* J Neurosci, 2014. **34**(45): p. 14890-900.

303. Hartig, W., et al., *Abolished perineuronal nets and altered parvalbumin-immunoreactivity in the nucleus reticularis thalami of wildtype and 3xTg mice after experimental stroke.* Neuroscience, 2016. **337**: p. 66-87.
304. Nichols, J., et al., *Parvalbumin fast-spiking interneurons are selectively altered by paediatric traumatic brain injury.* J Physiol, 2018. **596**(7): p. 1277-1293.
305. Kossoff, E.H., *The ketogenic diet and other dietary therapies for the treatment of epilepsy*, in *UpToDate*, J.F. Dashe, Editor.
306. Elman, I., et al., *The effects of pharmacological doses of 2-deoxyglucose on cerebral blood flow in healthy volunteers.* Brain Res, 1999. **815**(2): p. 243-9.
307. Washington, P.M., et al., *The effect of injury severity on behavior: a phenotypic study of cognitive and emotional deficits after mild, moderate, and severe controlled cortical impact injury in mice.* J Neurotrauma, 2012. **29**(13): p. 2283-96.
308. Rodriguez-Grande, B., et al., *Early to Long-Term Alterations of CNS Barriers After Traumatic Brain Injury: Considerations for Drug Development.* AAPS J, 2017. **19**(6): p. 1615-1625.